TECHNICAL REPORT STANDARD PAGE

1. Report No. **FHWA/LA. 12/495**	**2. Government Accession No.**	**3. Recipient's Catalog No.**
4. Title and Subtitle **Calibration of Resistance Factors for Drilled Shafts for the New FHWA Design Method**	**5. Report Date** January 2013 **6. Performing Organization Code** **LTRC Project Number: 11-4GT** **SIO Number: 30000280**	
7. Author(s) **Murad Y. Abu-Farsakh, Ph.D., P.E.,** **Qiming Chen, Ph.D., P.E., and Md Nafiul Haque**	**8. Performing Organization Report No.**	
9. Performing Organization Name and Address **Louisiana Transportation Research Center** **4101 Gourrier Avenue** **Baton Rouge, LA 70808**	**10. Work Unit No.** **11. Contract or Grant No.** **LTRC Number: 11-4GT** **SIO Number: 30000280**	
12. Sponsoring Agency Name and Address **Louisiana Transportation Research Center** **4101 Gourrier Avenue** **Baton Rouge, LA 70808**	**13. Type of Report and Period Covered** **Final Report** **Jan 2011 - June 2012** **14. Sponsoring Agency Code**	
15. Supplementary Notes **Conducted in Cooperation with the U.S. Department of Transportation, Federal Highway Administration**		

16. Abstract

The Load and Resistance Factor Design (LRFD) calibration of deep foundation in Louisiana was first completed for driven piles (LTRC Final Report 449) in May 2009 and then for drilled shafts using 1999 FHWA design method (O'Neill and Reese method) (LTRC Final Report 470) in September 2010. As a continuing effort to implement the LRFD design methodology for deep foundations in Louisiana, this report will present the reliability-based analyses for the calibration of the resistance factor for LRFD design of axially loaded drilled shafts using Brown et al. method (2010 FHWA design method). Twenty-six drilled shaft tests collected from previous research (LTRC Final Report 449) and eight new drilled shaft tests were selected for statistical reliability analysis; the predictions of total, side, and tip resistance versus settlement behavior of drilled shafts were established from soil borings using both 1999 FHWA design method (Brown et al. method) and 2010 FHWA design method (O'Neill and Reese method). The measured drilled shaft axial nominal resistance was determined from either the Osterberg cell (O-cell) test or the conventional top-down static load test. For the 30 drilled shafts that were tested using O-cells, the tip and side resistances were deduced separately from test results. Statistical analyses were performed to compare the predicted total, tip, and side drilled shaft nominal axial resistance with the corresponding measured nominal resistance. Results of this showed that the 2010 FHWA design method overestimates the total drilled shaft resistance by an average of two percent, while the 1999 FHWA design method underestimates the total drilled shaft resistance by an average of 21 percent. The Monte Carlo simulation method was selected to perform the LRFD calibration of resistance factors of drilled shaft under strength I limit state. The total resistance factors obtained at different reliability index (β) were determined and compared with those available in literature. Results of reliability analysis, corresponding to a target reliability index (β) of 3.0, reveals resistance factors for side (ϕ_{side}), tip (ϕ_{tip}), and total resistance factor (ϕ_{total}) are 0.26, 0.53, and 0.48, respectively for the 2010 FHWA design method and 0.39, 0.52, and 0.60, respectively for the 1999 FHWA design method. The side and total resistance factors calibrated using the 2010 FHWA design method are less than those calibrated using the 1999 FHWA design method.

17. Key Words		**18. Distribution Statement** **Unrestricted. This document is available through the National Technical Information Service, Springfield, VA 21161.**	
19. Security Classif. (of this report) **Unclassified**	**20. Security Classif. (of this page)** **Unclassified**	21. No. of Pages 122	22. Price

Project Review Committee

Each research project will have an advisory committee appointed by the LTRC Director. The Project Review Committee is responsible for assisting the LTRC Administrator or Manager in the development of acceptable research problem statements, requests for proposals, review of research proposals, oversight of approved research projects, and implementation of findings.

The dedication and work effort of the following Project Review Committee members to guide this research study to fruition are acknowledged and appreciated.

LTRC Administrator

Zhongjie "Doc" Zhang, Ph.D., P.E.
Pavement and Geotechnical Research Administrator

Members

Steve Meunier, DOTD
Arthur D'Andrea, DOTD
Chris Nickel, DOTD
Ching Tsai, DOTD
Jenny Fu, DOTD
Arturo Aguirre, FHWA

Directorate Implementation Sponsor

Richard Savoie, DOTD Chief Engineer

Calibration of Resistance Factors for Drilled Shafts for the New FHWA Design Method

by

Murad Y. Abu-Farsakh, Ph.D., P.E.
Qiming Chen, Ph.D., PE
Md Nafiul Haque

Louisiana Transportation Research Center
4101 Gourrier Avenue
Baton Rouge, LA 70808

LTRC Project No. 11-4GT
SIO No. 30000280

conducted for

Louisiana Department of Transportation and Development
Louisiana Transportation Research Center

January 2013

ABSTRACT

The Load and Resistance Factor Design (LRFD) calibration of deep foundation in Louisiana was first completed for driven piles (LTRC Final Report 449) in May 2009 and then for drilled shafts using 1999 FHWA design method (O'Neill and Reese method) (LTRC Final Report 470) in September 2010. As a continuing effort to implement the LRFD design methodology for deep foundations in Louisiana, this report will present the reliability-based analyses for the calibration of the resistance factor for LRFD design of axially loaded drilled shafts using Brown et al. method (2010 FHWA design method). Twenty-six drilled shaft tests collected from previous research (LTRC Final Report 449) and eight new drilled shaft tests were selected for statistical reliability analysis; the predictions of total, side, and tip resistance versus settlement behavior of drilled shafts were established from soil borings using both 1999 FHWA design method (Brown et al. method) and 2010 FHWA design method (O'Neill and Reese method). The measured drilled shaft axial nominal resistance was determined from either the Osterberg cell (O-cell) test or the conventional top-down static load test. For the 30 drilled shafts that were tested using O-cells, the tip and side resistances were deduced separately from test results. Statistical analyses were performed to compare the predicted total, tip, and side drilled shaft nominal axial resistance with the corresponding measured nominal resistance. Results of this showed that the 2010 FHWA design method overestimates the total drilled shaft resistance by an average of 2 percent, while the 1999 FHWA design method underestimates the total drilled shaft resistance by an average of 21 percent. The Monte Carlo simulation method was selected to perform the LRFD calibration of resistance factors of drilled shaft under strength I limit state. The total resistance factors obtained at different reliability index (β) were determined and compared with those available in literature. Results of reliability analysis, corresponding to a target reliability index (β) of 3.0, reveals resistance factors for side (ϕ_{side}), tip (ϕ_{tip}), and total resistance factor (ϕ_{total}) are 0.26, 0.53, and 0.48, respectively for the 2010 FHWA design method and 0.39, 0.52, and 0.60, respectively for the 1999 FHWA design method. The side and total resistance factors calibrated using the 2010 FHWA design method are less than those calibrated using the 1999 FHWA design method.

ACKNOWLEDGMENTS

This research project was funded by the LADOTD (SIO No. 30000280) and Louisiana Transportation Research Center (LTRC Project No. 11-4GT). Sean Ferguson with Mississippi Department of Transportation contributed the Mississippi drilled shaft load test database. The comments and suggestions of Mark Morvant and Zhongjie Zhang of LTRC are gratefully acknowledged.

IMPLEMENTATION STATEMENT

The Federal Highway Administration and American Association of Highway Transportation Officials (AASHTO) set a transition date of October 1, 2007, after which all new federal-funded bridges shall be designed using LRFD design methodology to ensure a consistent level of reliability in design of both substructure and superstructure. The current AASHTO specifications recommended resistance factors for drilled shaft design is somewhat conservative, based on Louisiana's experience. In order to provide an efficient and consistent design, it becomes necessary to calibrate the resistance factors for drilled shaft design using the local drilled shaft tests and soil databases. LRFD calibration of resistance factors for O'Neill and Reese design method (1999 FHWA design method) commonly used by LADOTD engineers based on a local database was completed in September 2010. In 2010, a new design manual (Brown et al. 2010), published by the FHWA, introduced a new design methodology in calculating the resistance of drilled shafts and load settlements. As a result, this research study focused on LRFD calibration of resistance factors for Brown et al. design method (2010 FHWA design method) based on a similar database. The resistance factors based on a reliability index of 3.0 recommended in this study will be available for immediate implementation of the LRFD methodology in the design of all future drilled shaft foundations. In addition, the calibration effort in this study is documented; therefore the calibration process becomes a heritage for LADOTD users, and thereby enhances future LRFD research and development. As experience is gained in the application of LRFD to design, the role of past Allowable Stress Design (ASD) practice will become less important; all the advantages of the LRFD design described in the problem statement can be fully addressed. Based on this research, the reliability indices and resistance factors for both 2010 FHWA design method and 1999 FHWA design method are recommended. These recommendations are expected to be used in the design of future projects involving using drilled shafts.

This project is a continuation of the previous project entitled "Calibration of Resistance Factors Needed in the LRFD Design of Driven Piles" *[1]* and "Calibration of Resistance Factors Needed in the LRFD Design of Drilled Shafts" *[2]*. This project will complete the effort of implementing the LRFD design for deep foundations in Louisiana.

TABLE OF CONTENTS

LIST OF TABLES

LIST OF FIGURES

INTRODUCTION

Bridge design philosophies and specifications have been developed over the years to result in bridges with a desired level of reliability. Prior to 1970, the sole design philosophy was allowable stress design (ASD), which has been around since the first AASHTO standard specification for highway bridges was published in 1931. Beginning in early 1970, a new design philosophy called load factor design (LFD) was introduced. It was adopted by AASHTO in 1970 as an alternate method and published in the 1971 AASHTO Interim Specifications. In 1993, AASHTO adopted the Load and Resistance Factor Design (LRFD) specifications for bridge design. The primary difference between LFD and LRFD lies in the calibration procedures to provide the minimum desired level of safety. In the LRFD specifications, the load and resistance factors are determined from a probability based calibration process to achieve a more uniform reliability index for the various components of the system than LFD, in which the load and resistance factors are determined based on judgment and experience *[3]*.In an effort to maintain a consistent level of reliability, FHWA mandated that the AASHTO LRFD Bridge Design Specification should be used for all federal-funded new bridges on which states initiate preliminary engineering after October 1, 2007.

Drilled shafts, as structural members placed in the ground and used to transfer loads from a structure to the foundation soil, have been used in the Louisiana for many years as a deep foundation alternative for bridges. Louisiana Department of Transportation and Development (LA DOTD) initially used ASD for the substructure and LRFD for the superstructure. Recently, LA DOTD started moving to the LRFD method for the substructure since AASHTO LRFD bridge design specification went into effect in 2007; and AASHTO national resistance factors (ϕ) are generally applied in design. However, the resistance factors proposed in the AASHTO specification were derived mainly based on fitting to the ASD factor of safety with consideration of the reliability-base analysis conducted by Paikowsky et al. *[4, 5]*. It is very clear that the concept of LRFD has been well established, but the factors adopted in AASHTO specification do not fully embody this concept. As such, many researchers have been working to develop a reasonable way to implement the LRFD method in bridge substructure design and to determine appropriate resistance factors for different regional soil conditions *[4, 6, 7, 8, 9, 10, 11, 12, 13, 14,* and *15]*.

Paikowsky et al. calibrated resistance factors for drilled shafts based on a database developed by the University of Florida, the FHWA, and O'Neill et al. *[4, 16]*. Resistance factors for total nominal resistance and side resistance were calibrated for drilled shafts in different types of soils considering the effect of construction methods. To reflect the change of load

factors and design method in the AASHTO LRFD specifications, Allen recalibrated resistance factors for drilled shafts based on the databases in the previous literature by fitting to ASD, as well as using the Monte Carlo Method *[*4, *15, 17, 18* and 19*]*. Yang et al. calibrated resistance factors for side resistance estimated by the O'Neill and Reese method based on 19 Osterberg cell (O-cell) test data in Kansas, Colorado, and Missouri *[17, 20]*. Based on the top-down test data of drilled shaft collected in the NCHRP Project 24-17, Liang and Li calibrated resistance factors of drilled shafts designed using the O'Neill and Reese method via the Monte Carlo approach *[14, 17]*.

The use of single drilled shafts to support individual columns in bridges and buildings is widely practiced. When superstructures are sensitive to foundation movements, the settlement of a drilled shaft is important to the normal operation of supported superstructures. According to the FHWA drilled shaft design method, the nominal resistance of drilled shafts is defined as the load carried by the shaft at the head displacement equal to five percent of the shaft diameter, if the shaft has not plunged prior to this displacement *[17, 21]*.

Currently, AASHTO specifications recommend axial compression resistance factors (ϕ_t) for a drilled shaft used in groups of two to four shafts range from 0.40 to 0.60 at the reliability index (β) of 3.0 depending on different soil conditions *[*5*]*. According to AASHTO, the recommended resistance factors for single shaft foundations should be reduced by 20 percent to reflect a higher reliability index of 3.5 due to a lack of redundancy. As mentioned earlier, the recommended resistance factors were derived mainly based on fitting to the ASD factor of safety. The LA DOTD, in conjunction with Louisiana Transportation Research Center (LTRC), began the calibration effort in July 2006, and the drilled shafts calibration is now completed for FHWA (1999) design method *[17]* recommended by AASHTO (2007). In 2010, a new design manual *[22]* published by the FHWA introduces a new design methodology in calculating the resistance of drilled shafts and load settlements. As a result, the resistance factors recommended by the previous report (Report 470) should be augmented to account for the changes of the new design methodology.

OBJECTIVE

The main objective of this study was to calibrate the resistance factors (ϕ_{total}, ϕ_{side}, and ϕ_{tip}) of axially loaded drilled shafts installed in Louisiana soils at strength I limit state using the new FHWA design methodology based on the available drilled shaft load test database collected from Louisiana and Mississippi Departments of Transportation. For comparison purposes, the resistance factors for both the 1999 FHWA design method (O'Neill and Reese design method) and the 2010 FHWA design method (Brown et al. design method), design methods used by LADOTD, will be developed at the target reliability. The findings of this research effort will aid the implementation of the LRFD design methodology for the design of drilled shafts.

SCOPE

To reach the objectives of this study, 26 drilled shaft tests collected from previous research and 8 new drilled shaft tests were collected; among those cases, 30 drilled shafts were tested using O-cells and 4 drilled shafts were tested using the conventional top-down static load test *[2]*. The load settlement curves of drilled shafts from soil borings were predicted using both the 1999 FHWA design method (O'Neill and Reese method) and the 2010 FHWA design method (Brown et al. method). Statistical analyses were conducted on the collected data to evaluate both design methods for predicting the measured drilled shaft resistance. Following the AASHTO specification, a target reliability index of 3.0 was selected for calibration of the resistance factors. Based on the collected database, LRFD calibration of drilled shaft using Monte Carlo simulation method was performed to determine resistance factors (tip, side, and total) for both design methods.

METHODOLOGY

As discussed earlier, the main objective of this research study was to calibrate the resistance factors for 2010 FHWA design method of drilled shafts based on the local database and experience. Background information on 2010 FHWA and 1999 FHWA drilled shaft design methodologies and LRFD calibration were introduced first. Then, a total of 34 drilled shaft load tests and their corresponding soil borings were identified and collected from LADOTD and MSDOT files. The collected drilled shaft load test data and soil properties were compiled and analyzed. The methodology of collecting, compiling, and analyzing the drilled shaft load test database is presented in this section.

Background

Prediction of Ultimate Resistance of Drilled Shafts

The ultimate axial resistance (Q_u) of a drilled shaft consists of the end-bearing resistance (Q_b) and the skin frictional resistance (Q_s). The ultimate drilled shaft resistance can then be calculated using the following equation:

$$Q_u = Q_b + Q_s = q_b.A_b + \sum_{i=1}^{n} f_i A_{si} \quad (1)$$

where, q_b is the unit tip bearing resistance, A_b is the cross-section area of the drilled shaft base, f_i is the average unit skin friction of the soil layer i, A_{si} is the area of the drilled shaft interfacing with layer i, and n is the number of soil layers along the drilled shaft.

In this research, the load-settlement behavior and ultimate drilled shaft resistance were determined according to FHWA suggestions based on the Brown et al. method (2010 FHWA design method) and the O'Neill and Reese method (1999 FHWA design method) *[22][17]*.

Skin Friction in Cohesive Soil. The skin friction for drilled shafts is calculated based on the static α-method as described by O'Neill and Reese *[17]*. The undrained shear strength, S_u, is used in the following equation to compute the ultimate load transfer in skin friction (f_{sz}) at any given depth (z) below the ground surface:

$$f_{sz} = \alpha_z S_{uz} \quad (2)$$

where, α_z is shear strength reduction factor at depth z, S_{uz} is the undrained shear strength at depth z, and f_{sz} is then used to calculate the nominal side resistance R_{SN} as:

$$R_{SN} = \int_0^L f_{sz} dA \quad (3)$$

where, dA is the differential area of the perimeter along the sides of the drilled shaft over the penetration depth, and L is the penetration of the drilled shaft below ground surface.

The α-value used in the equations is shown in Table 1 for the O'Neill and Reese's method (1999 FHWA design method) and Table 2 for the Brown et al. method (2010 FHWA design method). As can be seen from Tables 1 and 2, the difference between 2010 and 1999 FHWA design methods is whether the side resistance should be neglected over a distance of one diameter above the base of drilled shafts or not.

Table 1
α-value used to determine side resistance for O'Neill and Reese Method *[17]*

Location along drilled shaft	α-value	Value of S_{uz}/P_a^*
From ground surface to depth of 1.5 m (5 ft)	0	—
Bottom one diameter or one shaft diameter above the bell (if any)	0	—
All others	0.55	$S_{uz}/P_a \leq 1.5$
	$0.55 - 0.1\ (S_{uz}/P_a - 1.5)$	$1.5 \leq S_{uz}/P_a \leq 2.5$

P_a: atmospheric pressure

Table 2
α-value used to determine side resistance for Brown et al. Method *[22]*

Location along drilled shaft	α-value	Value of S_{uz}/P_a^*
From ground surface to depth of 1.5 m (5 ft)	0	—
All others	0.55	$S_{uz}/P_a \leq 1.5$
	$0.55 - 0.1\ (S_{uz}/P_a - 1.5)$	$1.5 \leq S_{uz}/P_a \leq 2.5$

P_a: atmospheric pressure

End Bearing in Cohesive Soil. Load transfer in end bearing is computed by the following equation, which was developed by O'Neill and Reese and other investigators, and has proven to be fairly effective *[17]*.

$$q_b = N_c S_{ub} \tag{4}$$

where, S_{ub} is the average undrained shear strength of the clay between the base and a depth of 2B (B: diameter of the drilled shaft) below the base. Values of N_c are given in Table 3. Linear interpolation can be used for values between those tabulated.

Table 3
α-value used to determine side resistance for O'Neill and Reese Method *[17]*

S_{ub} (psf)	$I_r = \frac{E_u}{3S_{ub}}$	N_c
500	50	6.5
1000	150	8.0
≥2,000	250 ~ 300	9.0

I_r is the rigidity index; E_s is the undrained Young's modulus

If the shaft depth L is less than 3B, the following equation for q_b is recommended for use *[17]*.

$$q_b = 2/3\,(1+1/6\,(L/B))\,N_c S_{ub} \tag{5}$$

Evaluation of end bearing of drilled shafts in cohesive soil in the Brown, et al.'s method (2010 FHWA design method) is not changed from the O'Neill and Reese's method (1999 FHWA design method).

Skin Friction in Cohesionless Soil. In cohesionless soil, the β-method is usually used to compute the ultimate unit side resistance, f_{sz}, at depth z as follows *[17]*:

$$f_{SZ} = \beta\sigma'_z \le 200\ \text{kPa}\ (2.1\ \text{tsf}) \tag{6}$$

$$R_{SN} = \int_0^L \beta\sigma'_z\, dA \tag{7}$$

In the O'Neill and Reese Method (1999 FHWA design method):

$$\beta = 1.5 - 0.135\,z^{0.5}\ \ 0.25 \le \beta \le 1.2 \text{ for } N_{60} \ge 15, \tag{8}$$

$$\beta = (N_{60}/15)(1.5 - 0.135\,z^{0.5})\ \ 0.25 \le \beta \le 1.2 \text{ for } N_{60} < 15 \tag{9}$$

where, σ'_z is the vertical effective stress in soil at depth z, and z is the depth below the ground surface. When N_{60} is greater than 50 blows/0.3 m (50 blows/ft.), the O'Neill and Reese method recommends that f_{sz} should be calculated using the method for cohesionless intermediate geomaterial (IGM) described later in this section. In the O'Neill and Reese method, β is a function of only depth.

In the Brown, et al. method (2010 FHWA design method):

$$\beta = (1-\sin\phi')\left(\frac{\sigma'_p}{\sigma'_z}\right)\tan\phi' \leq K_p\tan\phi' \quad (10)$$

where, σ_p' is the effective vertical preconsolidation stress and ϕ' is the effective friction angle. The value of β at shallow depths should be limited to the value corresponding to a depth of 7.5 ft.

$$\frac{\sigma'_p}{p_a} = 0.47(N_{60})^m \quad (11)$$

where, m = 0.6 for clean quartzitic sands and 0.8 for silty sands to sandy silts, and p_a is the atmospheric pressure. In Brown et al.'s method, β accounts for soil strength and in-situ state of stress.

In cases where the interface friction angle (δ) between concrete and soil is known, the above equations are exchanged as follows:

$$f_{SZ} = K\sigma'_z\tan\delta \quad (12)$$

$$Q_s = \int_0^L K\sigma'_z\tan\delta\, dA \quad (13)$$

where, K is the parameter that combines the lateral pressure coefficient and a correlation factor.

End Bearing in Cohesionless Soil. The value of q_b in cohesionless soil is based on the N_{SPT} (uncorrected SPT N value) value that is defined by the average blow count from standard penetration tests (SPT) in the zone between the base and a depth of 2B.

If N_{SPT} is less than 50 blows/0.3 m (50 blows/ft.), the following equations can be used to calculate q_b *[17]*:

$$q_b = 0.0575\ N_{SPT}\ (\text{MPa}) \leq 2.9\ \text{MPa} \quad (14)$$

$$q_b = 0.60\ N_{SPT}\ (\text{tsf}) \leq 30\ \text{tsf} \quad (15)$$

when N_{SPT} is greater than 50 blows/0.3 m (50 blows/ft.), the O'Neill and Reese method (1999 FHWA design method) recommends that the unit base resistance (q_b) should be calculated using the method for cohesionless intermediate geomaterial (IGM); while in Brown et al.'s method (2010 FHWA design method), the unit base resistance (q_b) in cohesionless soil is limited to the upper-bound value of 30 tsf with N-values exceeding 50.

Skin Friction in Cohesionless IGM. In the O'Neill and Reese method (1999 FHWA design method), the load transfer in skin friction can be estimated using the friction theory *[17]* as follows:

$$f_{SZ} = \sigma'_z\, K_{oz}\, \tan\phi_z \quad (16)$$

where, K_{oz} is the earth pressure coefficient at rest at depth z, and ϕ_z is the internal friction angle at depth z.

End Bearing in Cohesionless IGM. In O'Neill and Reese's method (1999 FHWA design method), if N_{SPT} exceeds 50 blows/0.3 m (50 blows/ft.), the soils can be classified as cohesionless IGM and q_b can be calculated using following equation:

$$q_b = 0.59\left(N_{60}\frac{p_a}{\sigma'_z}\right)^{0.8}\sigma'_z \quad (17)$$

where N_{60} is the average corrected SPT blow counts between the base of the drilled shaft, and 2B below the base for the condition in which 60 percent of the potential energy of the hammer is transferred to the top of the drive string, and p_a is the atmospheric pressure.

Prediction of Load-Settlement Behavior of Drilled Shaft

In the O'Neill and Reese Method (1999 FHWA design method). The load-settlement behavior of a drilled shaft under short-term compression loading can be calculated using the normalized relations proposed by O'Neill and Reese *[17]*. The normalized average trend curves for cohesive and cohesionless soils are shown in Figure 1. The side friction resistance (R_s) developed for each layer at a specific settlement can be calculated using the ratio of the average deflection along the sides of a drilled shaft (w_s) to the shaft diameter (B).

The average deflection along the side of a drilled shaft can be calculated using the following equation:

$$w_s = w_T - \delta_s/2 \quad (18)$$

where, δ_s is the approximate elastic compression of the drilled shaft, and w_T is the estimated deflection of the head of the drilled shaft.

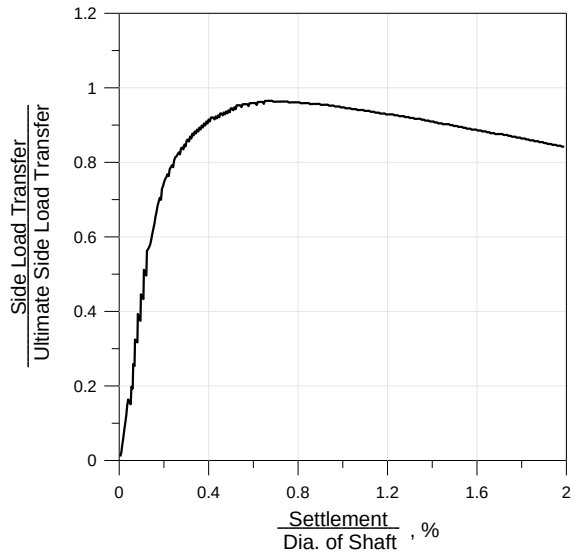

(a) Side load transfer in cohesive soil

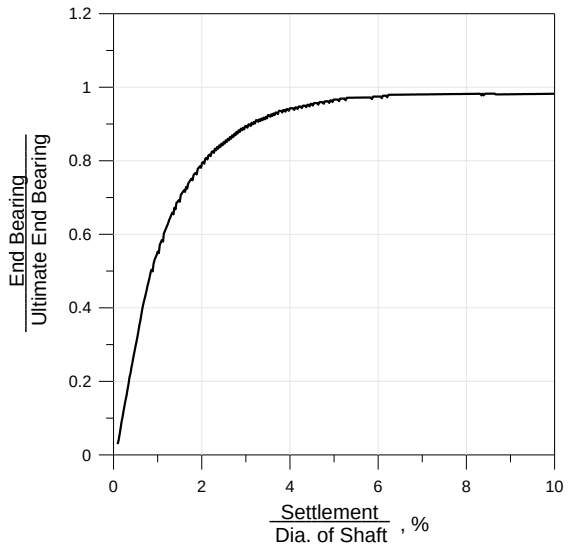

(b) Base load transfer in cohesive soil

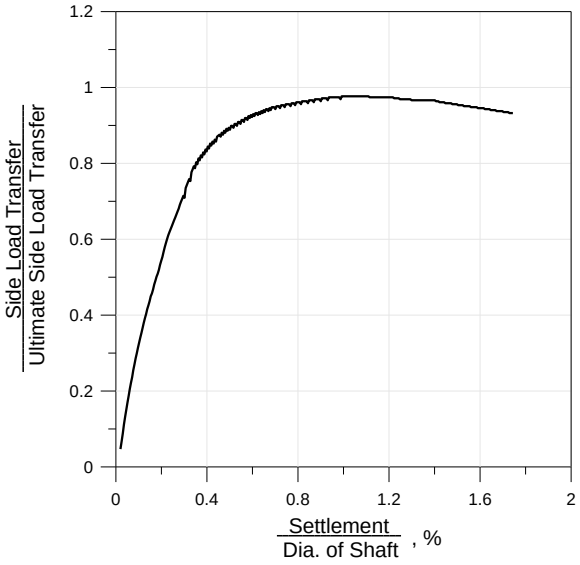

(c) Side load transfer in cohesionless soil

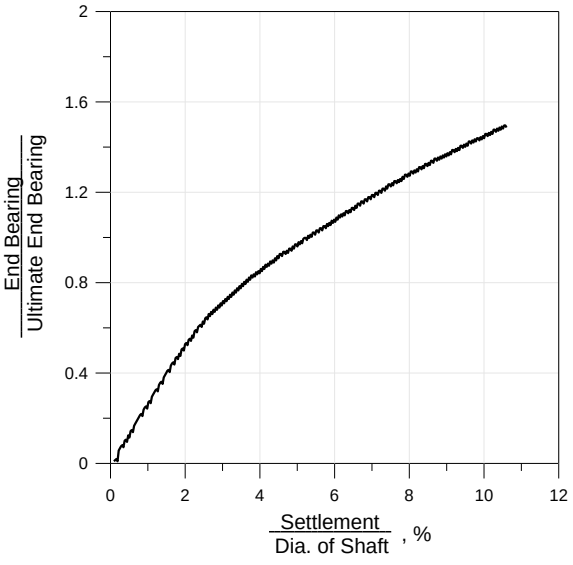

(d) Base load transfer in cohesionless soil

Figure 1
Normalized load transfer representing the average trend value for drilled shaft (after O'Neill and Reese *[17]*)

The developed side friction resistance (R_s) can be obtained from the vertical axis of Figure 1 (a) and (c) for cohesive soils and cohesionless soils, respectively.

The same procedure can be applied to calculate the base resistance developed at a specific settlement. The deflection at the base of a drilled shaft (w_b) can be computed using:

$$w_b = w_T - \delta_s \tag{19}$$

Using the ratio of the deflection at the base to the base diameter (w_b/B_b), the developed base resistance (R_B) can be calculated from the vertical axis of Figure 1 (b) and (d) for cohesive soils and cohesionless soils, respectively.

The developed load (Q_T) at a specific settlement can then be calculated as follows:

$$Q_T = R_B \text{ (developed)} + R_s \text{ (developed)} \tag{20}$$

An example of a predicted load-settlement curve for DS-29 is shown in Figure 2.

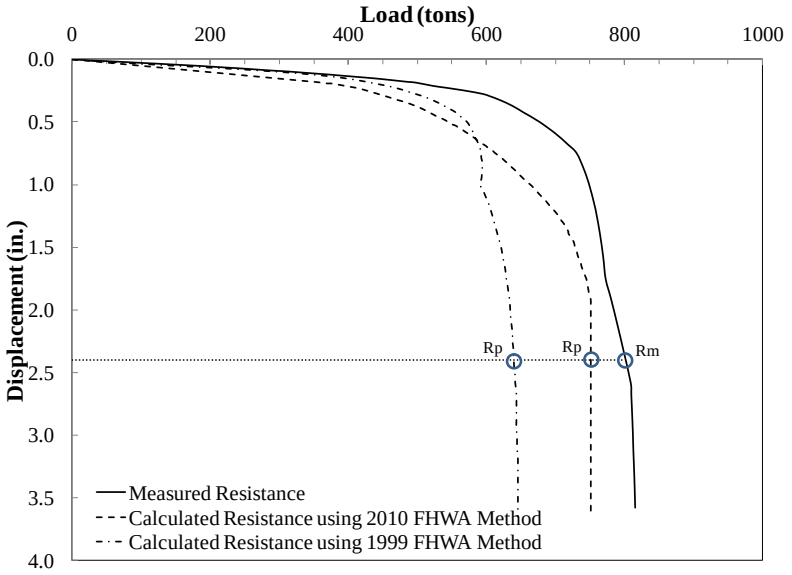

Figure 2
Example of load-settlement analysis and measured value (DS-29)

In Brown et al.'s Method (2010 FHWA design method). The load-settlement behavior of a drilled shaft under short-term compression loading can be calculated using the normalized relations proposed by Chen and Kulhawy [*23*].The normalized average trend curves for cohesive and cohesionless soils are shown in Figure 3. The failure threshold, which corresponds to the axial force at 4.0%B (B: diameter of the drilled shaft), is computed as the sum of nominal side and base resistance as:

$$Q_{\text{failure threshold}} = R_{SN} + \eta R_{BN} \quad (21)$$

where, R_{SN} and R_{BN} are nominal side and base resistance, respectively; $\eta = 1.0$ for cohesive soil and 0.71 for cohesionless soil.

The normalized axial force at a specific settlement can be obtained from the vertical axis of Figure 3 using the ratio of the average deflection (δ) to the shaft diameter (B). An example of a predicted load-settlement curve is shown in Figure 2.

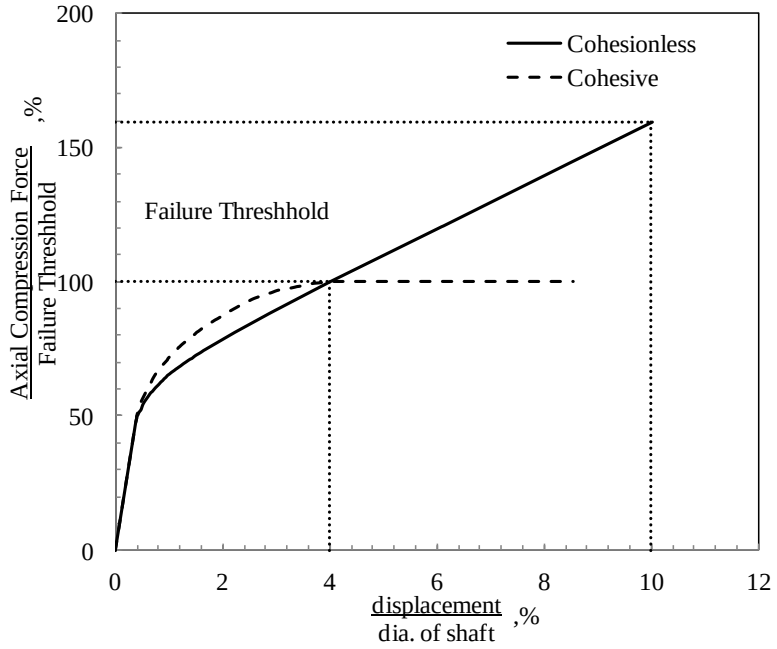

Figure 3
Normalized load transfer representing the average trend value for drilled shaft (after Brown et al. *[17]*)

Measured Load-Settlement Behavior of Drilled Shafts

The O-cell test has been widely used in the United States to determine resistance of drilled shafts. Unlike the conventional top-down load test, the load in an O-cell test is applied at the bottom or near the bottom of drilled shafts via a preinstalled hydraulic cell. During an O-cell load test, the shaft above the cell moves upward, and the shaft below the cell moves downward. As a result, both side friction and end bearing can be measured separately from O-cell test, as shown in Figure 4. The upward load shown in the figure was the net upward load (the O-cell measured upward load minus buoyant weight of the drilled shaft). An equivalent top-down curve can be constructed from the two component curves to investigate the combined total drilled shaft capacity. Construction of the equivalent top-down curve

begins by determining the side shear at an arbitrary deflection point on the side shear-deflection curve (the top curve in Figure 4). The shaft is assumed rigid; its top and bottom move together and have the same movement at this load. The end bearing at the same movement can be determined from the downward curve. By adding the side shear to the mobilized end bearing at the chosen displacement, one can determine a single point on the equivalent top-down curve [*24*]. The complete curve can be obtained by repeating this process. Figure 5 shows an example of the construction of an equivalent top-loaded settlement curve from O-cell test results (Figure 4). The solid line in Figure 5 shows the modified top-down curve to include the additional elastic compression of the shaft.

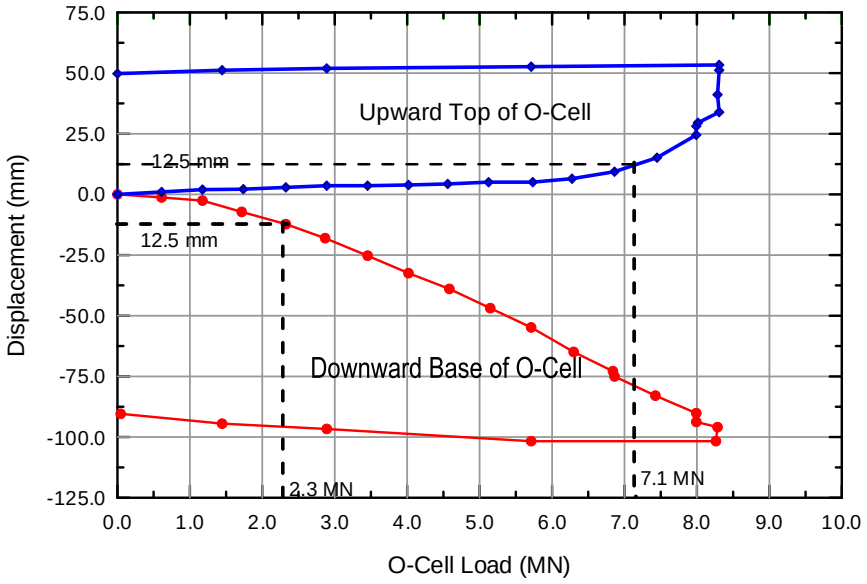

Figure 4
Settlement curves by O-cell

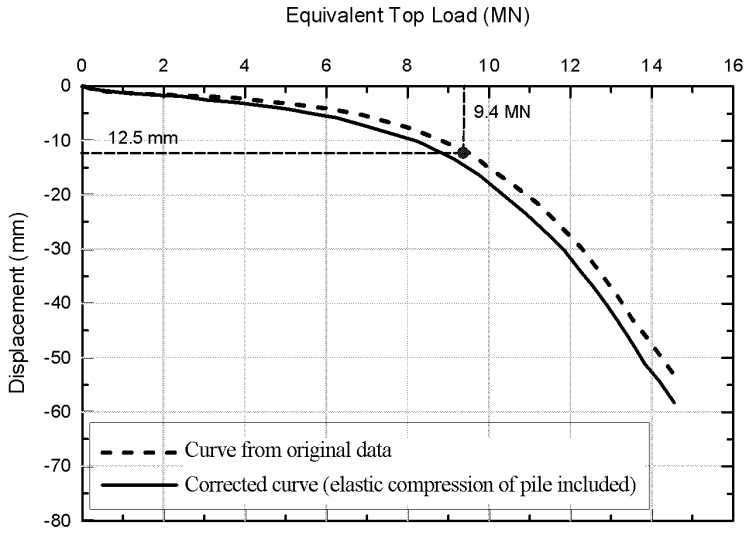

Figure 5
Equivalent top-down settlement curve

According to the comparison study available in the literature, the O-cell method has very similar results to the traditional top-down method in terms of measurement of equivalent top-down load-settlement curve [*24*]. Also the number of drilled shafts tested by top-down load tests in this study is small compared to total drilled shaft tests. Therefore, the difference of load test method has a negligible effect on the calibration of resistance factor for drilled shafts.

LRFD Calibration Using Reliability Theory

The basic concept behind LRFD is illustrated in Figures 6 and 7. Here, the distributions of random load (Q) and resistance (R) values are shown in Figure 6 as normal distributions. The performance limit state function for the state of the structural system can be described as follows:

$$g(R, Q) = R - Q \tag{22}$$

where, R is the resistance of a given structure, which is a random variable, and Q is the applied load, which is also a random variable.

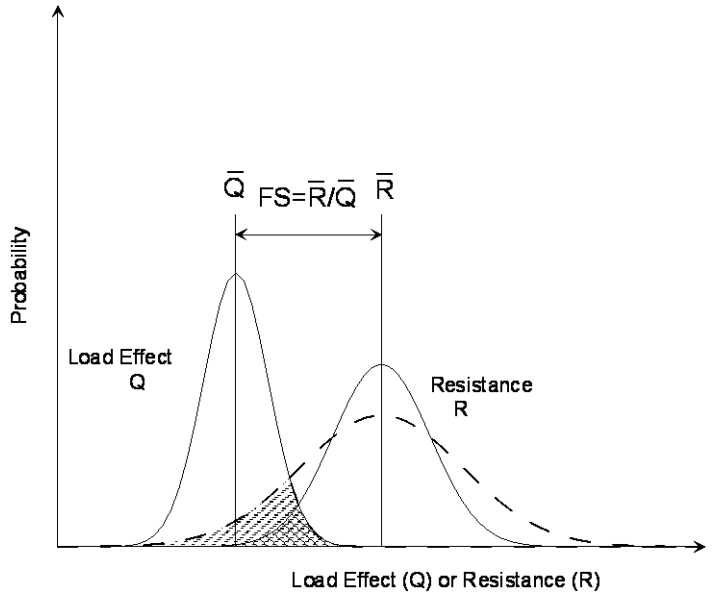

Figure 6
Probability density functions for load effect and resistance

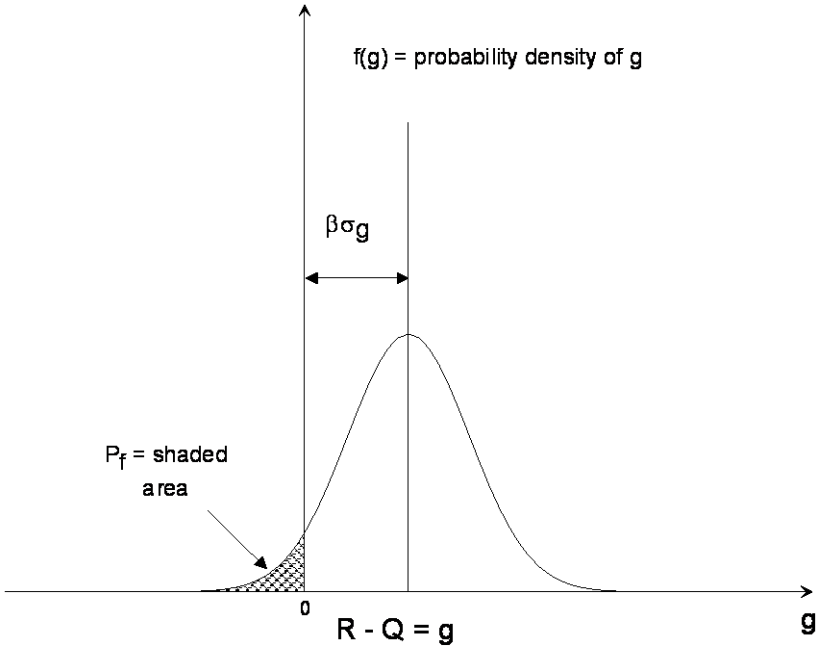

Figure 7
Probability density function of the safety margin *[25]*

The limit state, corresponding to the boundary between desired and undesired performance, would be when $g = 0$. If $g \geq 0$, the structure is safe (desired performance); if $g < 0$, the structure is unsafe (undesired performance).

The probability of failure is then defined as:

$$p_f = p[g(R, Q) < 0] = p[R < Q] \tag{23}$$

In general terms, if X is a random variable such that X = (x_1. x_2. x_3…..x_n) with joint probability density function (PDF) $f_x(x)$ and g(x) is a scalar function of input random variable, then g(x_1. x_2. x_3…..x_n) determines the state of structure such that g(X) > 0 means safe domain and g(X) < 0 indicates failure domain. Also, there exists a limit state surface at the boundary between the two domains defined as an n-dimensional hyper surface {x; g(x) = 0} or the limit state function.

The probability of failure is then given by:

$$P_F = \int_{g(x)\leq 0} f_X(x)dx \tag{24}$$

where, $f_x(x)$ is the probability density function for a random variable X.

Integration is carried out over the failure domain; in other words, the failure probability is the probability of being in the domain of the n-dimensional space bounded by $g(X) \leq 0$.

For a normal distribution of g values, the probability of failure can be equated explicitly to the value of reliability index $\beta = \mu_g/\sigma_g$, where μ_g is the mean value of g and σ_g is the standard deviation of g. The relationship between probability of failure and reliability index can be calculated using the following excel function:

$$p_f = 1 - NORMSDIST(\beta) \tag{25}$$

Also, if the load and resistance values are normally distributed and the limit state function is linear, then β can be determined from the following relation:

$$\beta = \frac{\mu_R - \mu_Q}{\sqrt{\sigma_R{}^2 + \sigma_Q{}^2}} \tag{26}$$

where, μ_R and μ_Q are the mean, and σ_R, and σ_Q are the standard deviation of resistance and load, respectively. If both the load and resistance distributions are lognormal and the limit state function is a product of random variables, then β can be calculated using a closed-form solution reported by Withiam et al. and Nowak as follows *[12* and *25]*:

$$\beta = \frac{\ln\left[\mu_R / \mu_Q \sqrt{\left(1+COV_Q^2\right)/\left(1+COV_R^2\right)}\right]}{\sqrt{\ln\left[\left(1+COV_Q^2\right)\left(1+COV_R^2\right)\right]}} \quad (27)$$

where μ_R is the mean value of the resistance R, and μ_Q is the mean value of the load Q; COV_R and COV_Q are the coefficients of variation for the resistance and load values, respectively.

The limit state function for LRFD design is given below *[5]*:

$$\phi R_n \geq \sum \gamma_i Q_{ni} \quad (28)$$

where, γ_i is the load factor applicable to specific load, Q_{ni} is the specific nominal load, R_n is the nominal resistance, and ϕ is the resistance factor.

The main objective of LRFD is to calibrate the resistance factor so that equation (28) is always fulfilled for the targeted reliability index (β_t). Thus, combining equations (22) and (28), the limit state function for LRFD is shown as follows:

$$g(R, Q) = \sum \gamma_i Q_n - \sum \phi R_n \quad (29)$$

Statistical Characterization of the Collected Data

To perform an LRFD calibration, the performance limit state equations must first be determined. The two limit states that are usually checked in the design of piles and drilled shafts are the ultimate limit state (ULS), or strength limit state, and the serviceability limit state (SLS). Both limit state designs are carried out to satisfy the following criteria *[26]*:

ULS: Factored resistance $\geq$ Factored load effects

SLS: Deformation $\leq$ Tolerable deformation to remain serviceable

It is usually considered that the design of deep foundations is controlled by the strength limit state. Therefore, in the following discussion, only the strength I limit state is considered. The following basic equation is recommended to represent limit states design by AASHTO *[5]*:

$$\phi R_n \geq \sum \eta . \gamma_i . Q_i \quad (30)$$

where, ϕ = resistance factor, R_n = nominal resistance, and η = load modifier to account for effects of ductility, redundancy, and operational importance. The value of η usually is taken as 1.00. The value Q_i = load effect, and γ_i =load factor.

It should be noted the calibrated resistance factors are valid only for the ranges of shaft dimensions (length and diameter) employed in this study.

Considering the load combination of dead load and live load for AASHTO Strength I case, the performance limit equation is as follows *[27]*:

$$\phi R_n = \gamma_D Q_D + \gamma_L Q_L \tag{31}$$

where, Q_D and Q_L are the dead load and live load, respectively; γ_D and γ_L are the load factors for dead load and live load, respectively.

The loads applied to the drilled shafts are traditionally based on superstructure analysis; whereas, the actual loads transfer to substructure is not fully researched. Most researchers employ the load statistics and the load factors from AASHTO LRFD specifications, which were originally recommended by Nowak, to make the deep foundation design consistent with the bridge superstructure design *[11]*. For example, Zhang et al., Kim et al., McVay et al., Abu-Farsakh and Titi, and Abu-Farsakh et al. selected the statistical parameters of dead and live loads, which used in the AASHTO LRFD specifications as follow *[1, 27, 28, 29, 30,* and *31]*:

$$\gamma_L = 1.75 \quad \lambda_L = 1.15 \quad COV_L = 0.18$$
$$\gamma_D = 1.25 \quad \lambda_D = 1.08 \quad COV_D = 0.13$$

where, λ_D and λ_L are the load bias factors (mean ratio of measured to predicted value) for the dead load and live load, respectively. COV_D and COV_L are the coefficient of variation values for the dead load and live load, respectively.

The Q_D/Q_L is the dead load to live load ratio, which varies depending on the span length *[32]*. In this research, Q_D/Q_L of 3 is used for calibration, since the calibration is insensitive to Q_D/Q_L ratio above 3.

The resistance statistics were calculated in terms of the bias factors. The resistance bias factor is defined as the ratio of the measured shaft resistance over the predicted shaft resistance, i.e.,

$$\lambda_R = \frac{R_m}{R_p} \tag{32}$$

where, R_m = measured resistance and R_p = predicted nominal resistance.

Monte Carlo Simulation Method

For more complicated limit state functions, the application of the general statistical method for the calculation of the reliability index is either extremely difficult or impossible. Under this circumstance, Monte Carlo simulation provides the only feasible way to determine the reliability index or the probability of failure.

The Monte Carlo method is a technique utilizing a random number generator to extrapolate cumulative density function (CDF) values for each random variable. Extrapolation of CDF makes estimating β possible; otherwise, a limited quantity of data has restricted the reliable estimate of β. Once reliability index, β, is estimated, the probability of failure can be estimated by assuming the distribution of g(x). The steps of Monte Carlo simulation method are as follows:

1. Select a trial resistance factor (ϕ). Generate random numbers for each set of variables. Here there are three variables (resistance and dead load and live load bias factor), so three sets of random variables have to be generated independently for each case. The number of simulation points required is found using the following equation:

$$N = \frac{1 - P_{true}}{V_p^{\,2} * (P_{true})} \tag{33}$$

where, P_{true} is the lowest magnitude of probability that is to be determined using Monte Carlo simulation, and V_p is the desired coefficient of variation of the simulation result. For estimating probability as low as 10^{-2} and keeping variance under 10 percent, the number of points to be generated in Monte-Carlo simulation is 9900.

For each lognormal variable, sample value x_i is estimated as:

$$x^*_i = \exp(\mu_{lnx} + z_i \sigma_{lnx}) \tag{34}$$

where, $\sigma^2_{\ln x} = \ln(V_x^2 + 1)$ and $\mu_{\ln x} = \ln(\mu_x) - \frac{1}{2}\sigma^2_{\ln x}$

In the above expressions, μ_x and V_x are the arithmetic mean and variance of x; μ_{lnx} and σ_{lnx} are equivalent lognormal mean and standard deviation of ln(x); and z_i = NORMSINV(RAND()) is the random standard normal variable generated using EXCEL function.

2. Define the limit state function.

$$Q = \lambda_D\, Q_D + \lambda_L\, Q_L \tag{35}$$

From (31) and (35)

$$g(R,Q) = \left(\frac{\gamma_D Q_D + \gamma_L Q_L}{\phi}\right)\lambda_R - \left(\lambda_D\, Q_D + \lambda_L\, Q_L\right) \tag{36}$$

Equation (36) can be rearranged as:

$$g(R,Q) = \left(\frac{\gamma_D + \gamma_L \kappa}{\phi}\right)\lambda_R - \left(\lambda_D + \lambda_L\, \kappa\right) \tag{37}$$

Where $\kappa = Q_L/Q_D$.

3. Find the number of cases where $g(x_i) \le 0$. The probability of failure is then defined as:

$$Pf = \frac{\text{count}(g \le 0)}{N} \tag{38}$$

and reliability index β is estimated as:

$$\beta = \Phi^{-1}(Pf) \tag{39}$$

4. If the calculated reliability index (β) is different from the selected target reliability index (β_T), the trial resistance factor (ϕ) in step 1 should be changed and iteration needs to be done until $|\beta - \beta_T|$ < tolerance (0.01 in this study).

Drilled Shaft Load Test Database

In a previous research project, an extensive search was conducted to collect all available drilled shaft test data in Louisiana and Mississippi *[2]*. A total of 26 drilled shaft cases, which meet the FHWA 5%B (B: diameter of the drilled shaft) settlement criterion, were collected at that time. Since the completion of that project, eight new drilled shaft test data were added to the database in this report. The final combined database has 34 cases as shown in Table 4 that represents the typical subsurface soils in Louisiana. The measured and predicted tip, side, and total resistance, which are based on FHWA 5%B interpretation criterion, are presented in Table 5. The approximate geographical locations of drilled shafts for the final selected database are shown in the maps of Figure 8.

The diameter of drilled shafts included in the database ranges from 2 ft. to 6 ft. and length ranges from 35.1 ft. to 138.1ft. Fifteen cases collected from Mississippi and fifteen cases collected from Louisiana were O-cell tests; In addition, 4 cases in Louisiana were conventional top-down load tests. The soils encountered in the investigated database include silty clay, clay, sand, clayey sand, and gravel. Most of the soil strata are not homogenous and contain inter-bedded layers. The soil type description in Table 2 is a brief approximation/description for the entire shaft length/base.

Compilation of Drilled Shaft Test Data

All collected drilled shaft load test reports were compiled along with information and data regarding the project (soil stratification and properties, drilled shaft characteristics, load test data, etc.) and then processed and transferred from each load test report to tables, forms, and graphs. The following data and information were collected and compiled for each drilled shaft load test report.

The soil data consists of information on the soil boring location (station number); soil stratigraphy; unit weight; laboratory testing (shear strength, physical properties, etc.); and in-situ test results (e.g., Standard Penetration Test (SPT) for cohesionless soil). An example figure of soil condition for each shaft location is shown in Figure 9. The summary of geotechnical data for all projects investigated in this research is presented in Appendix A.

As shown in Table 4, a few cases have only either sand or clay type of soil. Most sites have layered soils. So the soil type for this database can be classified as mixed soils. The total resistance factor calibrated in this study is therefore considered for mixed soil.

Table 4
Summary of the characteristics of the investigated drilled shafts

I.D.	Location	Dia.	Length	Soil Type	Load Test
DS-01	Caddo, LA	2.5	53.1	Silty Clay, Sand Base	Top Down
DS-02	Caddo, LA	2.5	35.1	Clay and Sand with Sand Base	Top Down
DS-03	E. Baton Rouge, LA	3	54.1	Clayey Silt, Sand Base	O-cell
DS-04	Ouachita, LA	5.5	76.1	Silty Sand with Sand Base	O-cell
DS-05	Calcasieu, LA	6	86.9	Stiff Clay with Clay Base	O-cell
DS-06	Winn, LA	2.5	77.4	Sand Clay with Sand Base	O-cell
DS-07	Winn, LA	2.5	65	Fully Sand with Clay Base	O-cell
DS-08	E. Baton Rouge, LA	2.5	49.9	Silt,Clay with Clay Base	O-cell
DS-09	Beauregard, LA	5.5	40.7	Clay,Silt with Clay Base	O-cell
DS-10	Caddo, LA	3	44.9	Clay, Silty Clay with Clay Base	Top Down
DS-11	Caddo, LA	3	62	Clay with Sand Base	Top Down
DS-12	Union, MS	4.5	49.9	Fully SAND	O-cell
DS-13	Union, MS	4	73.1	Sand with Clay, Sand base	O-cell
DS-14	Washington, MS	4	123	CLAY/SAND-Sand Base	O-cell
DS-15	Washington, MS	4	138.1	SAND	O-cell
DS-16	Washington, MS	4	119.1	CLAY, SAND with SAND Base	O-cell
DS-17	Washington, MS	5.5	94.1	SAND/CLAY with SAND Base	O-cell
DS-18	Washington, MS	4	96.1	SAND with Sand Base	O-cell
DS-19	Washington, MS	4	82	SAND/GRAVEL/Sand Base	O-cell
DS-20	Washington, MS	4	97.1	Sand with Clay Interlayer and	O-cell
DS-21	Washington, MS	4	82	SAND with SAND Base	O-cell
DS-22	Lee, MS	4	89	Clay	O-cell
DS-23	Forrest, MS	6	47.9	SAND	O-cell
DS-24	Perry, MS	4.5	64	SAND/CLAY, Clay Base	O-cell
DS-25	Wayne, MS	4	64	Sand with Clay Base	O-cell
DS-26	Madison, MS	2	40	CLAY with Clay Base	O-cell
DS-27	E. Baton Rouge, LA	4	67.5	Fully Clay, Clay Base	O-cell
DS-28	E. Baton Rouge, LA	2.5	81.5	Fully Clay, Clay Base	O-cell
DS-29	E. Baton Rouge, LA	4	77.5	Fully Clay, Clay Base	O-cell
DS-30	Caddo, LA	6	43	Clay, Sand with Sand Base	O-cell
DS-31	Caddo, LA	5.5	47.5	Fully Sand wth Sand Base	O-cell
DS-32	Caddo, LA	5.5	48	Sand, Clay with Sand Base	O-cell
DS-33	Caddo, LA	5.5	53.85	Clay, Sand with Sand Base	O-cell
DS-34	Caddo, LA	5.5	51.12	Clay, Sand with Sand Base	O-cell

Table 5
Summary of total, tip, and side resistance of the investigated drilled shafts

ID NO	2010 FHWA Method			1999 FHWA Method			Measured		
	Tip	Side	Total	Tip	Side	Total	Tip	Side	Total
DS-01	148	436	584	174	312	485	-[*]	-[*]	1007[$]
DS-02	147	308	455	210	172	382	-[*]	-[*]	784[&]
DS-03	55	271	326	51	196	247	84	260	344[$]
DS-04	328	1774	2102	307	1264	1571	496	1064	1560[$]
DS-05	196	1029	1225	186	859	1045	550	1200	1750[$]
DS-06	143	696	839	197	324	521	413	475	888[$]
DS-07	8[#]	580	588	8[#]	382	390	384[#]	286	670[$]
DS-08	95	282	377	87	238	325	69	216	285[&]
DS-09	115	451	566	74	381	455	313	218	531[$]
DS-10	24	303	327	22	249	270	-[*]	-[*]	405[&]
DS-11	72	416	488	67	351	418	-[*]	-[*]	428[$]
DS-12	363	703	1066	338	543	881	656	575	1230[&]
DS-13	332	700	1032	315	585	900	492	529	1020[&]
DS-14	265	1163	1428	254	666	920	681	834	1515[$]
DS-15	377	1254	1631	409	638	1047	695	718	1413[&]
DS-16	302	1777	2079	294	1316	1610	667	610	1277[$]
DS-17	235	1743	1978	223	1407	1630	1196	949	2145[&]
DS-18	119	1340	1459	113	747	860	609	473	1082[$]
DS-19	301	1166	1467	290	920	1210	773	485	1258[$]
DS-20	128	808	936	126	488	614	575	534	1109[&]
DS-21	219	940	1159	211	629	840	449	426	875[$]
DS-22	344	2214	2558	329	1771	2100	945	1258	2203[$]
DS-23	291	1294	1585	279	1002	1280	784	518	1302[$]
DS-24	198	815	1013	189	526	715	266	232	498[$]
DS-25	163	437	600	153	343	496	210	235	445[$]
DS-26	61	254	315	62	200	262	91	125	215[$]
DS-27	127	298	425	122	238	360	255	294	549[$]
DS-28	86	369	455	82	302	384	156	415	570[$]
DS-29	253	498	751	242	397	639	302	500	802[$]
DS-30	848	1583	2431	895	1019	1914	1472	1294	2766[$]
DS-31	613	1261	1874	585	952	1537	1251	1092	2343[$]
DS-32	713	611	1324	765	373	1139	332	350	682[$]
DS-33	713	794	1507	776	571	1347	507	380	887[$]
DS-34	428	721	1149	412	490	902	739	439	1178[$]

[*]Top-down load tests; [#]This case was excluded from the tip resistance factor calibration; [$]extrapolated value; [&]actual measured value

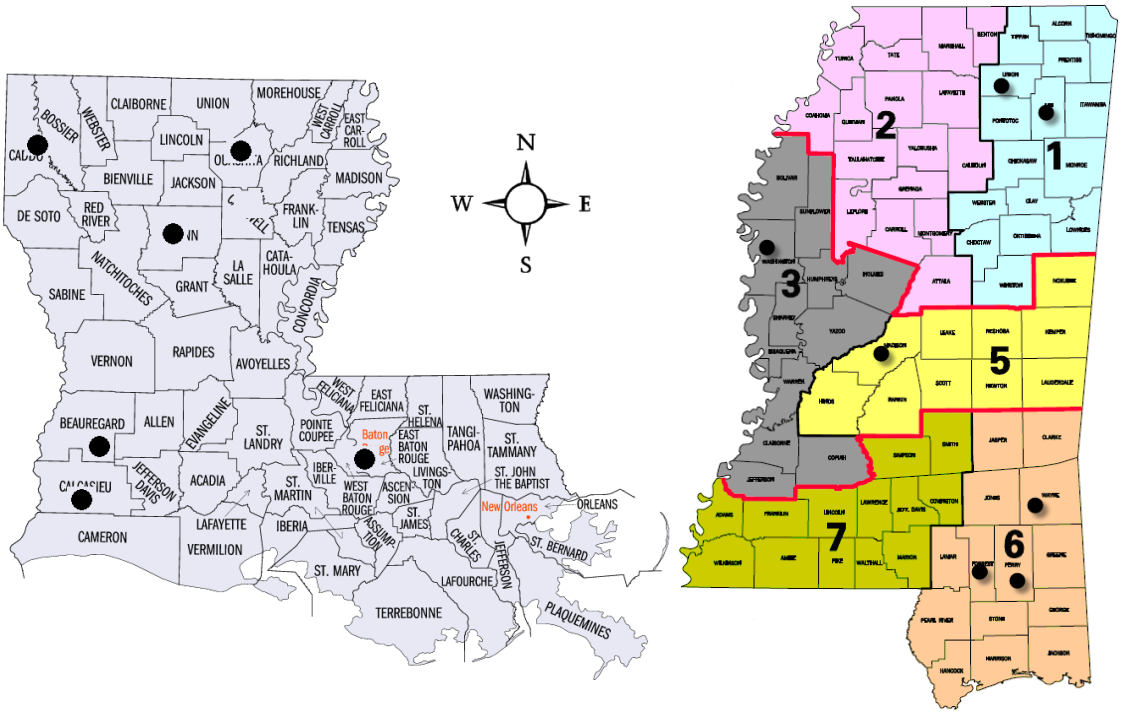

Figure 8
Approximate locations of the investigated drilled shafts

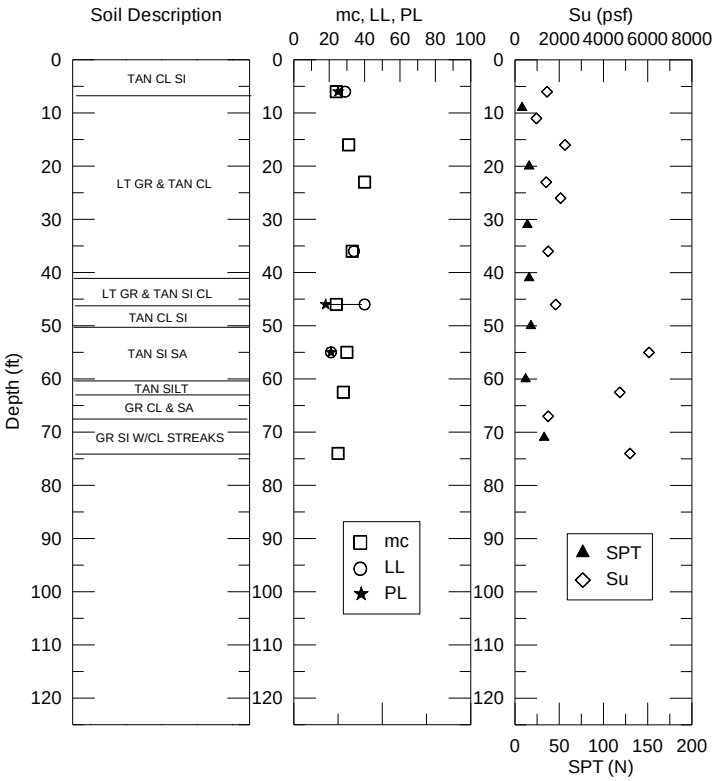

Figure 9
An example summary of geotechnical data for a tested drilled shaft (DS03)

Nominal Resistance of Drilled Shafts from Load Test

In this study, a total dataset of 34 drilled shaft cases constructed in silty clay, sand, sand-clay, and mixed soils were collected from the project libraries. The nominal resistance of a drilled shaft was defined as the test load corresponding to a settlement of 5 percent of the shaft diameter or the plunging load whichever occurs first *[16]*. Selection of this criterion was based on a recommendation from a previous study performed by Paikowsky for LRFD calibration consistency *[4]*. Statistical analysis showed that the FHWA's "5%B" method produced the closest and most consistent capacities with the mean value of the capacities determined by seven methods, which has been further confirmed and used by Zhang et al., Liang and Li, and Abu-Farsakh et al. *[13, 33,* and *34]*.

Nominal resistance of drilled shafts at a settlement of 5 percent of the shaft diameter can be determined by interpreting the calculated results. The measured nominal resistance can be obtained from measured load-settlement curves by O-cell tests or top-down conventional tests. Figure 2 shows an example of the determination of shaft nominal resistance according to the criterion thereof. Some of the measured settlements did not meet the 5 percent of the shaft diameter criterion. Therefore, it was necessary to extrapolate the measured load-settlement curves. Extrapolation of the measured load-settlement curves has been carefully performed on some cases that have settlements close to the settlement criterion to determine the estimated load at a settlement of 5 percent of the shaft diameter. After a comparison study of several extrapolation techniques (hyperbolic, Chin's method, cubic spline, and exponential curve fitting) the exponential curve fitting was chosen as the best method for extrapolation. The extrapolation has been examined to ensure a most reasonable estimation. Figure 10 shows an example of extrapolating the measured load-settlement curve using the proposed exponential curve fitting method. Data that needed large extrapolation were discarded. The final results of drilled shaft test database are summarized earlier in Table 4.

Separation of Resistance Components

As mentioned earlier, among the selected 34 drilled shaft test cases (Dataset 1), 30 drilled shaft cases were tested using O-cells. For those 30 cases (Dataset 2), the measured tip and side resistance components for each drilled shaft can be determined separately from O-cell results (Appendix B) using the FHWA interpretation criterion.

The determined measured total resistance of drilled shafts can be determined from the corrected equivalent top-down settlement curve (solid line in Figure 5) using the FHWA interpretation criterion as described in Figure 2. The O-cell test results can provide separate

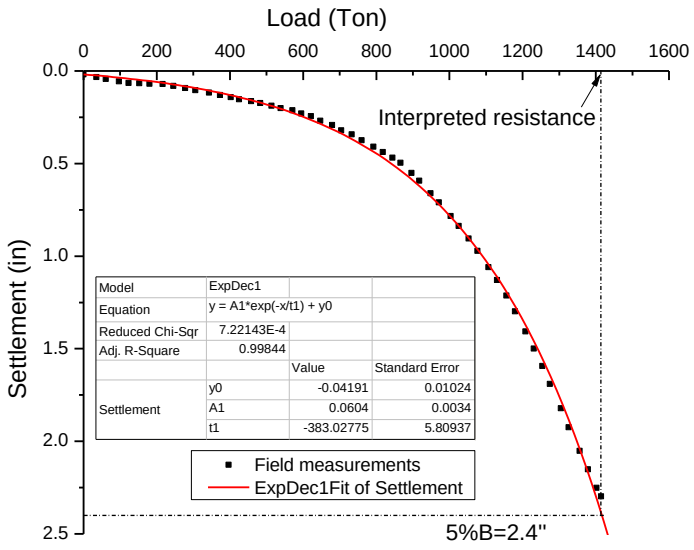

Figure 10
An example of extrapolation of measured top-down load-settlement curve

side friction and tip resistance as described in Figure 4. The side friction is the net upward force which equals the friction resistance as in a top-down load test based on O-cell test assumptions. The interpreted side resistance or tip resistance is determined from the measured curves from O-cell tests at a settlement of 5%B minus elastic compression (Figure 5). The elastic compression can be calculated or measured from the plots that are available in load test reports. For drilled shafts that need extrapolation, either the side friction or tip resistance needs to be determined by such an approach. Usually, the component with the larger displacement was preferred to determine the component resistance at 5%B settlement. Once one resistance component is estimated, the other component can be determined as the difference between the total resistance and the known component. This can help minimize the possible errors induced by extrapolation of load-settlement curves if needed. If neither side nor tip displacement reaches 5%B, the component with larger displacement will be extrapolated using hyperbolic method. The interpretation results will be presented in a later section.

DISCUSSION OF RESULTS

Predicted and Measured Drilled Shaft Resistance

Statistical analyses were performed on two sets of data: total resistance for 34 test cases (Dataset 1) including 4 top-down tests and 22 O-cell tests and total separated resistance for 30 O-cell test cases (Dataset 2). Total resistance of drilled shafts was analyzed using both datasets to compare the effect of the 4 top-down test cases on the final calibrated resistance factor. Statistical analyses were conducted to evaluate both the 2010 FHWA design method (i.e., Brown et al. method) and the 1999 FHWA design method (i.e., O'Neill and Reese method).

Total Resistance Analyses

From the results of Table 4, a statistical analysis was first conducted on the collected database of 34 drilled shaft cases to evaluate the statistical characteristics of the total nominal drilled shaft resistance. The corresponding resistance bias factor ($\lambda_R=R_m/R_p$), which is the mean ratio between the measured resistance and the predicted resistance (R_m/R_p), was determined. The standard deviation (σ) and the coefficient of variation (COV) of the bias (λ_R) were also calculated and summarized in Table 6 and Table 7 for the 2010 FHWA design method and for the 1999 FHWA design method, respectively.

Table 6
Statistical analysis of the 2010 FHWA drilled shaft design method (34 cases)

Summary Statistics				Best fit calculations
R_m/R_p			R_p/R_m	
Mean (λ_R)	σ	COV	Mean	R_{fit}/R_m
0.99	0.30	0.30	1.10	1.02

Table 7
Statistical analysis of the 1999 FHWA drilled shaft design method (34 cases)

Summary Statistics				Best fit calculations
R_m/R_p			R_p/R_m	
Mean (λ_R)	σ	COV	Mean	R_{fit}/R_m
1.27	0.38	0.30	0.87	0.79

Figure 11 and Figure 12 present the comparison between the measured and predicted total drilled shaft resistances using the 2010 FHWA design method and 1999 FHWA design method, respectively. A simple regression analysis was also conducted to obtain a line of best fit of the predicted/measured drilled shaft resistances. The mean ratio of R_p/R_m equals 1.10 for the 2010 FHWA design method, while the slope of the best fit line is 1.02 and

indicates a 2 percent overestimation of shaft resistance using the 2010 FHWA design method in Louisiana soils. On the other hand, the mean ratio of R_p/R_m equals 0.87 for the 1999 FHWA design method, while the slope of the best fit line is 0.79 and indicates a 21 percent underestimation of shaft resistance using the 1999 FHWA design method in Louisiana soils. The COV of R_m/R_p for both 2010 and 1999 FHWA design method is 0.30, which agrees well with the COV for the O'Neill and Reese design method (0.27 - 0.74) as reported by Paikowsky *[4]*.

Figure 13 and Figure 14 present the histogram and the normal and lognormal distributions of bias of the drilled shaft (R_m/R_p) using the 2010 and 1999 FHWA design methods, respectively. Figure 15 and Figure 16 illustrate the CDFs of the resistance bias for the 2010 and 1999 FHWA design method, respectively. As shown in these figures, for 2010 FHWA design method, lognormal distribution matches the histogram and the CDF of drilled shaft data better than the normal distribution; The goodness of fit test (Anderson-Darling test) showed that both normal and lognormal distribution provides a good fit to the observed data at a significance level 0.05. For the 2010 FHWA design method, lognormal distribution (a p-value of 0.60) gives a better fit than the normal distribution (a p-value of 0.43), while for the 1999 FHWA design method, the opposite was observed with a p-value of 0.54 for lognormal distribution and 0.90 for normal distribution. However, to be consistent, the lognormal distribution was used here in the reliability calibration analysis. The predicted lognormal distribution, obtained by the "best fit to tail" method recommended by Allen et al., is also shown in Figure 15 *[36]*. For the 2010 FHWA design method, the mean and standard deviation of λ_R obtained from the fit-to-tail curve are 1. 01 and 0.37, respectively; while the mean and standard deviation of λ_R obtained from the fit-to-tail curve for the 1999 FHWA design method, are 1.33 and 0.52, respectively The mean and standard deviation of λ_R obtained by both statistic calculation and best fit to tail were used in the LRFD calibration as are described in the following section.

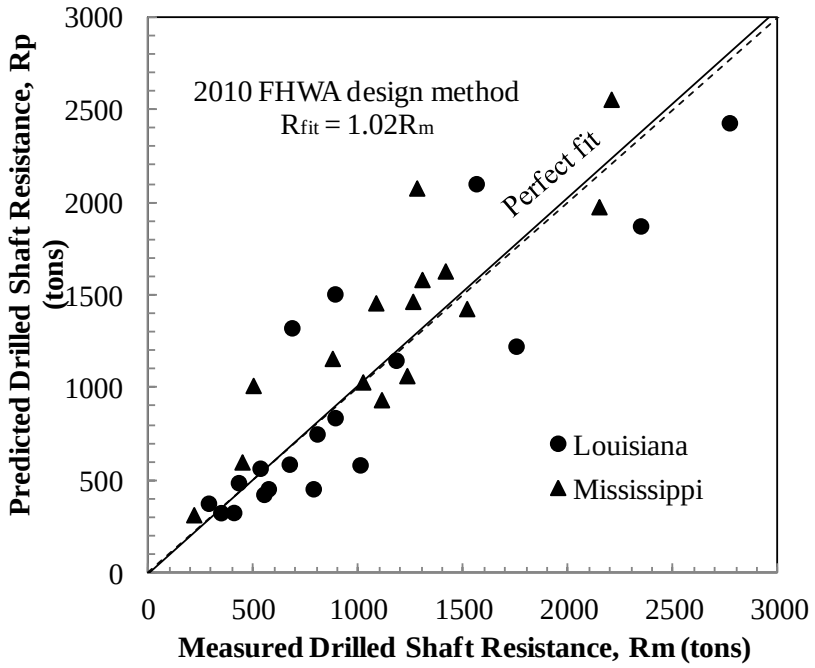

Figure 11
Measured (R_m) versus predicted (R_p) drilled shaft resistance using 2010 FHWA design method

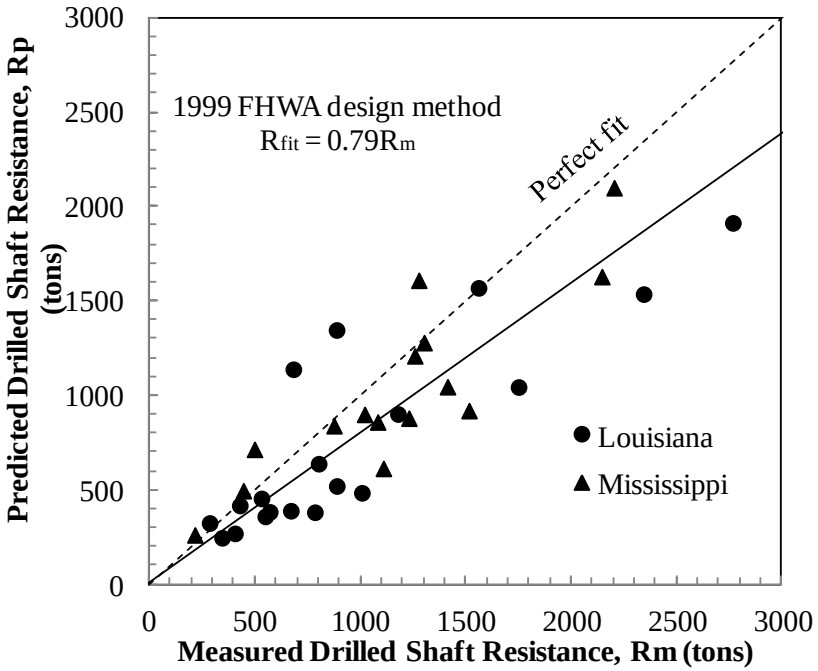

Figure 12
Measured (R_m) versus predicted (R_p) drilled shaft resistance using 1999 FHWA design method

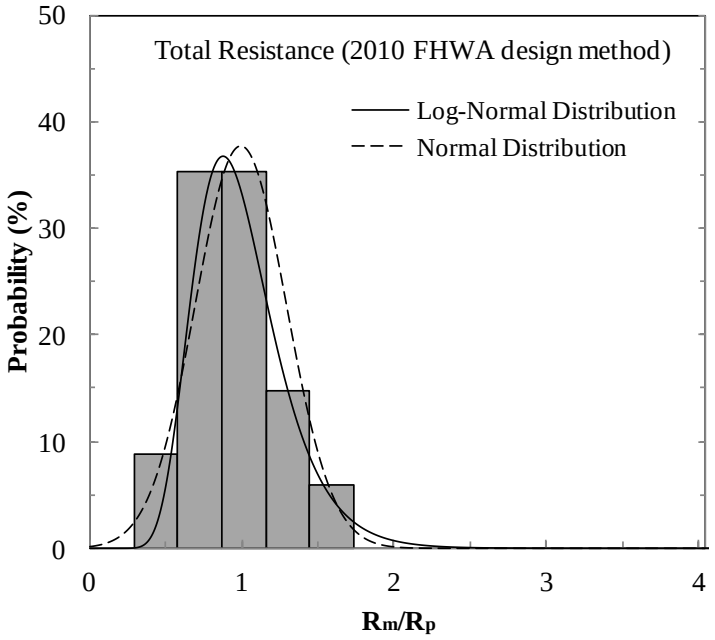

Figure 13
Histogram and probability density function of resistance bias for 2010 FHWA design method

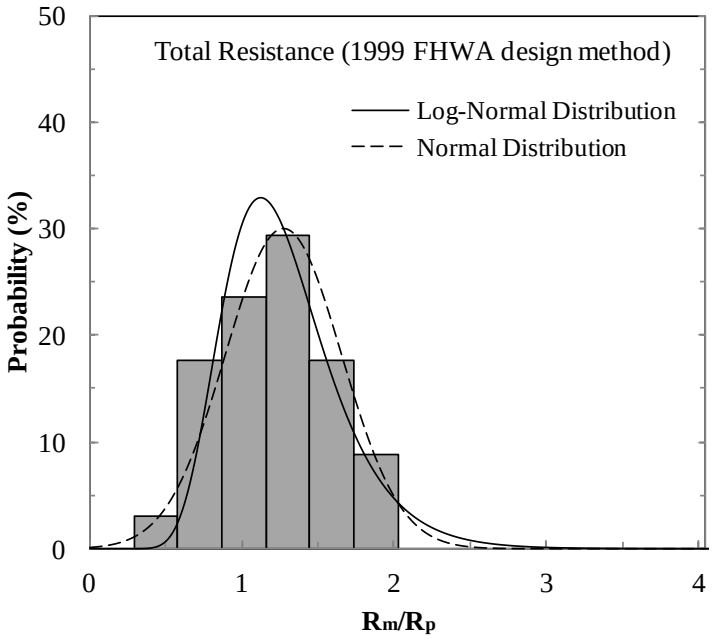

Figure 14
Histogram and probability density function of resistance bias for 1999 FHWA design method

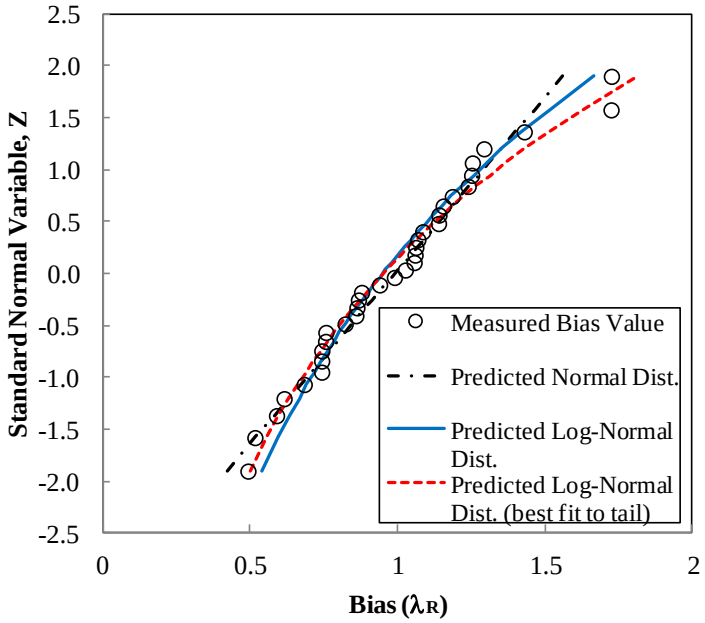

Figure 15
Cumulative distribution function (CDF) of bias values (2010 FHWA design method)

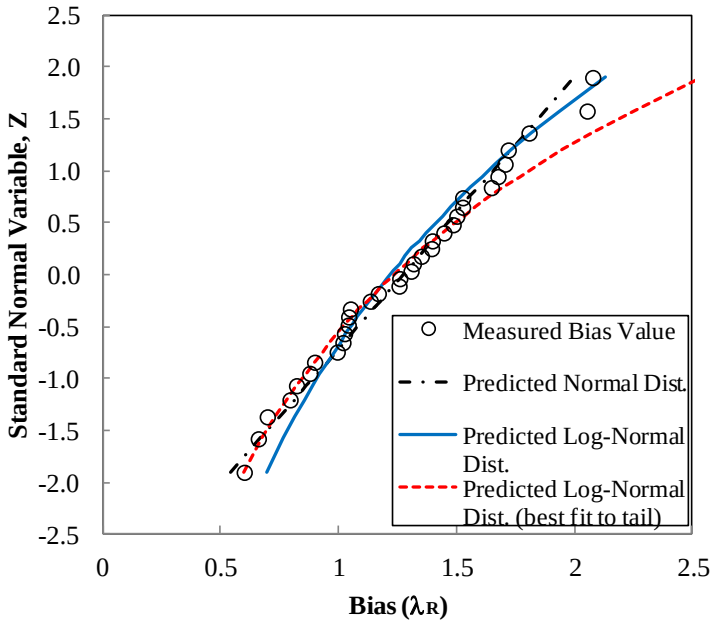

Figure 16
Cumulative distribution function (CDF) of bias values (1999 FHWA design method)

Separate Resistance Analysis

The tip and side resistance contributions of the investigated 30 O-cell drilled shaft cases are plotted in Figure 17. The average contribution of the side resistance to the total resistance is

about 52 percent. Both side resistance and tip resistance contribute significantly to the total resistance of investigated drilled shafts. However, both 2010 and 1999 FHWA design methods significantly underestimate tip resistance, as indicated in Figure 18 and Figure 19. The majority of total resistance (77 percent for the 2010 FHWA design method and 71percent for the 1999 FHWA design method) comes from side resistance. Tip resistance only contributes 23 percent of total resistance for the 2010 FHWA design method and 29 percent for the 1999 FHWA design method. The measured resistances are compared to the predicted resistances using the 2010 FHWA design method, as shown in Figure 20 and Figure 21 for tip and side resistances. The comparison between the measured resistances and the predicted resistances using the 1999 FHWA design method is shown in Figure 22 and Figure 23 for tip and side resistances. The average predicted total resistances using the 2010 FHWA design method and the 1999 FHWA design method are 103 and 80 percent of the measured total resistance as shown in Figure 26 and Figure 27, respectively, which are almost the same as the value fit using 34 cases, as shown in Figure 11 and Figure 12. The underestimation is observed for tip resistance as indicated with predicted resistances of only 47 percent of the measured resistance by using both 2010 FHWA design method and 1999 FHWA design method. The overestimation of side resistance is shown in Figure 21 and Figure 23 with predicted resistance of 154 and 110 percent of the measured resistance using 2010 FHWA design method and 1999 FHWA design method.

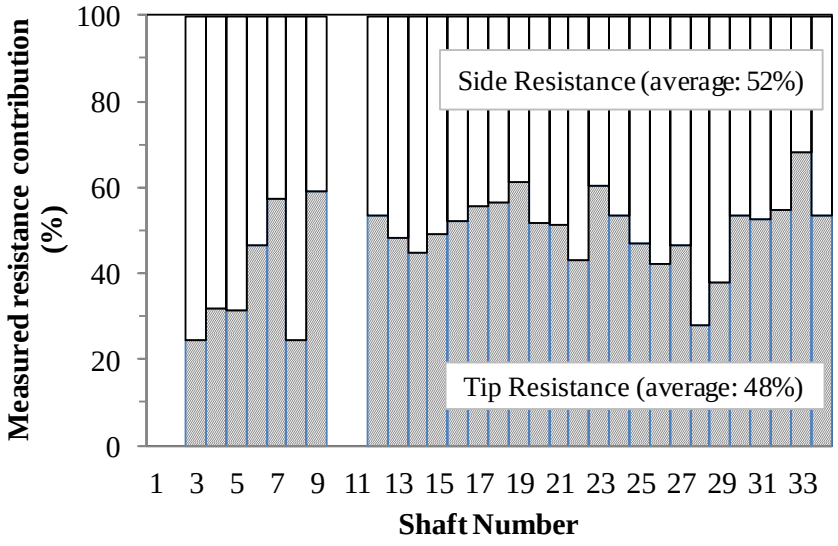

Figure 17
Contribution of measured side and tip resistances

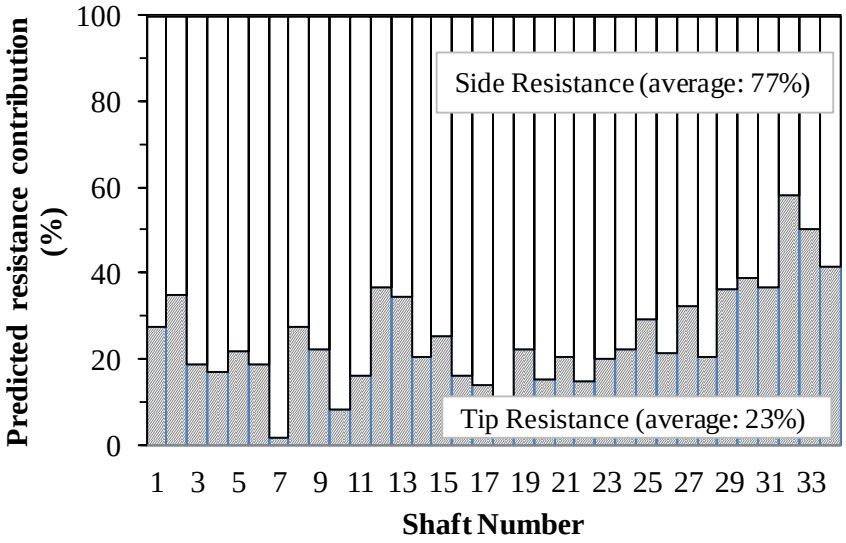

Figure 18
Contribution of predicted side and tip resistances using 2010 FHWA design method

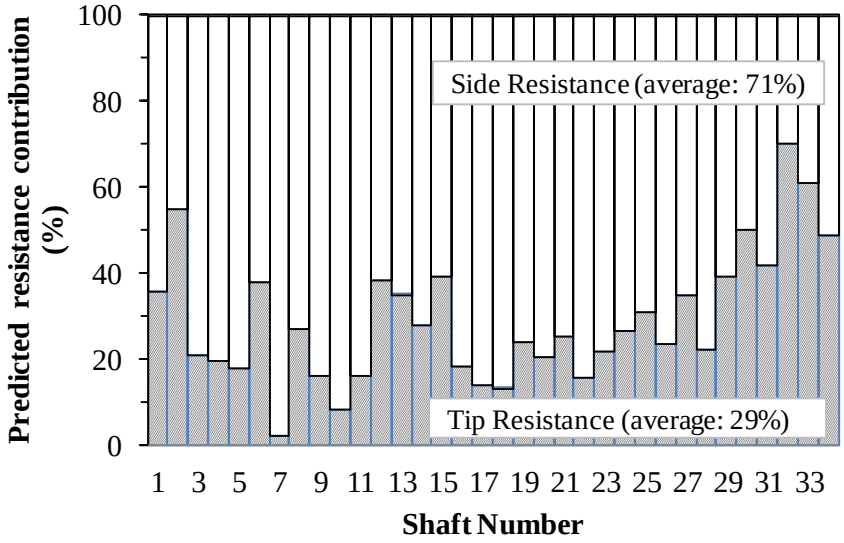

Figure 19
Contribution of predicted side and tip resistances using 1999 FHWA design method

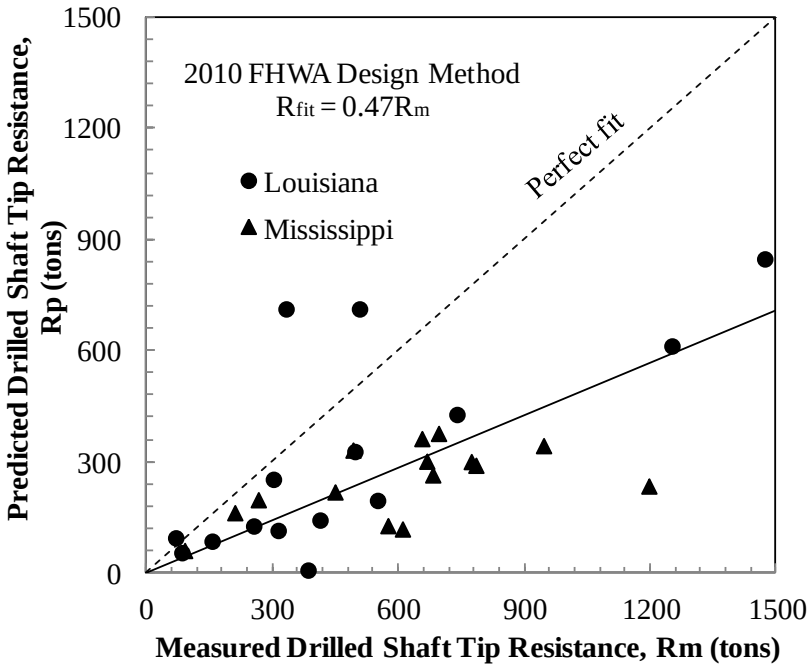

Figure 20
Measured versus predicted tip resistance of drilled shafts using 2010 FHWA design method

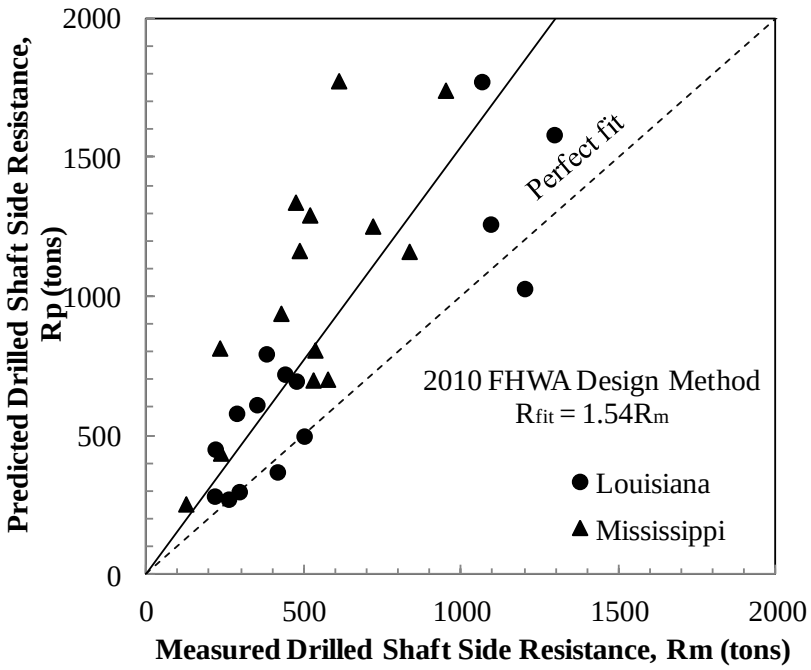

Figure 21
Measured and predicted side resistance of drilled shafts using 2010 FHWA design method

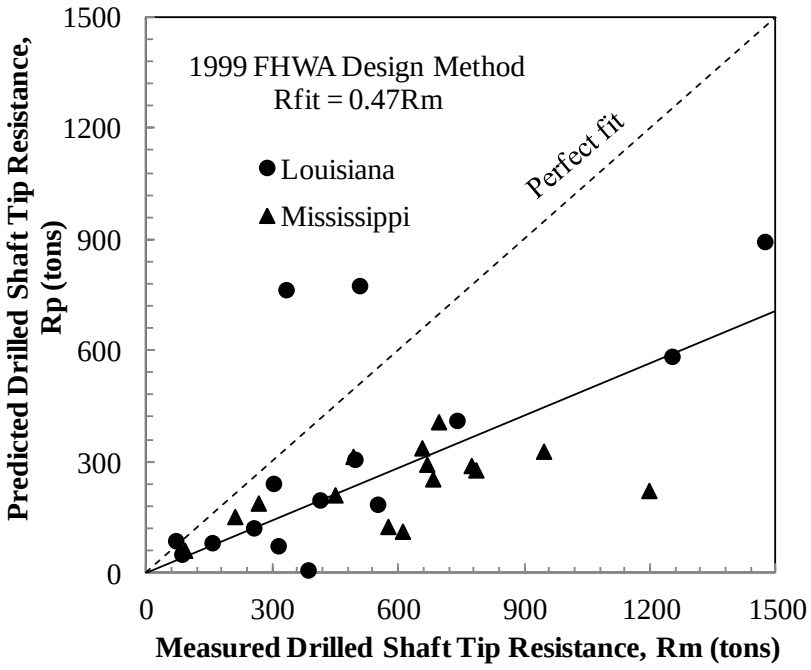

Figure 22
Measured versus predicted tip resistance of drilled shafts using 1999 FHWA design method

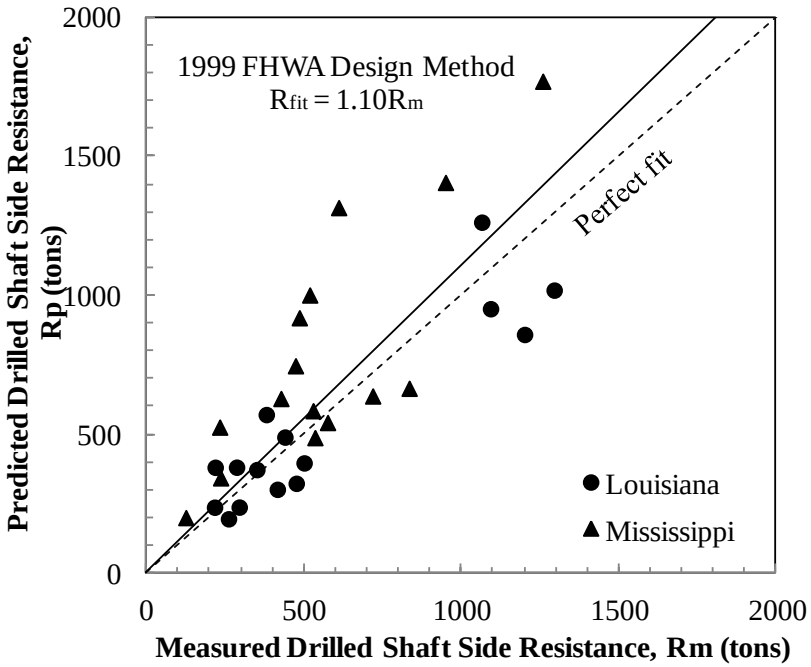

Figure 23
Measured and predicted side resistance of drilled shafts using 1999 FHWA design method

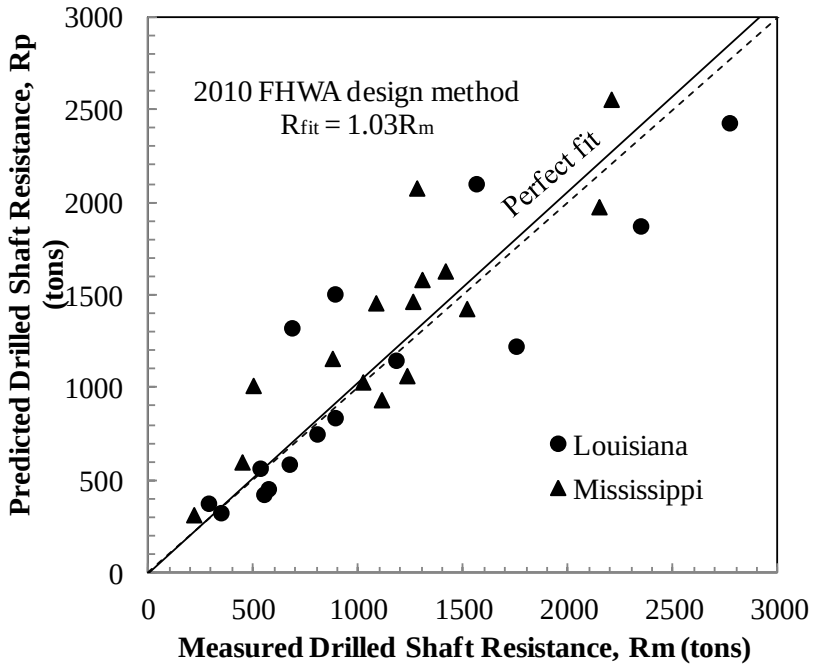

Figure 24
Measured (R_m) versus predicted (R_p) drilled shaft resistance using 2010 FHWA design method (O-cell)

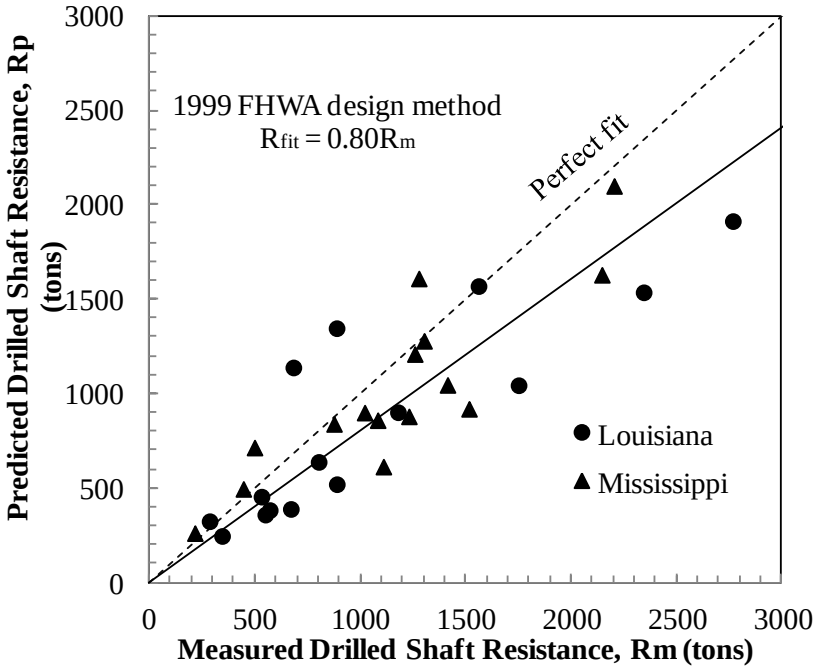

Figure 25
Measured (R_m) versus predicted (R_p) drilled shaft resistance using 1999 FHWA design method (O-cell)

A statistical analysis was conducted on the interpreted resistances to evaluate the statistical characteristics of the nominal drilled shaft resistances of different components. The

maximum, minimum, mean (μ), and COV of the bias for different resistance components were calculated and summarized in Table 8 for the 2010 FHWA design method and Table 9 for the 1999 FHWA design method. It can be observed that the resistance components have larger variation than that of the total resistance for both design methods. Prediction of tip resistance is more conservative as the model bias factor is the largest among the three.

Table 8
Summary of bias using 2010 FHWA design method (O-cell)

Statistics	Tip	Side	Total
Max.	5.12	1.17	1.43
Min.	0.47	0.28	0.49
Mean	2.16	0.65	0.94
COV	0.53	0.36	0.26

Table 9
Summary of bias using 1999 FHWA design method (O-cell)

Statistics	Tip	Side	Total
Max.	5.39	1.47	1.81
Min.	0.43	0.44	0.60
Mean	2.26	0.91	1.22
COV	0.55	0.34	0.28

Figure 26 and Figure 27 present the histogram and the normal and lognormal distributions of the bias of different resistance components for the 2010 FHWA design method, while Figure 28 and Figure 29 show the histogram and the normal and lognormal distributions of the bias of different resistance component for the 1999 FHWA design method. For tip resistance, the goodness of fit test (Anderson-Darling test) showed that normality assumption is invalid and lognormal distribution provides a good fit to the observed data at a significance level 0.05. The goodness of fit test for side resistance (Anderson-Darling test) showed that both normal and lognormal distribution provides a good fit to the observed side data at a significance level 0.05; and the lognormal distribution provides a better fit for both design methods. As such, lognormal distribution was used in reliability calibration analyses.

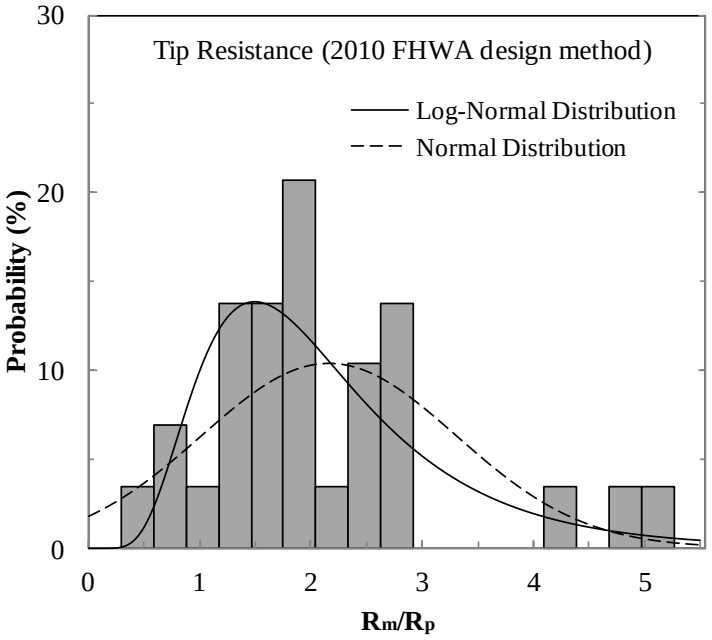

Figure 26
Histograms of bias for tip resistance using 2010 FHWA design method

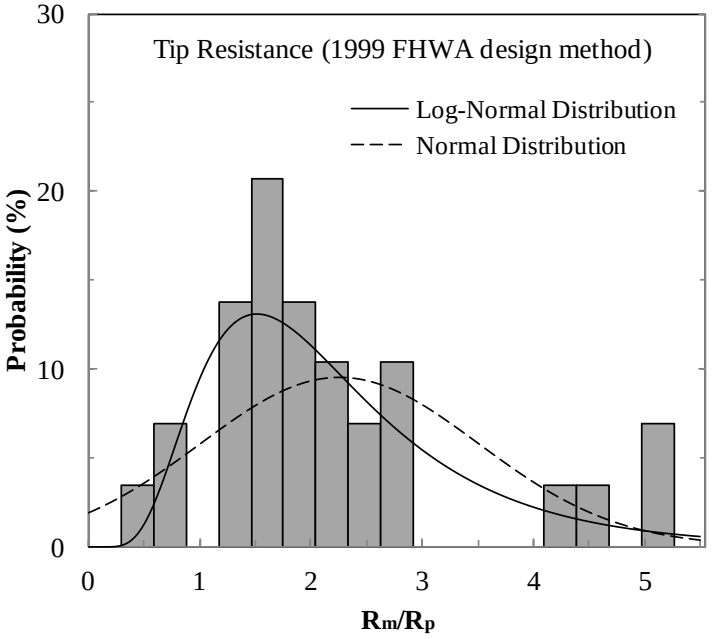

Figure 27
Histograms of bias for tip resistance using 1999 FHWA design method

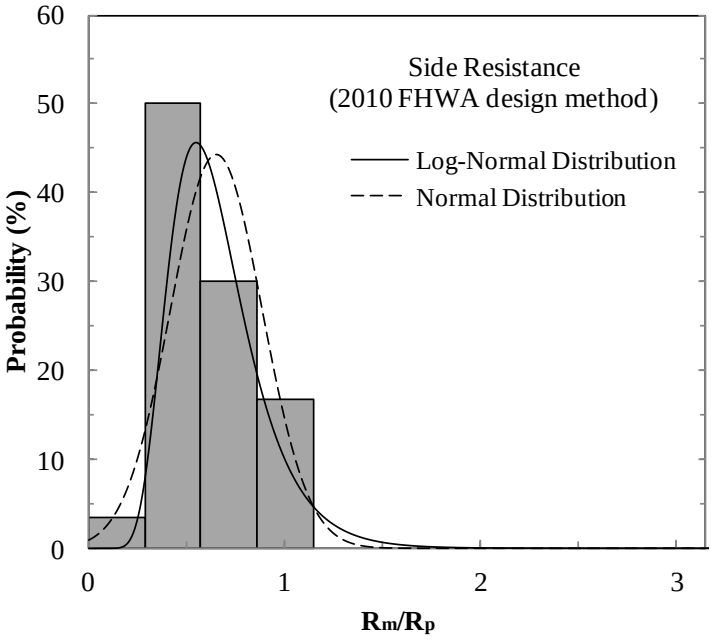

Figure 28
Histograms of bias for side resistance using 2010 FHWA design method

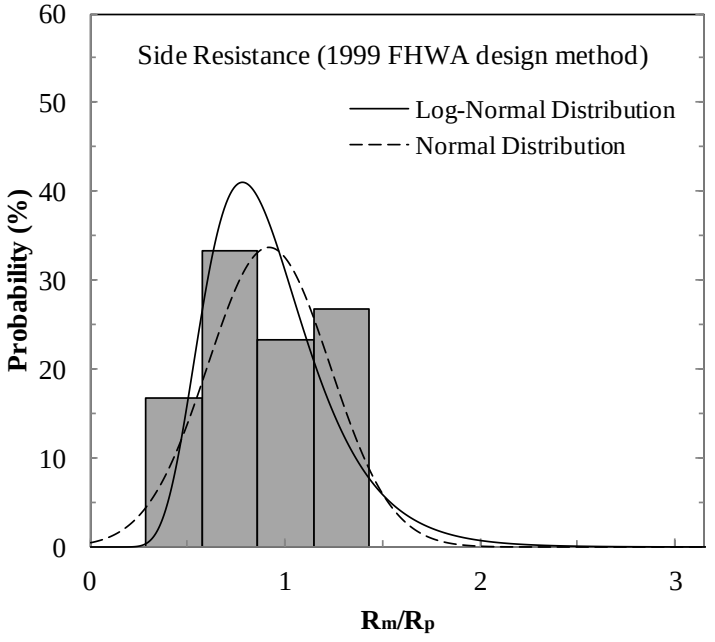

Figure 29
Histograms of bias for side resistance using 1999 FHWA design method

LRFD Calibration

Total Resistance Factor

This study follows the calibration procedure based on the Monte Carlo simulation method recommended in the Transportation Research Circular E-C079 to determine the total resistance factor of drilled shafts *[36]*. The required number of Monte Carlo trials is based upon achieving a particular confidence level for a specified number of random variables and is not affected by the variability of the random variables *[36, 38,* and *39]*. Using the procedure described by Harr, the number of Monte Carlo trials required for a confidence level of 90 percent is approximately 9,900 *[38]*. For the probabilistic calculations reported in this study, Monte Carlo simulation with 50,000 trials was conducted. The calculated reliability index and the corresponding resistance factor are plotted in Figure 30 and Figure 31 for the 2010 FHWA design method and the 1999 FHWA design method, respectively.

The calibration was conducted with a dead load to live load ratio of 3.0 since it is a typical value used in previous research as discussed previously *[5, 18]*. AASHTO suggested a required reliability index of 3.0 for the drilled shaft foundation with small amount of redundancy (i.e., two to four shafts in a group) . According to AASHTO, for larger shaft groups (i.e., five or more shafts in a group), the recommended resistance factor may be increased by up to 20 percent to reflect a lower reliability index of 2.3, while for single shaft foundations, the recommended resistance factors should be reduced by 20 percent to achieve a higher reliability index of 3.5 due to a lack of redundancy. Total resistance factors (ϕ) for the 2010 FHWA design method corresponding to a target reliability index of 3.0 is 0.41 using "best fit to tail" method and 0.48 using the measured bias (Figure 30). For the 1999 FHWA design method, total resistance factors (ϕ) corresponding to a target reliability index of 3.0 is 0.50 using "best fit to tail" method and 0.60 using the measured bias (Figure 31). The authors believe the resistance factor based on measured bias is more favorable since the measured bias data can be utilized to its full extent. Total resistance factors from this study as well as reported in previous literature are listed in Table 10. It should be noted that the resistance factors of cohesive and cohesionless soils calibrated by AASHTO and Paikowsky were based on O'Neill and Reese (1988) method *[4, 5,* and *40]*. The work by Liang and Li is based on O'Neill and Reese (1999) method via SHAFT program *[14, 17,* and 39*]*. The resistance factors calibrated using the 2010 FHWA design method is less than those calibrated using the 1999 FHWA design method. However, the 2010 FHWA design method gives a relatively higher efficiency factor than the 1999 FHWA design method does.

Separated Resistance Factors

The statistical parameters used for the calibration of separated resistance components are listed in Table 11. The side resistance and tip resistance were determined at the same settlement of the shaft top. The bias of side resistance and tip resistance can be considered as independent variables. Therefore, the resistance factor from side and tip can be calibrated separately following the same calibration procedure as for the total resistance. The calculated resistance factors for each resistance component are proposed in Table 11 for both the 2010 FHWA design method and the 1999 FHWA design method. Only measured bias data were used in this calibration. "Best-fit-to-tail" was not used. It is interesting to notice that the tip resistance factor is higher than the side resistance factor. This may be due to variation of soil type along the shafts. It is also interesting note that the side and total resistance factors calibrated using the 2010 FHWA design method are less than those calibrated using the 1999 FHWA design method. This might be due to the fact that when the β in the 2010 FHWA design method is able to account for soil strength and in-situ state of stress, it also introduces more variation, i.e., site variation. While both the 2010 and the 1999 FHWA design methods overestimate the side resistance, the overestimation by the 2010 FHWA design method is much more significant. Meanwhile, both design methods significantly underestimate the tip resistance. The calibrated total resistance factor using 30 tests (O-cell tests only) (Table 11) is higher than the one calibrated using the 34 cases (Table 10), e.g., total O-cell and top down tests with no separation.

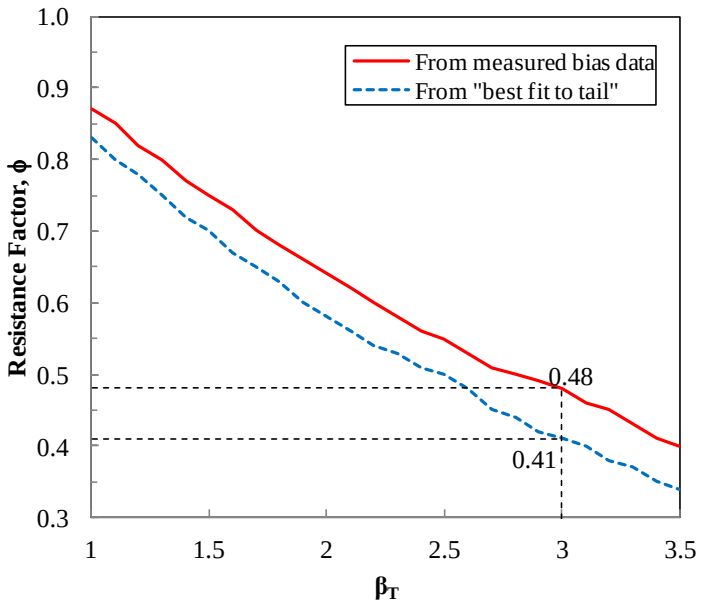

Figure 30
Resistance factors for different reliability indexes for 2010 FHWA design method

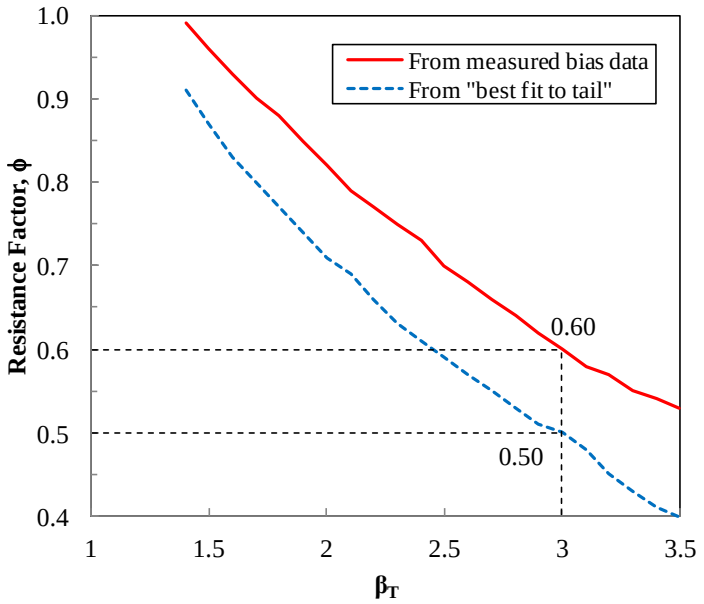

Figure 31
Resistance factors for different reliability indexes for 1999 FHWA design method

Table 10
Resistance factors (ϕ) and efficiency factors (ϕ/λ) for drilled shaft (Dataset 1)

$\beta_T = 3.0$	Resistance Factor, ϕ	Efficiency Factor, ϕ/λ
Current study (2010 FHWA design method)	0.48 in mixed soils 0.41 in mixed soils (best fit to tail)	0.48 in mixed soils 0.41 in mixed soils (best fit to tail)
Current study (1999 FHWA design method)	0.60 in mixed soils 0.50 in mixed soils (best fit to tail)	0.47 in mixed soils 0.38 in mixed soils (best fit to tail)
Liang and Li *[14]*	0.45 in clay 0.50 in sand 0.35 in mixed soils	-
Paikowsky *[**4**]* and AASHTO *[**5**]*	0.45 in cohesive soils 0.55 in cohesionless soils	-

Table 11
Separated resistance factors and efficiency factors (Dataset 2)

Resistance component	Tip		Side		Combined	
	ϕ	ϕ/λ	ϕ	ϕ/λ	ϕ	ϕ/λ
2010 FHWA design method	0.53	0.25	0.26	0.40	0.50	0.53
1999 FHWA design method	0.52	0.23	0.39	0.43	0.61	0.50

SUMMARY AND CONCLUSIONS

This study presented the LRFD calibration of the 2010 FHWA (Brown et al.) and the 1999 FHWA (O'Neill and Reese) design method for drilled shaft design based on the 5% B criterion. A drilled shaft load test database of 34 drilled shafts with different sizes and lengths was collected and used to calibrate the total and separated resistance factors. This collected database has four top-down tests and 30 O-cell tests. For each drilled shaft, the load-settlement behavior was estimated using both the 2010 and the 1999 FHWA methods. Tip, side, and total resistance factors (ϕ) needed in the LRFD design methodology of drilled shafts in Louisiana were determined at a reliability index (β_T) of 3.0 and are ready for implementation.

Statistical analyses comparing the predicted and measured drilled shaft resistances were conducted to evaluate the accuracy of both the 2010 and the 1999 FHWA design methods in estimating the measured drilled shaft capacity. Results of the analyses showed that the 2010 FHWA design method overestimates the total drilled shaft resistance by an average of two percent, while the 1999 FHWA design method underestimates the total drilled shaft resistance by an average of 21 percent. The prediction of tip resistance is much more conservative than that of side resistance.

LRFD calibration based on the Monte Carlo simulation method was conducted to determine the resistance factors (ϕ) at different reliability indexes (β_T) that are needed to implement the LRFD design of axially loaded drilled shafts. Design input parameters for loads were adopted from the AASHTO LRFD design specifications for bridge substructure. Total resistance factor (ϕ_{total}) for mixed soils corresponding to a dead load to live load ratio (Q_D/Q_L) of 3.0 with a target reliability index (β_T) of 3.0 was found to be 0.48 for the 2010 FHWA design method and 0.60 for the 1999 FHWA design method. The total resistance factor determined from 30 dataset (O-cell) only was found to be 0.50 for the 2010 FHWA design method and 0.61 for the 1999 FHWA design method. Based on the 30 O-cell drilled shaft tests, a tip resistance factor (ϕ_{tip}) of 0.53 and a side resistance factor (ϕ_{side}) of 0.26 were determined for the 2010 FHWA design method and 0.52 and 0.39 for the 1999 FHWA design method. The side and total resistance factors calibrated using the 2010 FHWA design method are less than those calibrated using the 1999 FHWA design method. The presented resistance factors can be valuable reference values for the LADOTD engineers to design drilled shafts in Louisiana using the LRFD methodology.

RECOMMENDATIONS

1. LADOTD engineers need to start implementing the resistance factors (ϕ) determined in this research study in design of drilled shafts for all future state projects.

2. A few projects should be selected to demonstrate the comparison between the LRFD design and the traditional ASD design and conduct a cost benefit study.

3. A workshop should be held to train LADOTD engineers in the LRFD design of deep foundations.

4. It is recommended to continue collecting drilled shaft test data from new projects, especially for those cases in which the end bearing and side frictional capacities can be separated for possible future re-calibration of resistance factors. A database of a minimum 20 load tests is considered statistically reliable to perform LRFD calibration.

5. It should be noted that performing complete reliability analyses of deep foundations requires the inclusion of all risk factors. Scour is a critical factor in the selection of drilled shaft tip elevations. The risk associated with scour directly impacts the reliability of drilled shaft foundations. This is mainly due to expected changes on the in-situ stress state (overburden and stress history) of the subsurface soil that will affect the laboratory and in-situ test results. However, the scope of this study does not include the evaluation of scour and is recommended to be considered in the future.

6. Global resistance factors are recommended herein for the design of axially loaded drilled shafts in Louisiana. However, further research should be conducted to evaluate site variability and in-situ load tests' effect on the selection of resistance factor values.

ACRONYMS, ABBREVIATIONS, AND SYMBOLS

AASHTO	American Association of Highway and Transportation Officials
ASD	Allowable Stress Design
CDF	Cumulative Distribution Function
COV	Coefficient of Variation
DOT	Department of Transportation
FHWA	Federal Highway Administration
IGM	Intermediate Geomaterial
LA	Louisiana
LADOTD	Louisiana Department of Transportation and Development
LRFD	Load and Resistance Factor Design
LTRC	Louisiana Transportation Research Center
MS	Mississippi
MDOT	Mississippi Department of Transportation
NCHRP	National Cooperative Highway Research Program
PDF	Probability Density Function
SHAFT	Computer program for drilled shaft design
SLS	Serviceability Limit State
SPT	Standard Penetration Test
ULS	Ultimate Limit State

REFERENCES

1. Abu-Farsakh, Y. M., Yoon, S., and Tsai, C. *Calibration of Resistance Factors Needed in the LRFD Design of Driven Piles*. Report No. 449, Louisiana Transportation Research Center, May, 2009.
2. Abu-Farsakh, Y. M., Yu, X., and Tsai, C. *Calibration of Resistance Factors Needed in the LRFD Design of Drilled Shafts*. Report No. 470, Louisiana Transportation Research Center, September, 2010.
3. California Department of Transportation, *Bridge Design Practice Manual*, http://www.dot.ca.gov/hq/esc/techpubs/manual /bridgemanuals/bridge-design-practice/pdf/bdp_1.pdf, Accessed on March, 2012.
4. Paikowsky, S. G. *Load and Resistance Factor Design (LRFD) for Deep Foundations*, Publication NCHRP-507. Transportation Research Board, Washington D.C., 2004. pp. 87.
5. AASHTO. *LRFD Bridge Design Specifications*, 4th Edition, American Association of State Highway and Transportation Officials, Washington, D.C., 2007. pp. 40.
6. Yang, X., Han, J., Parsons, R., and Henthorne, R. "Resistance Factors for Drilled Shafts in Weak Rocks Based on O-Cell Test Data." In *Transportation Research Record 2045*. Transportation Research Board, National Research Council, Washington, D.C., 2008, pp. 62-67.
7. Allen, T. M. *Development of the WSDOT Pile Driving Formula and Its Calibration and Resistance Factor Design (LRFD)*, Publication FHWA-WA-RD 610.1. FHWA, Washington State Department of Transportation, 2005. pp. 57.
8. McVay, M., Birgisson, B., Zhang L., Perez, A., and Putcha, S. "Load and Resistance Factor Design (LRFD) for Driven Piles Using Dynamic Methods—A Florida Perspective." *Geotechnical Testing Journal*, Vol. 23, No. 1, 2000, pp. 55–66.
9. McVay, M., Birgisson, B., Nguyen, T., and Kuo, C. "Uncertainty in LRFD phi, ϕ, Factors for Driven Prestressed Concrete Piles." In *Transportation Research Record 1808*. Transportation Research Board, National Research Council, Washington, D.C., 2002, pp. 99–107.
10. Allen, T.M. "Development of a New Pile Driving Formula and Its Calibration for Load and Resistance Factor Design." Proceedings for the 86th TRB Annual Meeting, Washington, D.C., TRB, 2006.
11. Yang, L. and Liang, R. "Incorporating Setup into Load and Resistance Factor Design of Driven Piles in Sand." Proceedings for the 86th TRB Annual Meeting. Washington, D.C., TRB, 2006.

12. Nowak, A.S. *Calibration of LRFD Bridge Design Code*, Publication NCHRP-368, Transportation Research Board, Washington, D.C., 1999. pp.218.
13. Kuo, C. L., McVay, M., and Birgisson, B. "Calibration of Load and Resistance Factor Design." In *Transportation Research Record 1808*. Transportation Research Board, National Research Council, Washington, D.C., 2002, pp. 108-111.
14. Liang, R. and Li, J. "Resistance Factors Calibrated from FHWA Drilled Shafts Static Top-Down Test Data Base." GSP 186: *Contemporary Topics in In-Situ Testing, Analysis, and Reliability of Foundations*, 2009.
15. Barker, R. M., Duncan, J. M., Rojiani, K. B., Ooi, P. S. K., Tan, C. K., and Kim, S. G. *Manuals for the Design of Bridge Foundations*. NCHRP-343, Transportation Research Board, National Research Council, Washington, D.C., 1991, pp. 306.
16. O'Neill, M., Townsend, F., Hassan, K., Buller, A., and Chang, P. *Load Transfer for Drilled Shafts in Intermediate Geomaterials*. FHWA-RD-95-172, FHWA, 1996, pp. 184.
17. O'Neill, M.W. and Reese, L.C. *Drilled Shafts: Construction Procedures and Design Methods*, Publication FHWA-IF-99-025, FHWA, Washington, D.C., 1999, pp. 758
18. AASHTO. *LRFD Bridge Design Specifications*, 4th Edition, American Association of State Highway and Transportation Officials, Washington, D.C., USA, 2007. pp.582.
19. Allen, T.M. *Development of Geotechnical Resistance Factors and Downdrag Load Factors for LRFD Foundation Strength Limit State Design*, Publication FHWA-NHI-05-052, FHWA, Washington, D.C., 2005. pp.49.
20. Yang, X.M., Han, J., Parsons, R.L., and Henthorne, R. "Resistance Factors for Drilled Shafts in Weak Rocks Based on O-cell Test Data." In *Transportation Research Record 2045*. Transportation Research Board, National Research Council, Washington, D.C., 2008, pp. 62-67.
21. DFI. *Guidelines for the Interpretation and Analysis of the Static Loading Test*, 1st Edition. Sparta, NJ: Deep Foundations Institute, 1990. pp. 20.
22. Brown, D.A., Turner, J.P., and Castelli, R.J. Drilled Shafts: Construction Procedures and LRFD Designm Methods, Publication FHWA-NHI-10-016, FHWA, Washington, D.C., 2010, pp. 753
23. Chen, Y-J, and Kulhawy, F.H. (2002), "Evaluation of Drained Axial Capacity for Drilled Shafts," Geotechnical Special Publication No. 116, Deep Foundations 2002, M.W. O'Neill and F.C. Townsend, Editors, ASCE, Reston, VA, pp. 1200-1214.
24. Schmertmann, J. H. and Hayes, J. A. "The Osterberg Cell and Bored Pile Testing – A Symbiosis." *3rd International Geotechnical Engineering Conference*, Cairo, Egypt; 1997. pp. 139–66.

25. Withiam, J., Voytko, E., Barker, R., Duncan, M., Kelly, B., Musser, S., and Elias, V. *Load and Resistance Factor Design (LRFD) of Highway Bridge Substructures*. FHWA-HI-98-032. FHWA, Washington, D.C., 1998.
26. Becker, D. E. "Eighteenth Canadian Geotechnical Colloquium: Limit States Design for Foundations. Parts I and II. An Overview of the Foundation Design Process." *Canadian Geotechnical Journal*, Vol. 33, 1996, pp. 956-1007.
27. Zhang, L., Tang, W. H., and Ng, C.W.W. "Reliability of Axially Loaded Driven pile Groups." *Journal of Geotechnical and Geoenvironmental Engineering*, ASCE, Vol. 127, No. 12, 2001, pp. 1051-1060.
28. Kim, J., Gao, X., and Srivatsan, T.S. "Modeling of Void Growth in Ductile Solids: Effects of Stress Triaxiality and Initial Porosity." *Engineering Fracture Mechanics*, Vol. 71, No. 3, 2004. pp. 379-400.
29. McVay, M., Ellis, Jr. R., Birgisson, B., Consolazio, G., Putcha, S., and Lee, S. "Load and Resistance Factor Design, Cost, and Risk: Designing a Drilled-Shaft Load Test Program in Florida Limestone." In *Transportation Research Record 1849.* Transportation Research Board, National Research Council, Washington, D.C., 2003, pp. 98-106.
30. Abu-Farsakh, M., and Titi, H. "Probabilistic CPT Method for Estimating the Ultimate Capacity of Friction Piles." *Geotechnical Testing Journal*, ASTM, Vol. 30, No. 5, 2007, pp. 387-398.
31. McVay, M.C. "Load and Resistance Factor Design, Cost, and Risk: Designing a Drilled Shaft Load Test in Florida Limestone." *Soil Mechanics*, 2003, pp. 98-106.
32. Hansell, W. C. and Viest, I. M. "Load Factor Design for Steel Highway Bridges." *AISC Engineering Journal*, Vol. 8, No. 4, 1971, pp. 113-123.
33. Zhang L.M., Li, D.Q., and Tang, W.H. "Reliability of Bored Pile Foundations Considering Bias in Failure Criteria." *Canadian Geotechnical Journal*, Vol. 42., 2005, pp. 1086-1093.
34. Abu-Farsakh, M., Yong, S., Yu, X., Tsai, C., and Zhang, Z. "Calibration of Resistance Factor for LRFD Design of Drilled Shafts in Louisiana." Proceedings for the 89th TRB Annual meeting, Washington, D.C., TRB, 2010, pp.12.
35. Zhang, Z., and Tumay, M.T. "Statistical to Fuzzy Approach Toward CPT Soil Classification." *Journal of Geotechnical and Geoenvironmental Engineering,* ASCE, Vol. 125, No. 3, 1999, pp. 179-186.
36. Allen, T.M., Nowak, A., and Bathurst, R. *Calibration to Determine Load and Resistance Factors for Geotechnical and Structural Design*. Publication TRB Circular E-C079, Transportation Research Board, Washington, D.C., 2005. pp.93.

37. Fishman, G. S. *Monte Carlo: Concepts, Algorithms, Applications*. Springer-Verlag, New York, 1995.
38. Harr, M. E. *Reliability-Based Design in Civil Engineering*. Dover Publications, Mineola, NY, 1996. pp. 291.
39. Baecher, G. B. and Christian, J. T. *Reliability and Statistics in Geotechnical Engineering*. Wiley, Chichester, England, 2003, pp. 619.
40. Reese, L.C. and O'Neill, M.W. *Drilled Shafts: Construction Procedures and Design Methods*. Report No. FHWA-HI-88-042, FHWA, Washington, DC, 1988, pp. 564.

APPENDIX A

Summary of Geotechnical Data for the Projects Investigated

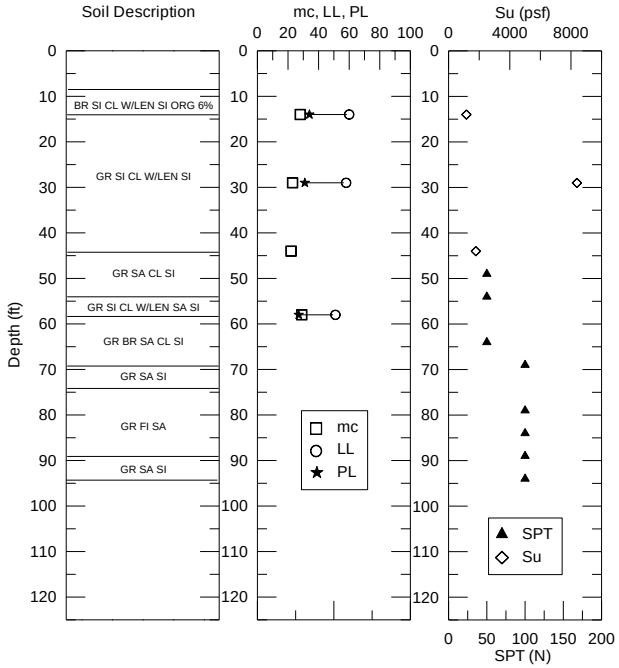

Figure 32
DS01

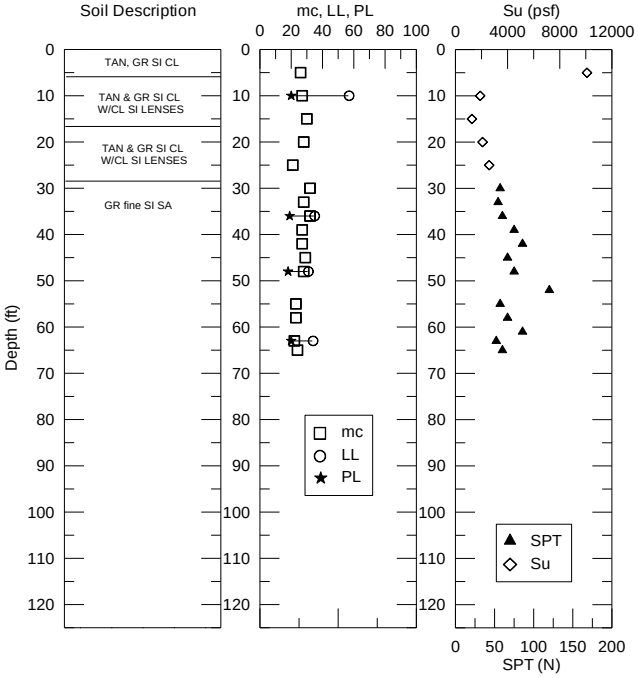

Figure 33
DS02

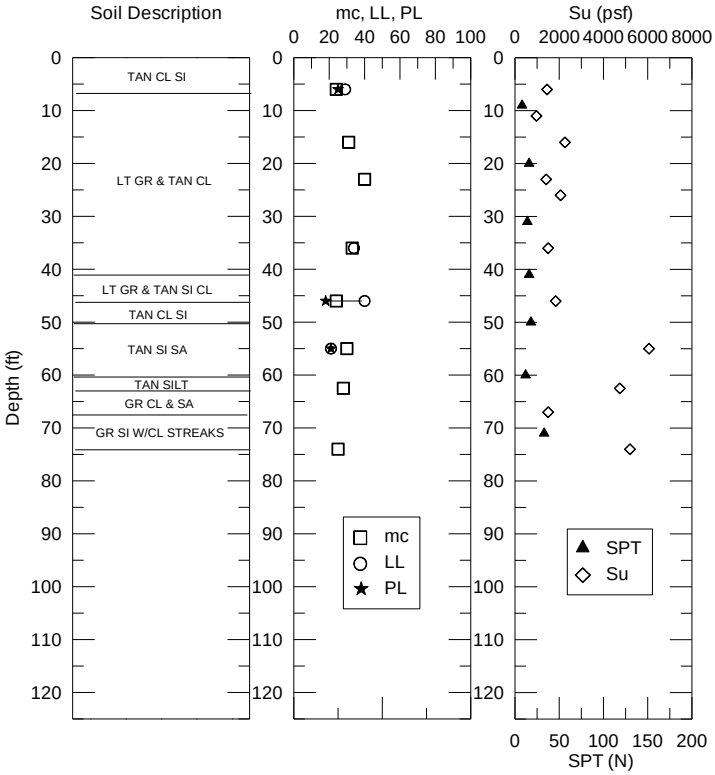

Figure 34
DS03

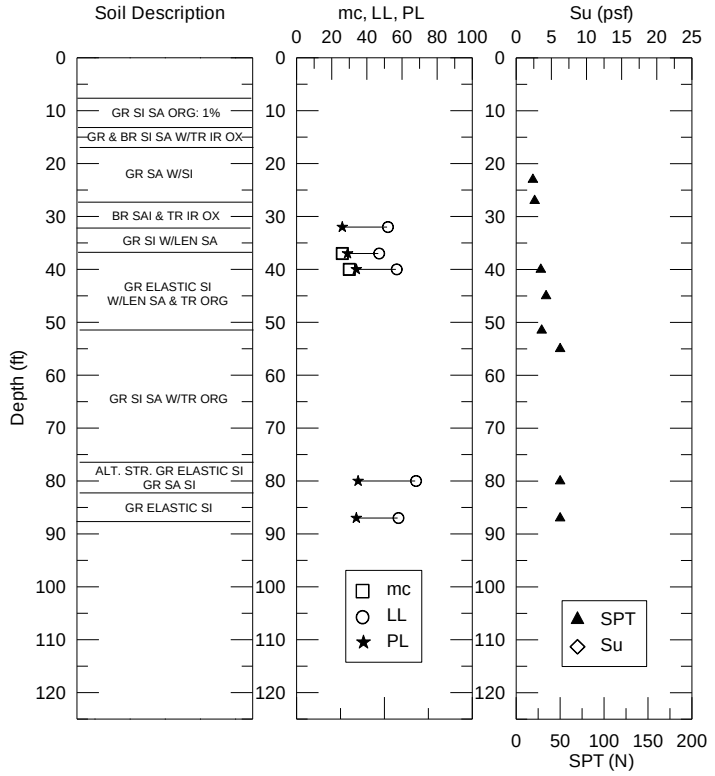

Figure 35
DS04

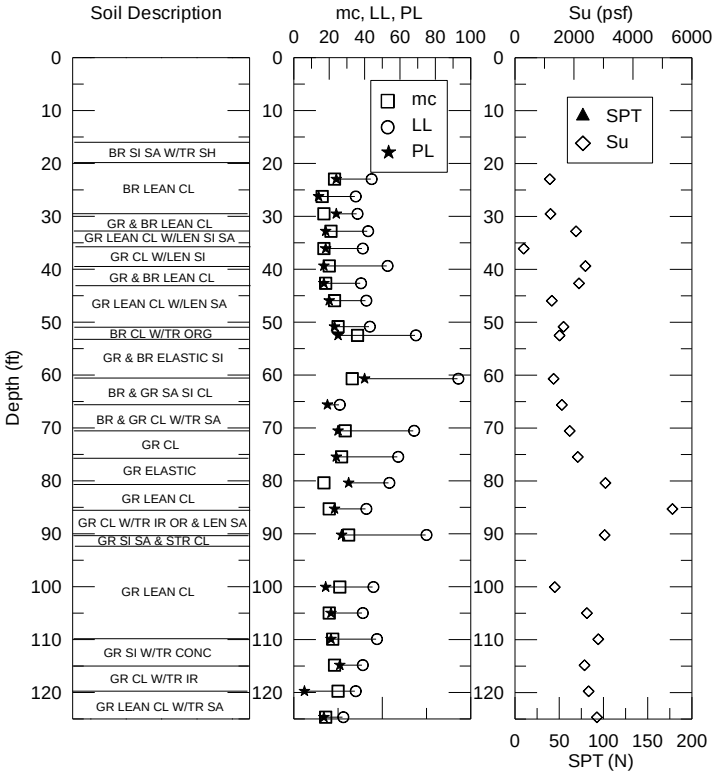

Figure 36
DS05

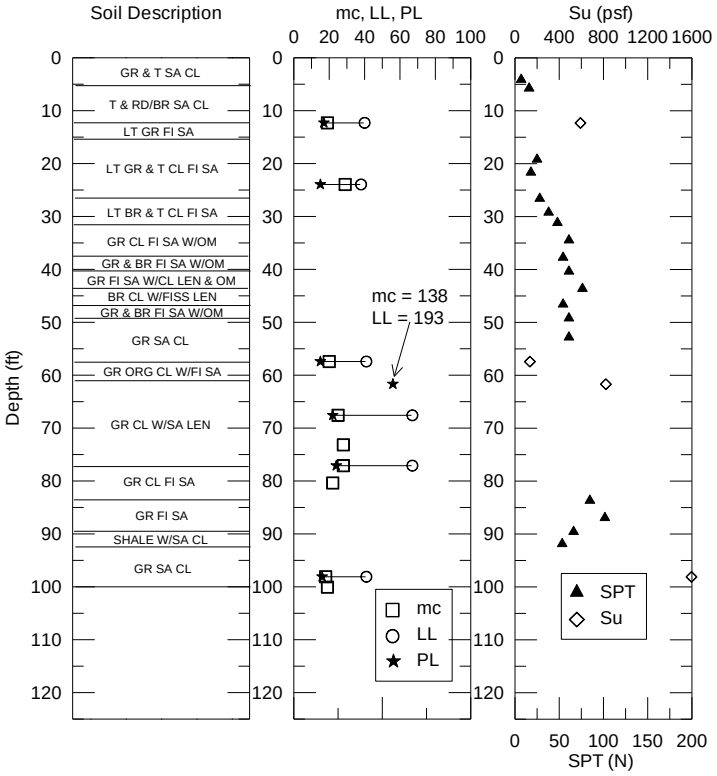

Figure 37
DS06

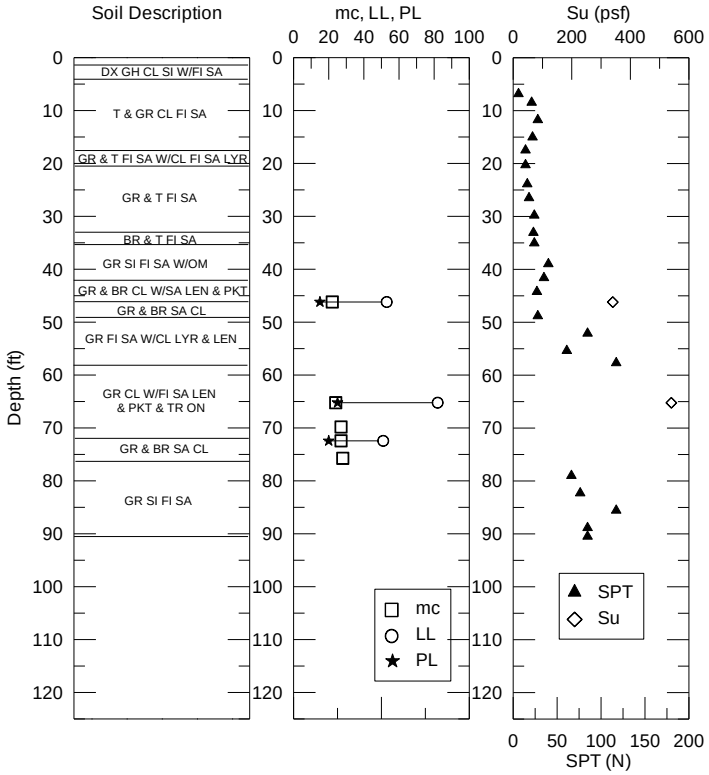

Figure 38
DS07

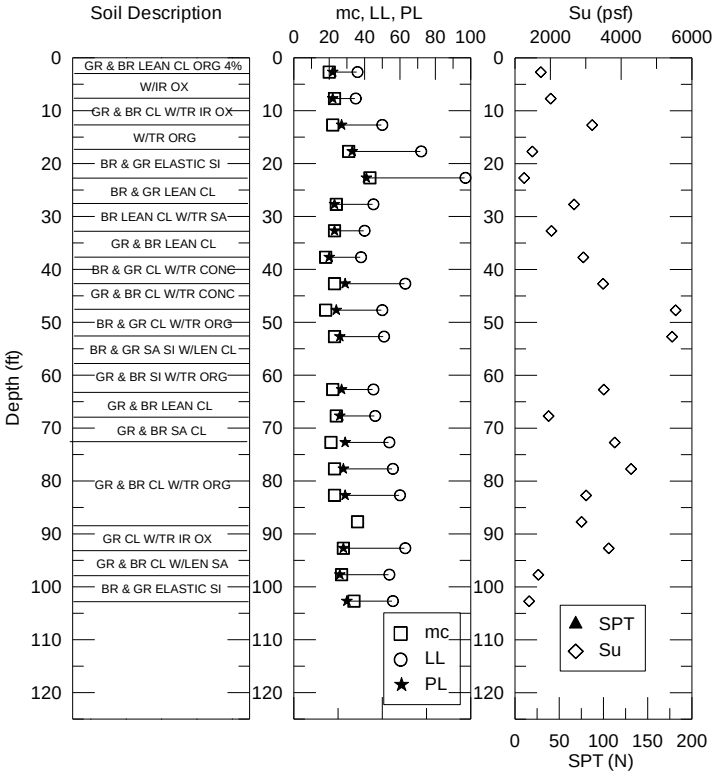

Figure 39
DS08

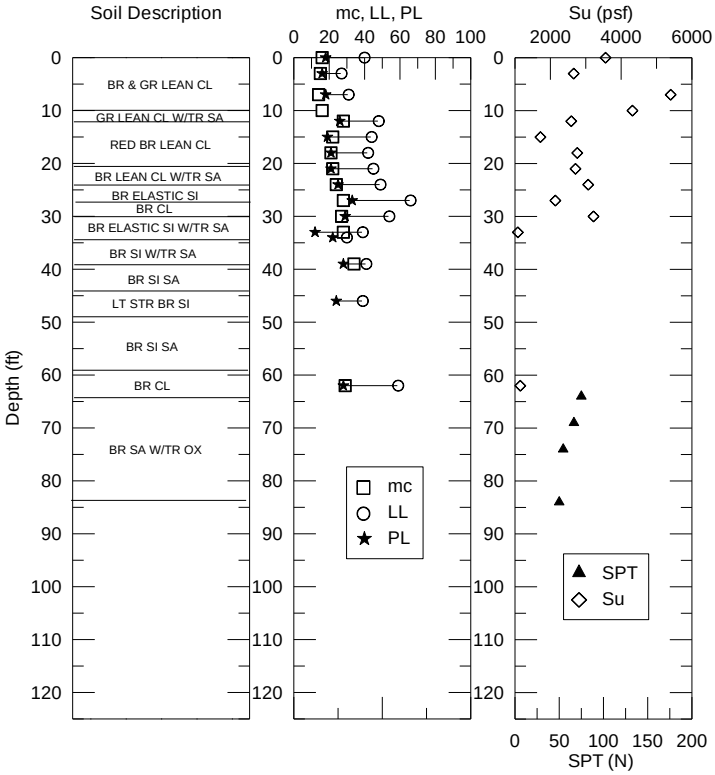

Figure 40
DS09

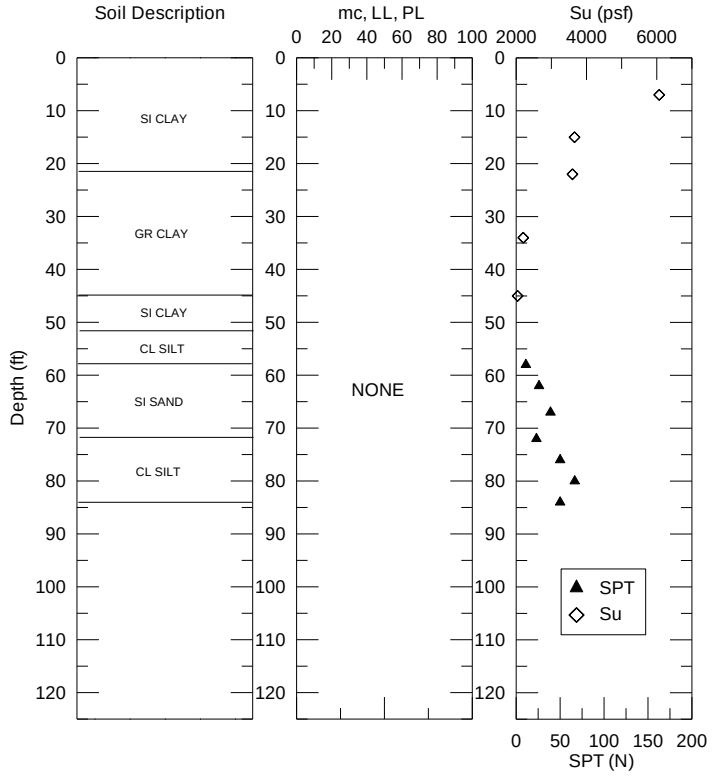

Figure 41
DS10 and DS11

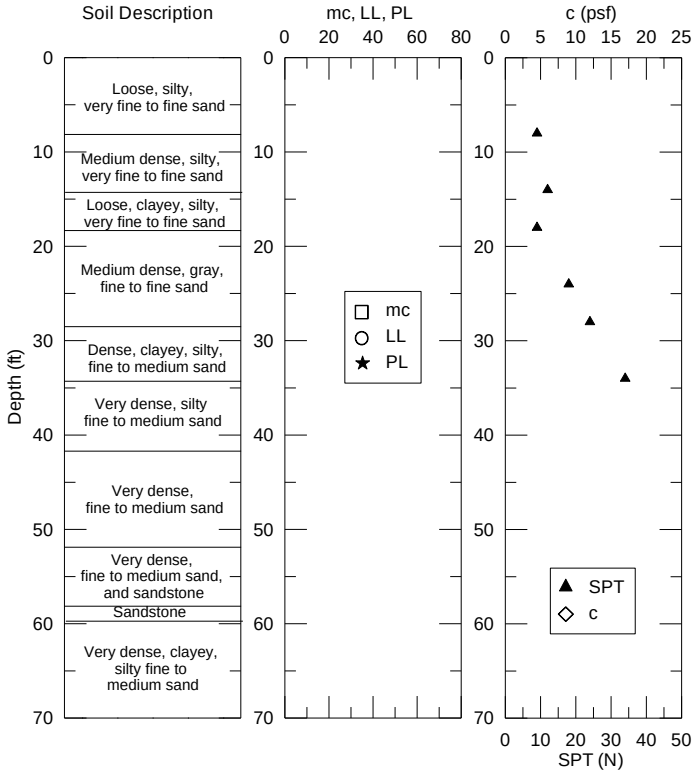

Figure 42
DS12

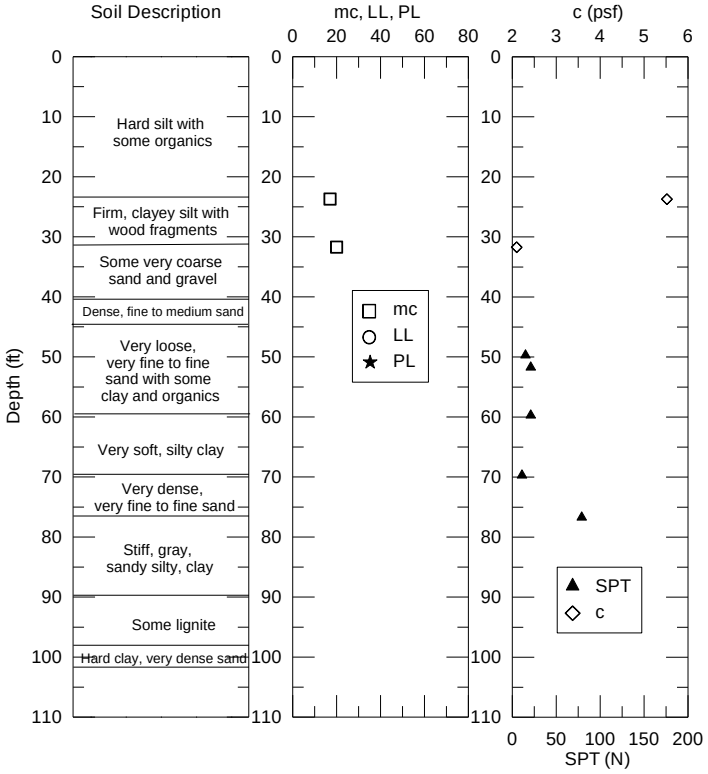

Figure 43
DS13

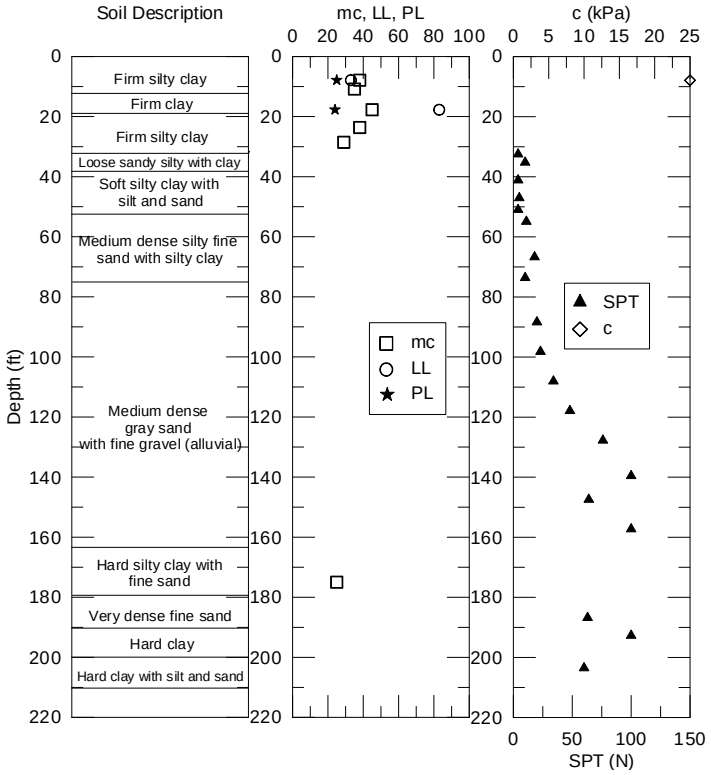

Figure 44
DS14

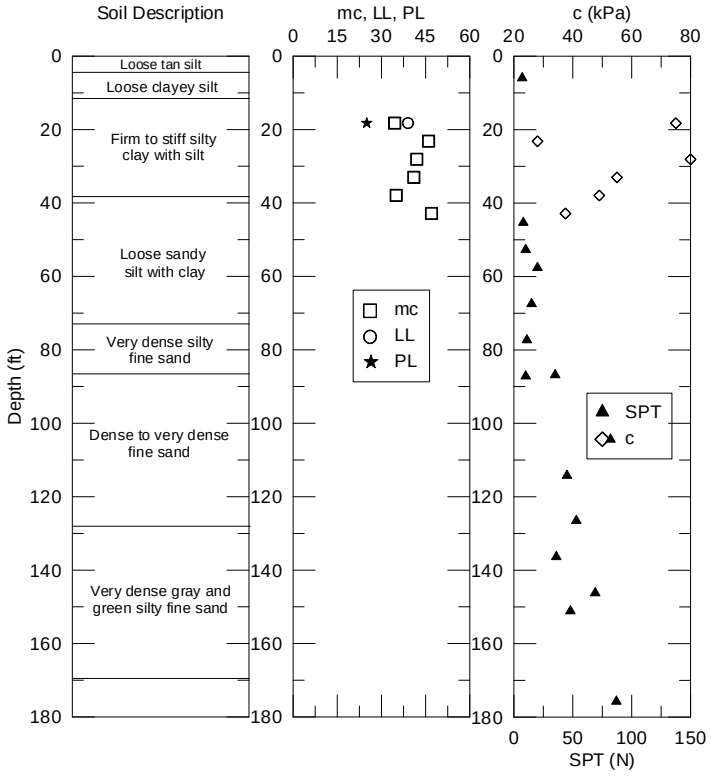

Figure 45
DS15

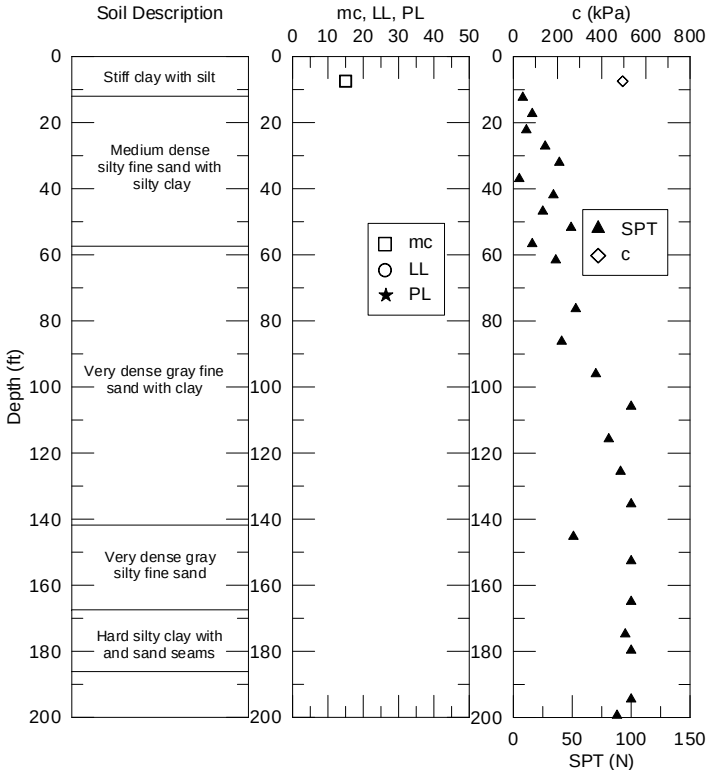

Figure 46
DS16

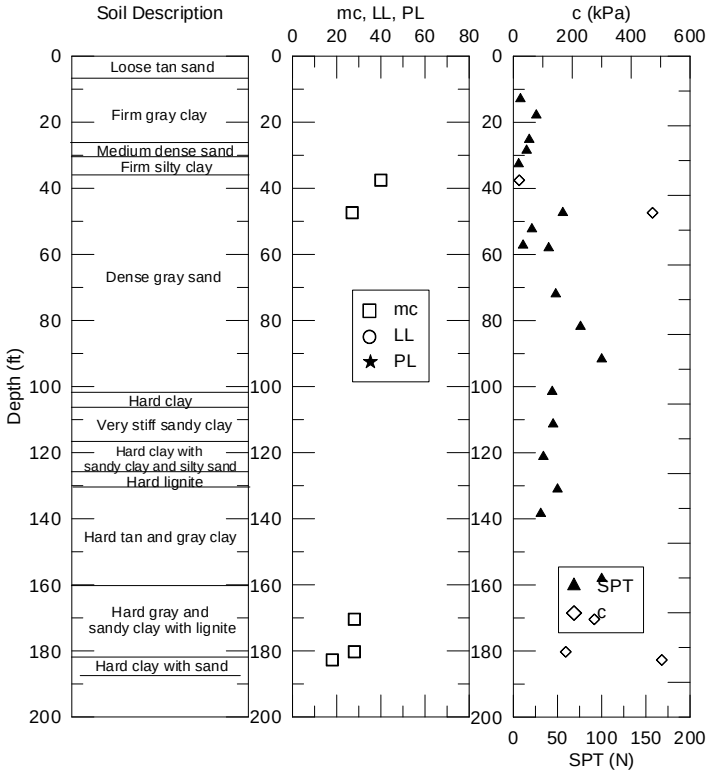

Figure 47
DS17

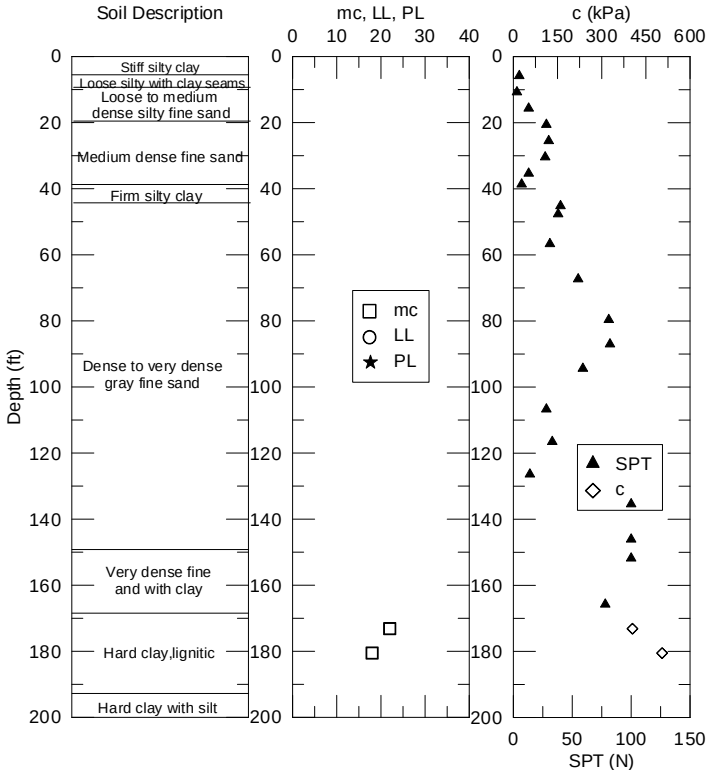

Figure 48
DS18

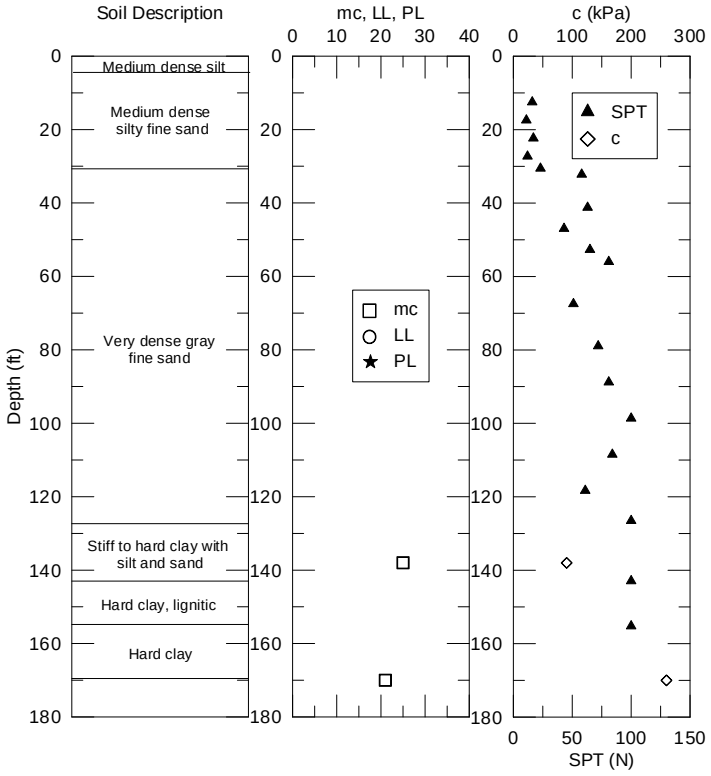

Figure 49
DS19

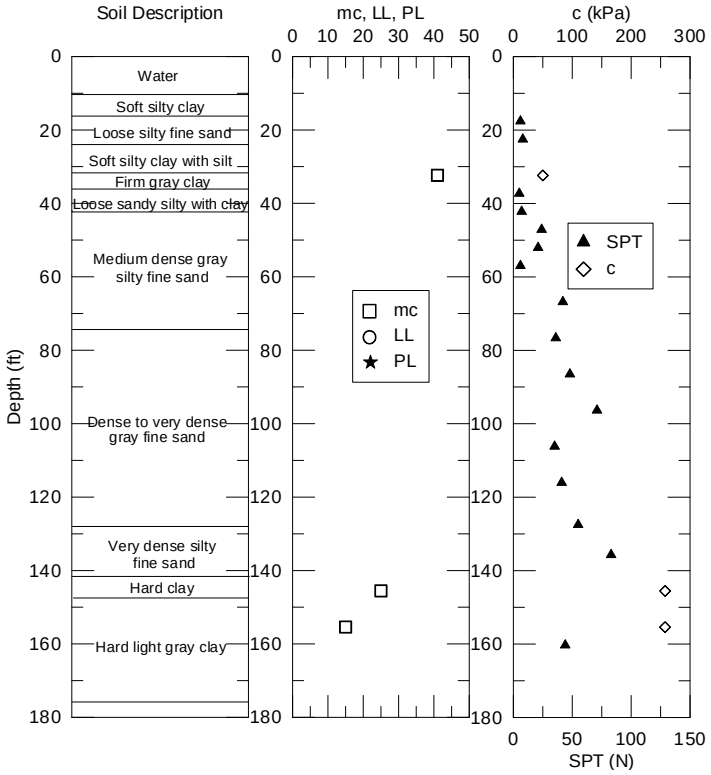

Figure 50
DS20

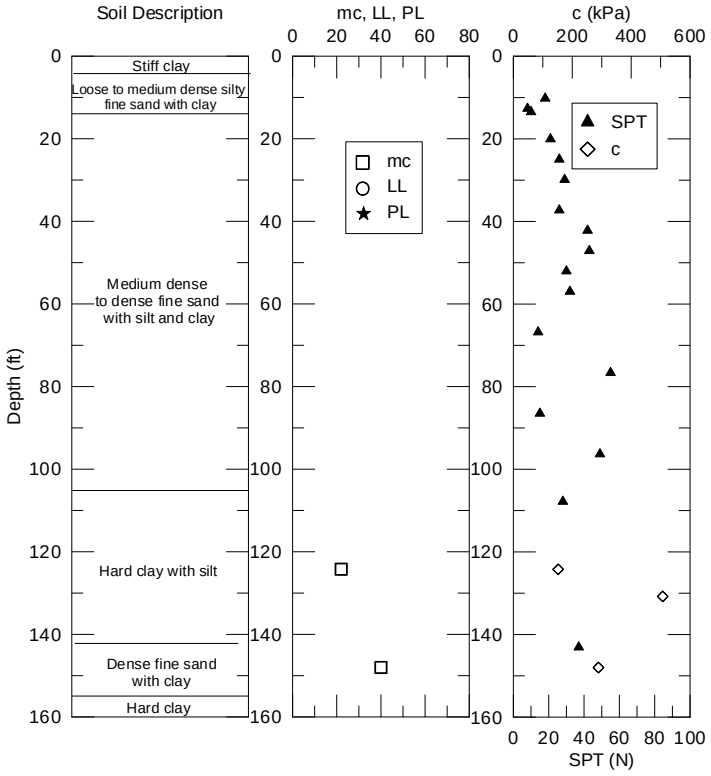

Figure 51
DS21

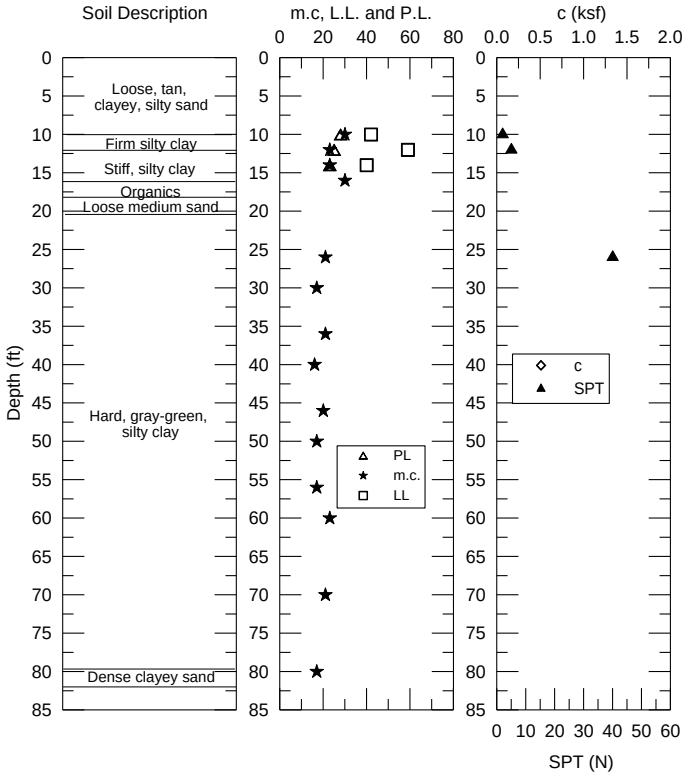

Figure 52
DS22

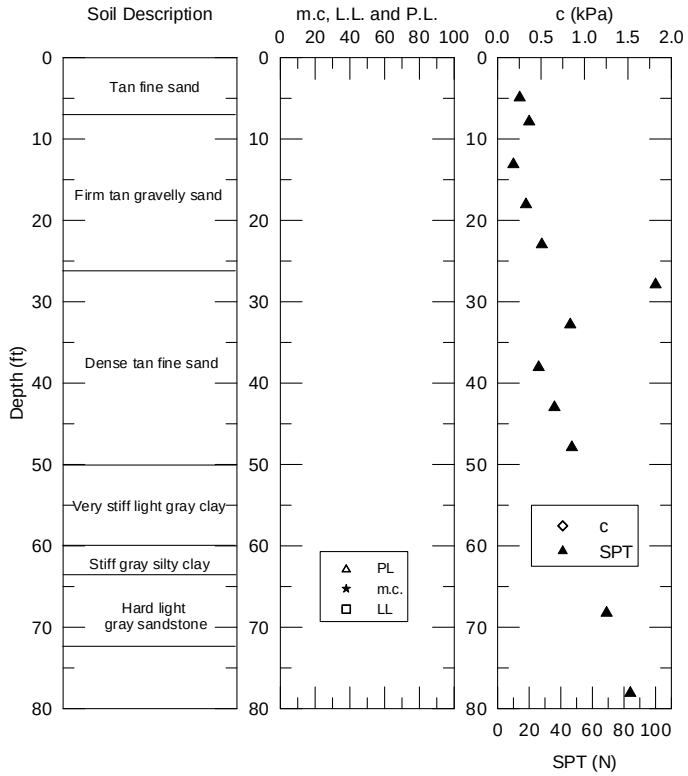

Figure 53
DS23

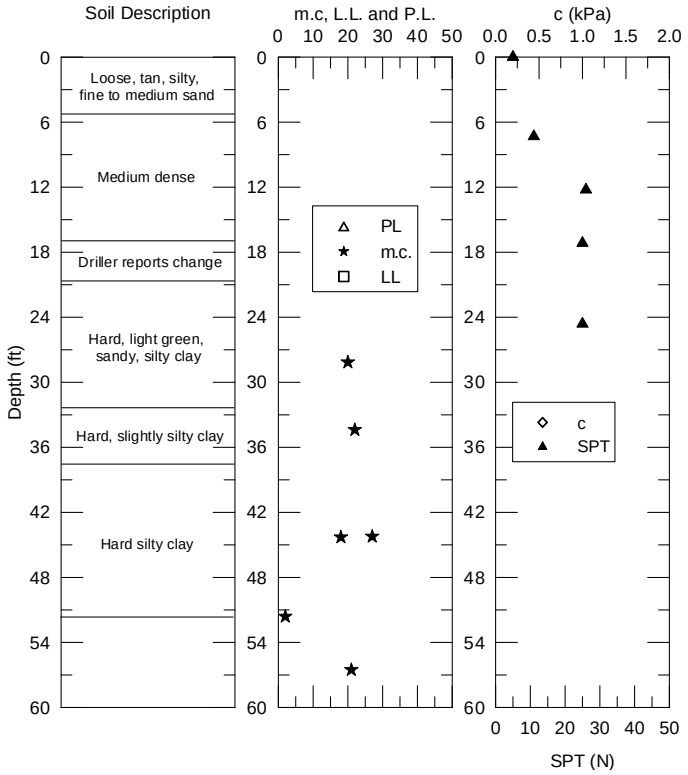

Figure 54
DS24

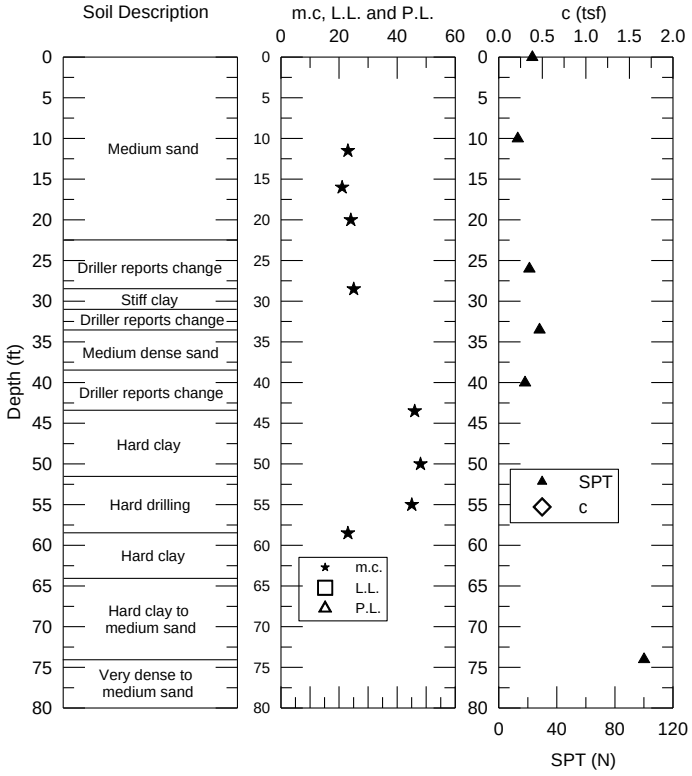

Figure 55
DS25

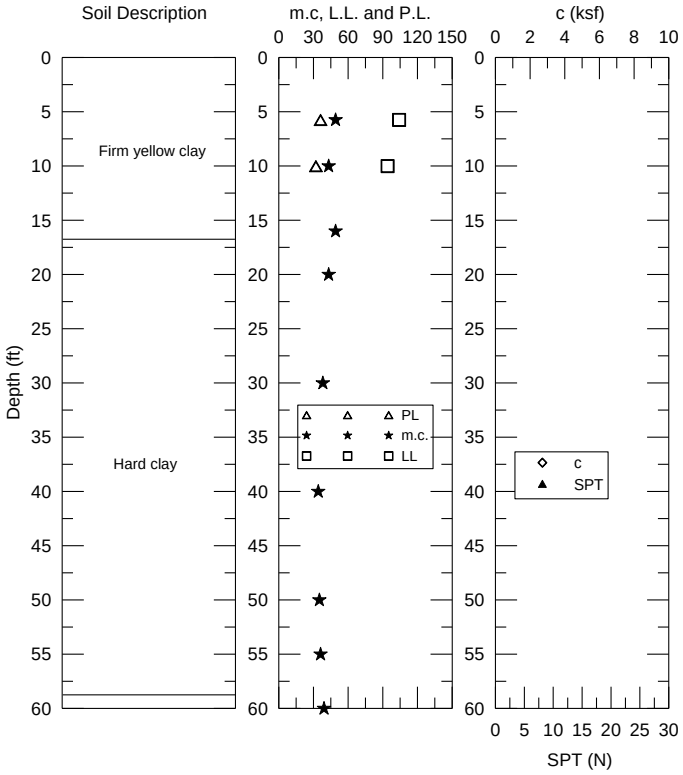

Figure 56
DS26

APPENDIX B

Measured Load-settlement Curves

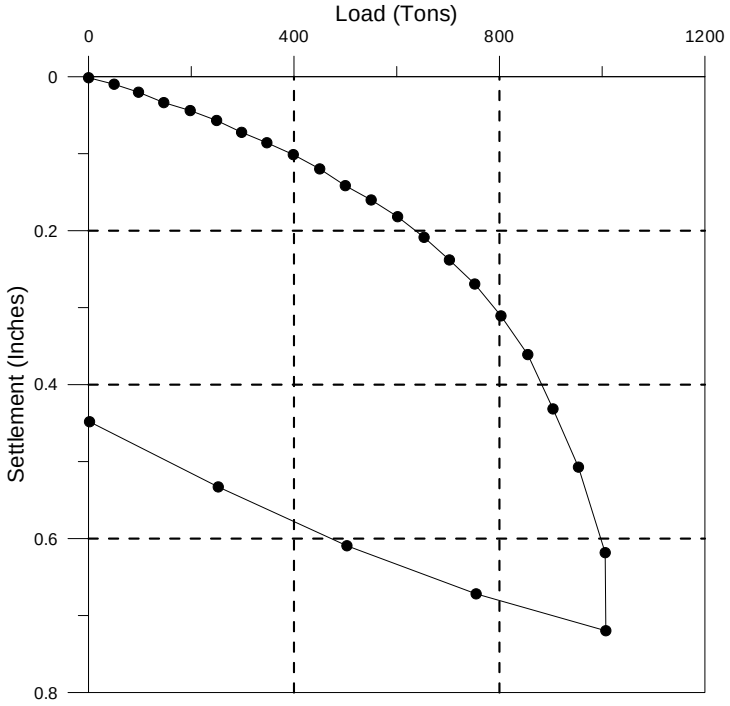

Figure 57
Top-down load settlement curve of DS01

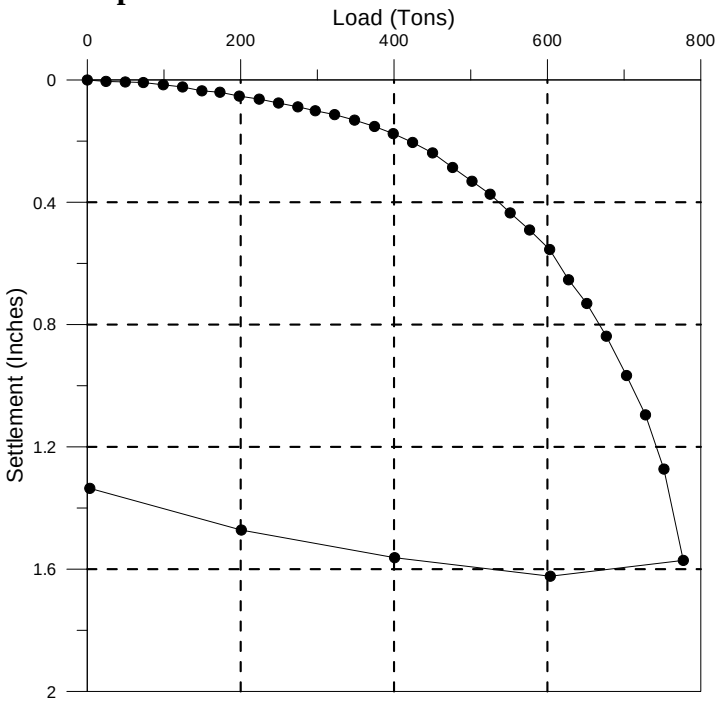

Figure 58
Top-down load settlement curve DS02

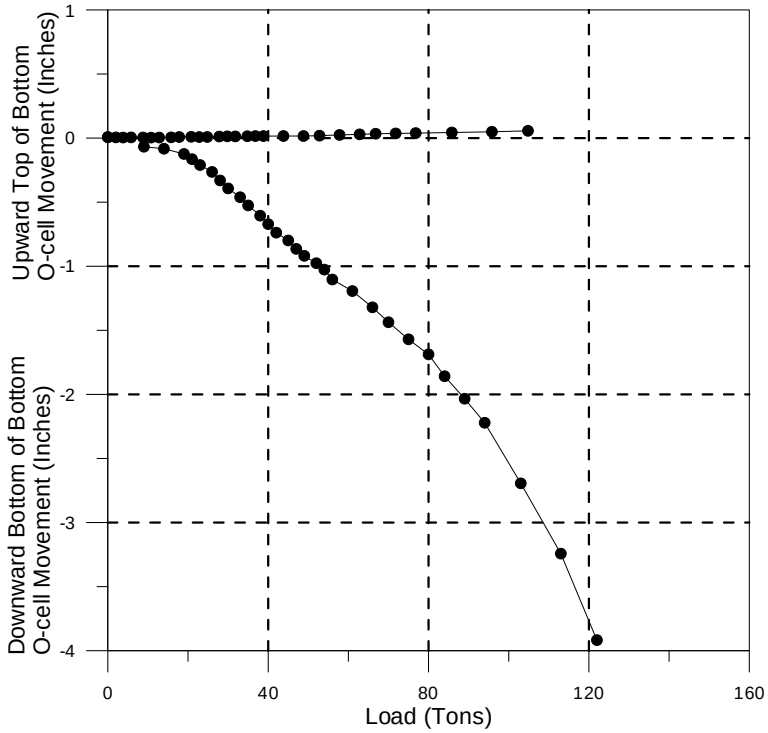

Figure 59
Lower O-cell load movement curves-stage 1 DS03

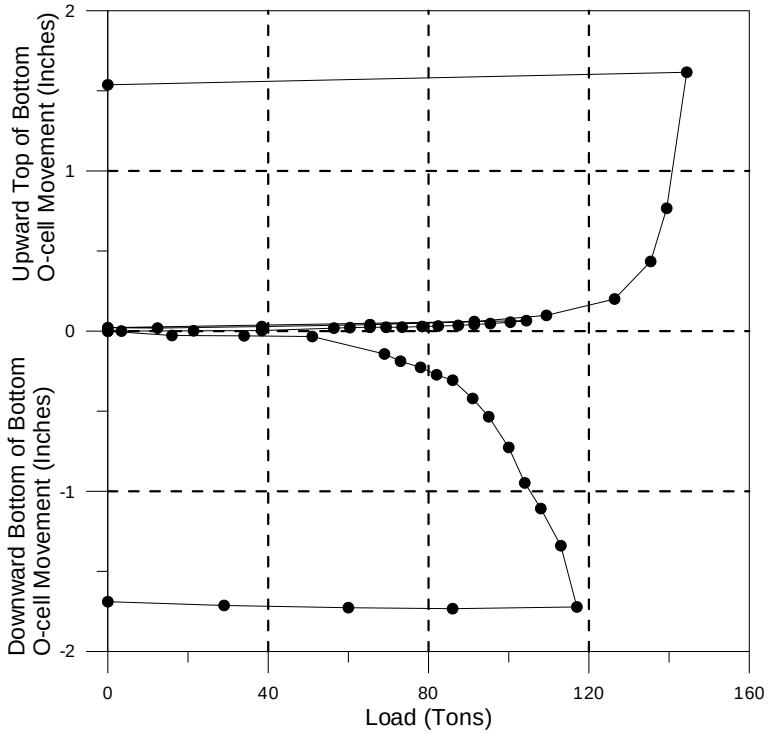

Figure 60
Upper O-cell load movement curves-stage 2 DS03

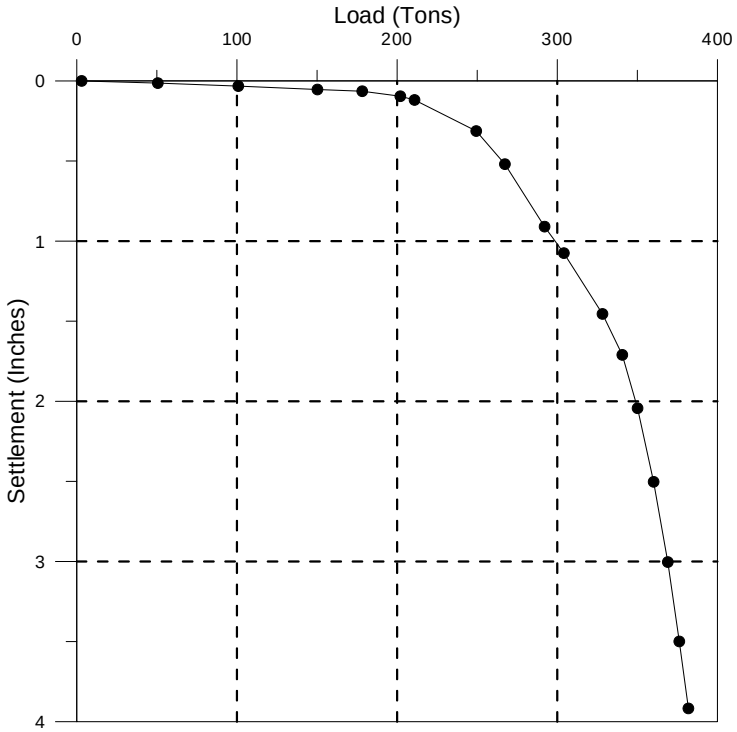

Figure 61
Equivalent top-down load settlement curve DS03

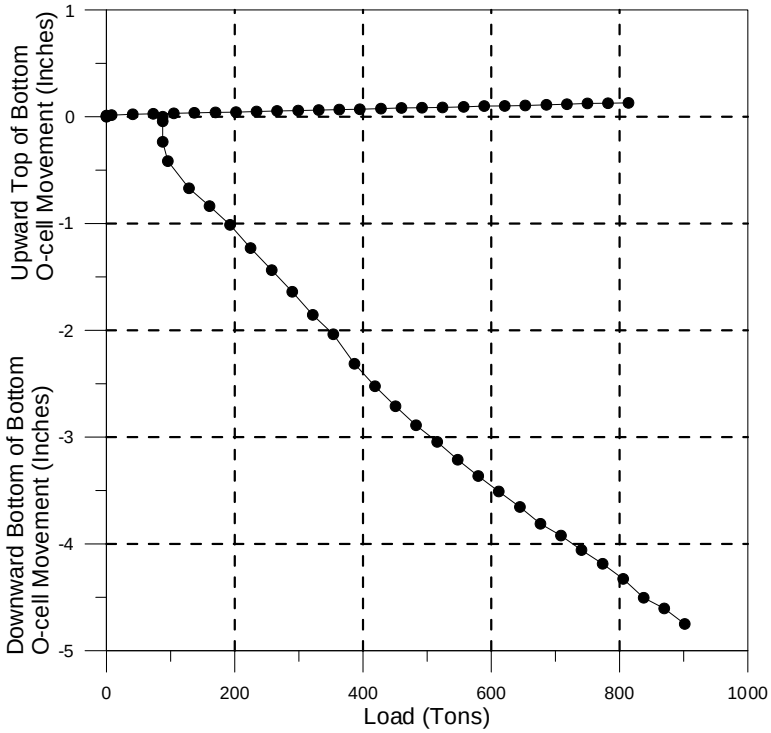

Figure 62
O-cell load settlement curve DS04

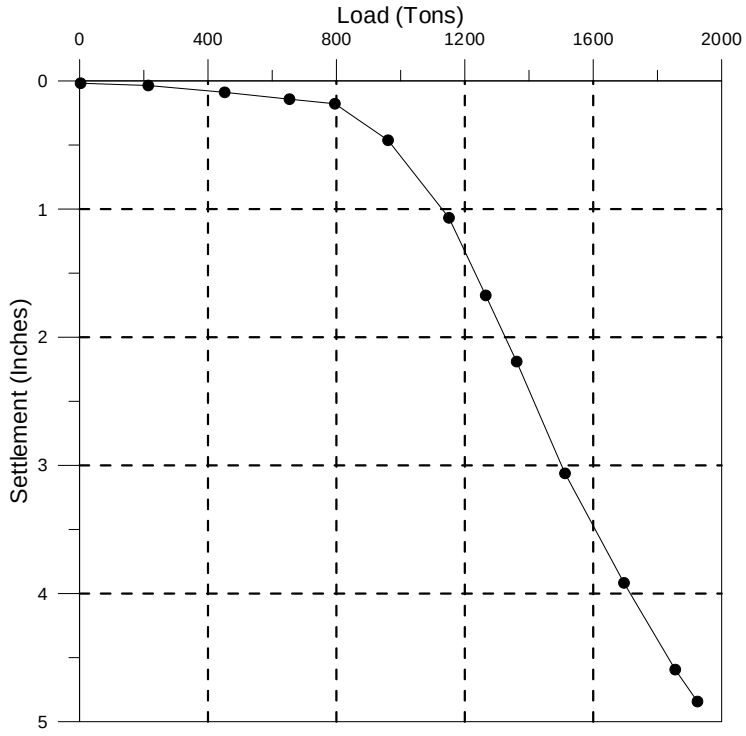

Figure 63
Equivalent top-down load settlement curve DS04

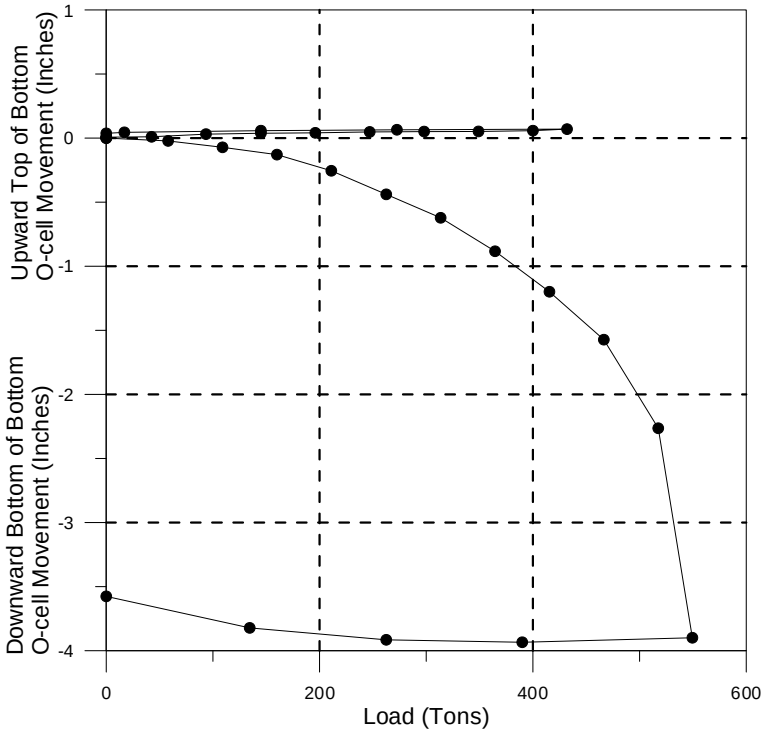

Figure 64

Lower O-cell load movement curves-stage 1 DS05

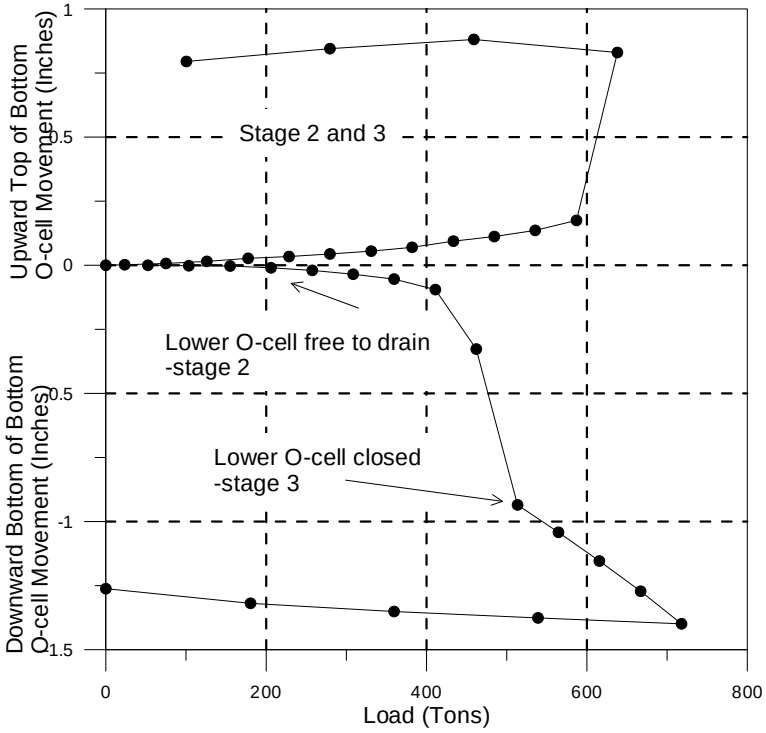

Figure 65

Upper O-cell load movement curves-stage 2 DS05

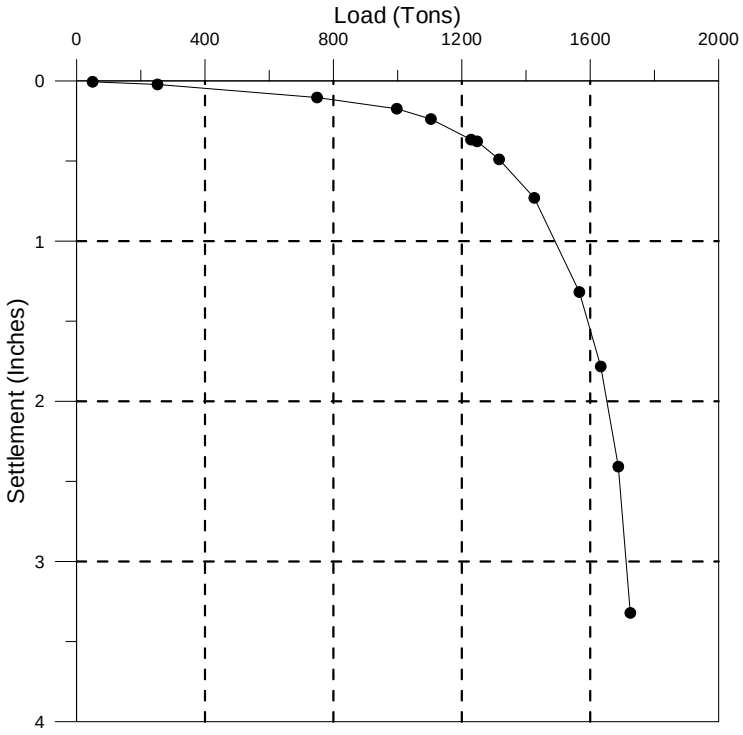

Figure 66
Equivalent top-down load settlement curve DS05

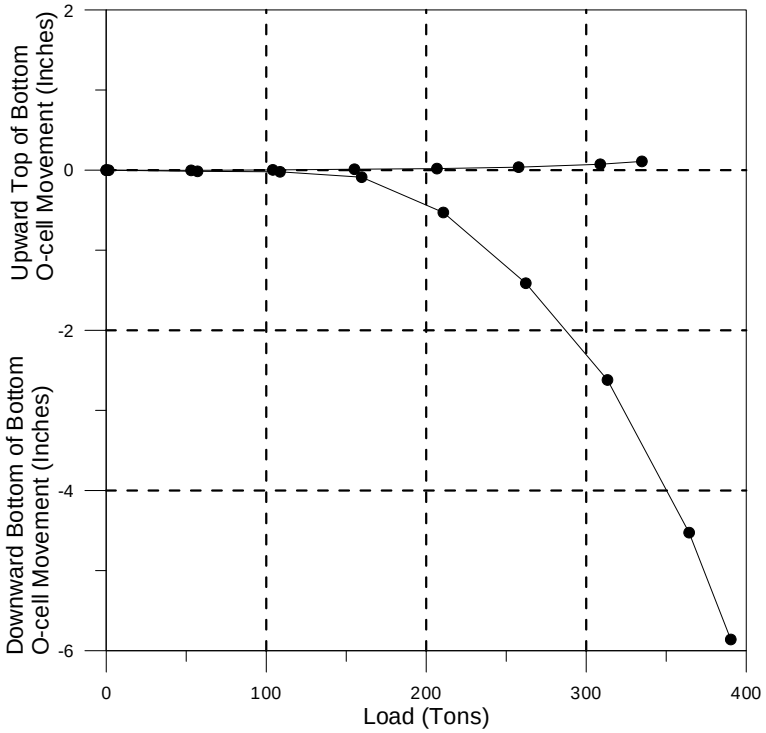

Figure 67
O-cell load settlement curve DS06

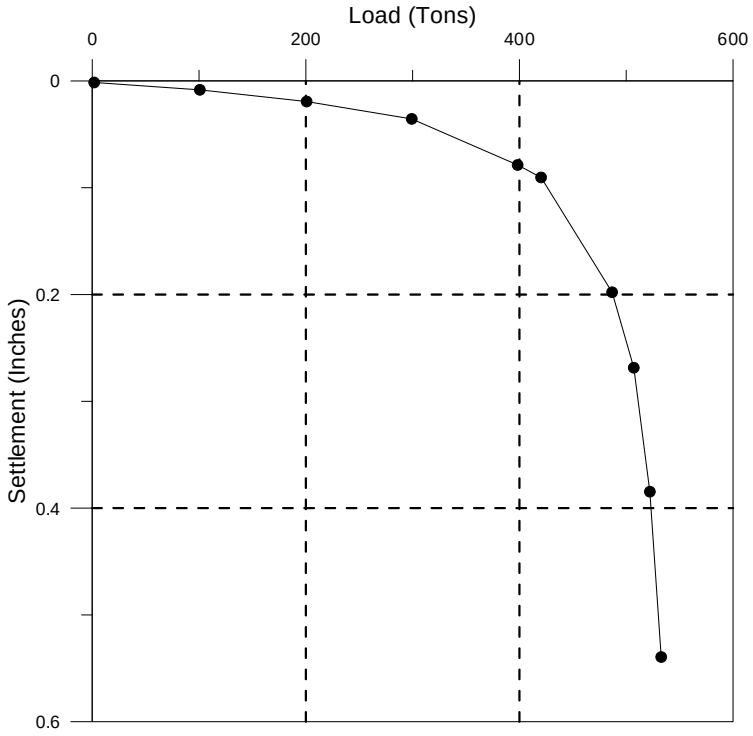

Figure 68
Equivalent top-down load settlement curve DS06

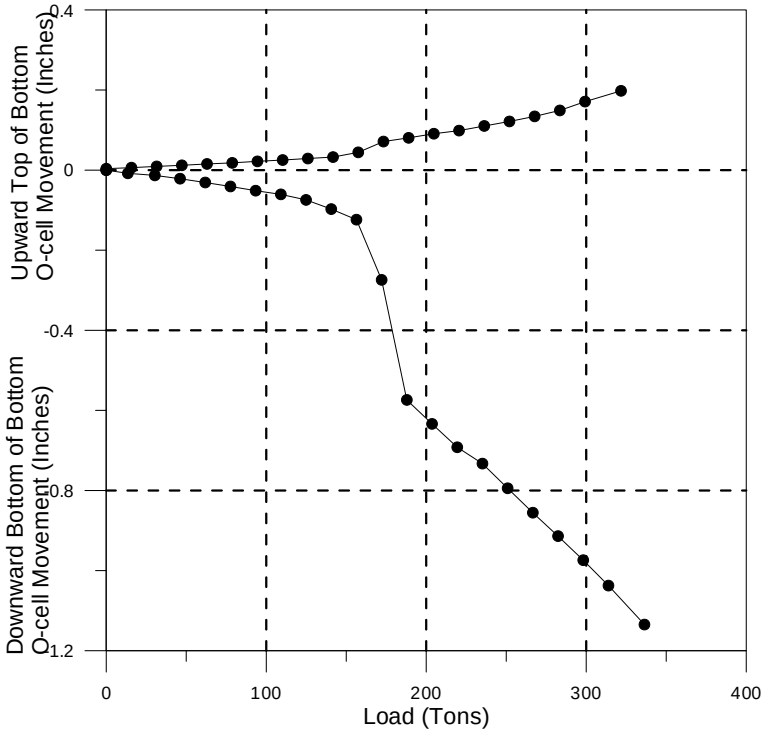

Figure 69
O-cell load settlement curve DS07

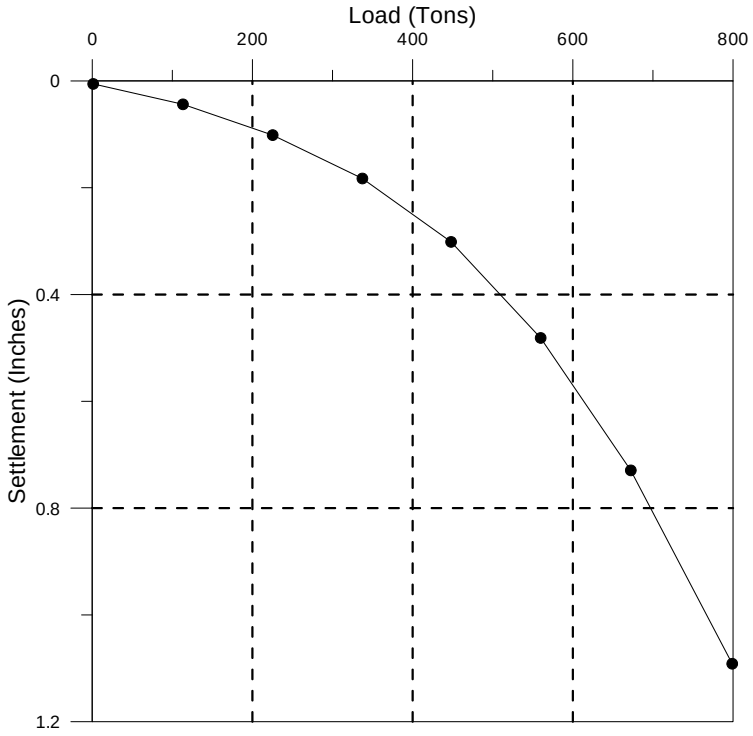

Figure 70
Equivalent top-down load settlement curve DS07

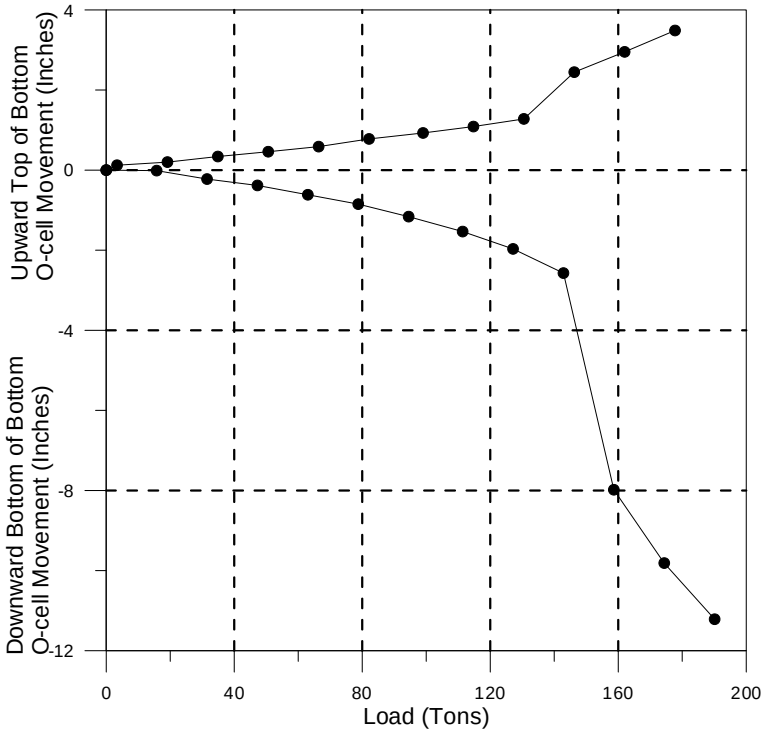

Figure 71
O-cell load settlement curve DS08

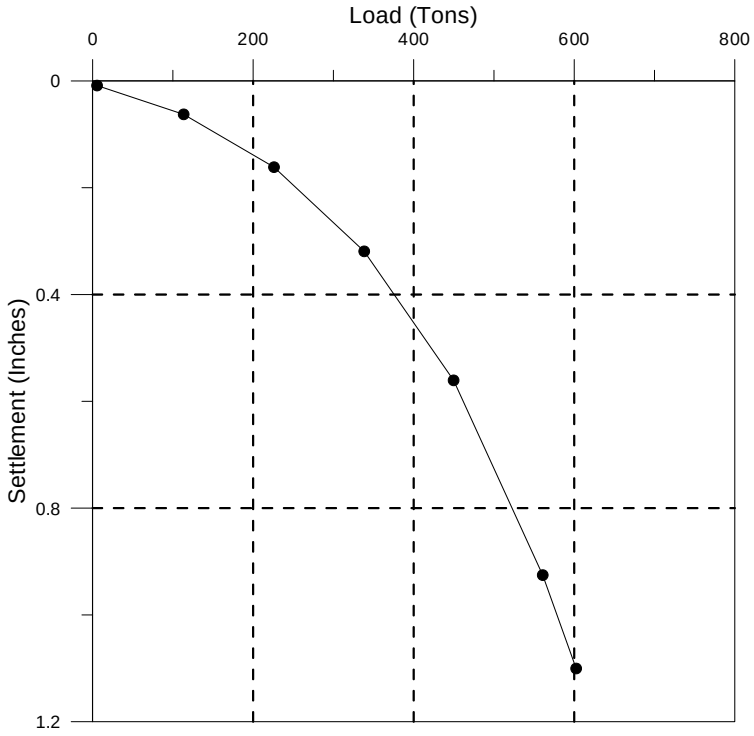

Figure 72
Equivalent top-down load settlement curve DS08

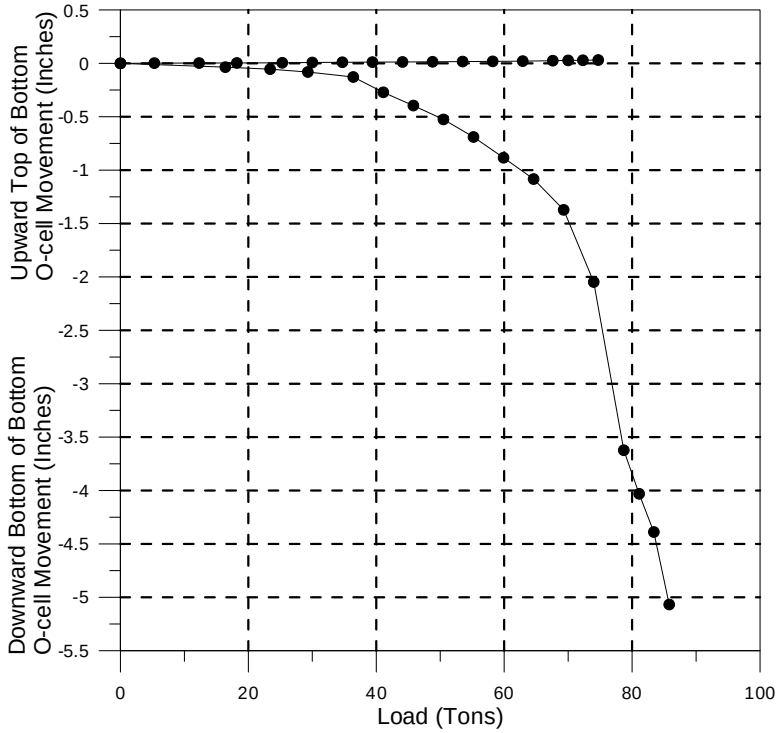

Figure 73

Lower O-cell load movement curves-stage 1 DS09

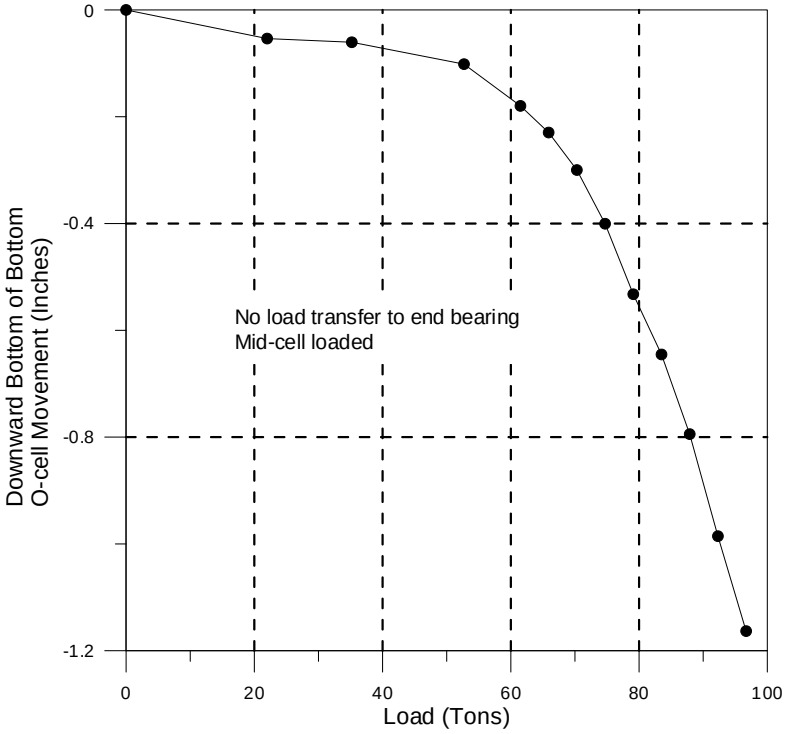

Figure 74

Upper O-cell load movement curves-stage 2 DS09

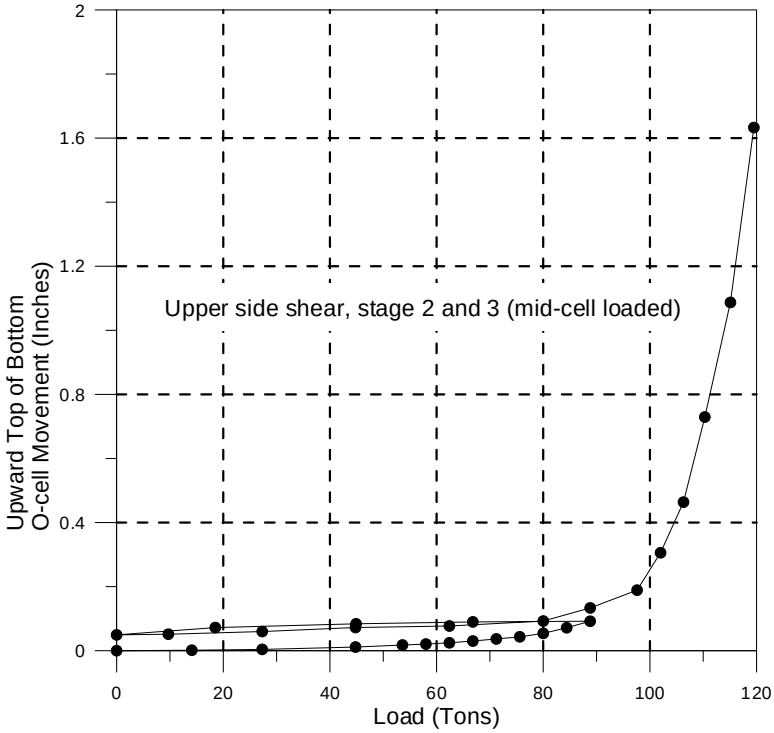

Figure 75
Upper O-cell load movement curves-stage 2 and 3 DS09

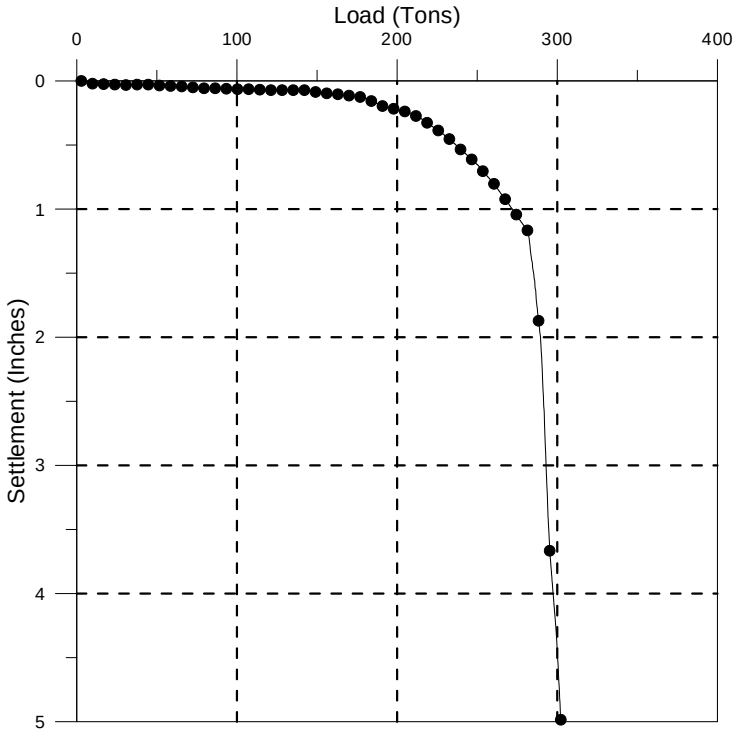

Figure 76
Equivalent top-down load settlement curve DS09

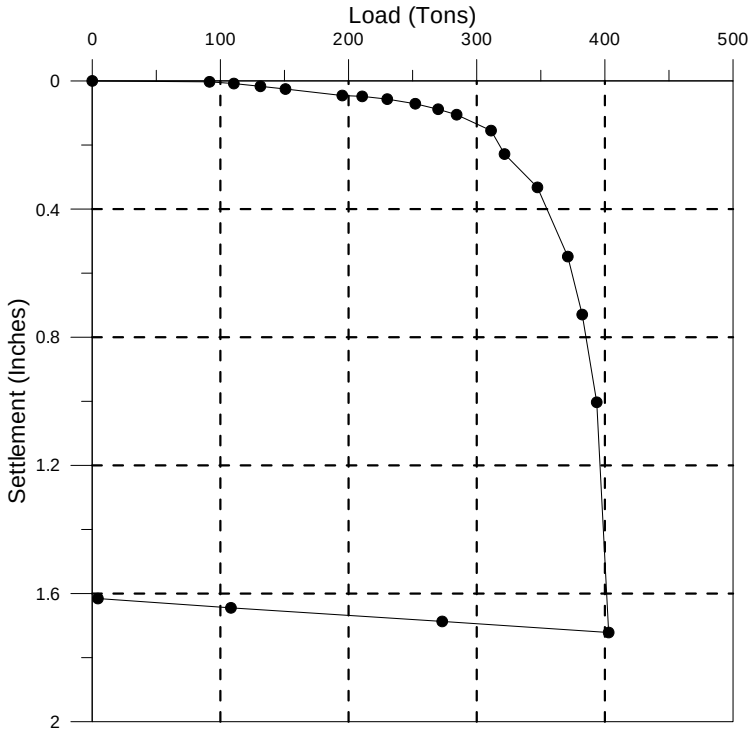

Figure 77
Top-down load settlement curve of DS10

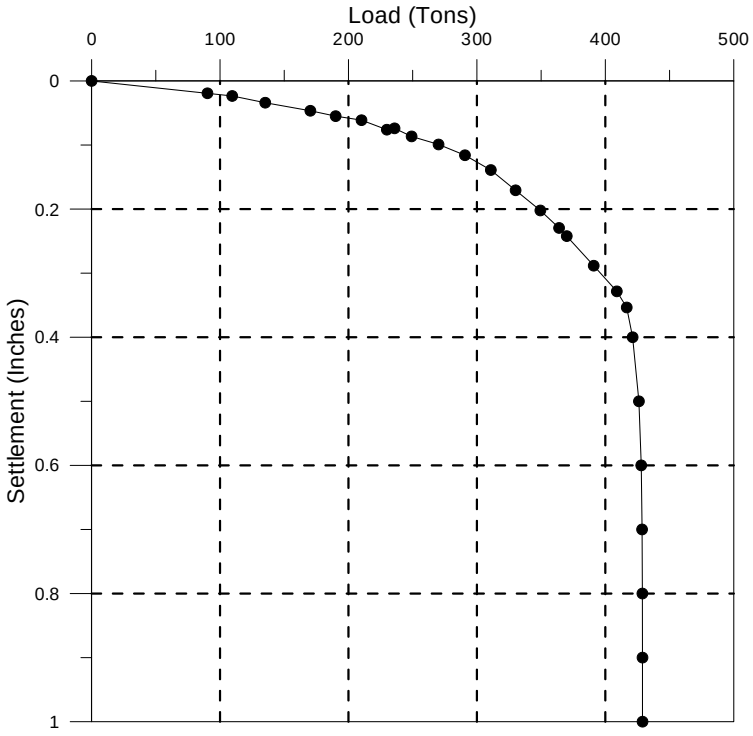

Figure 78
Top-down load settlement curve of DS11

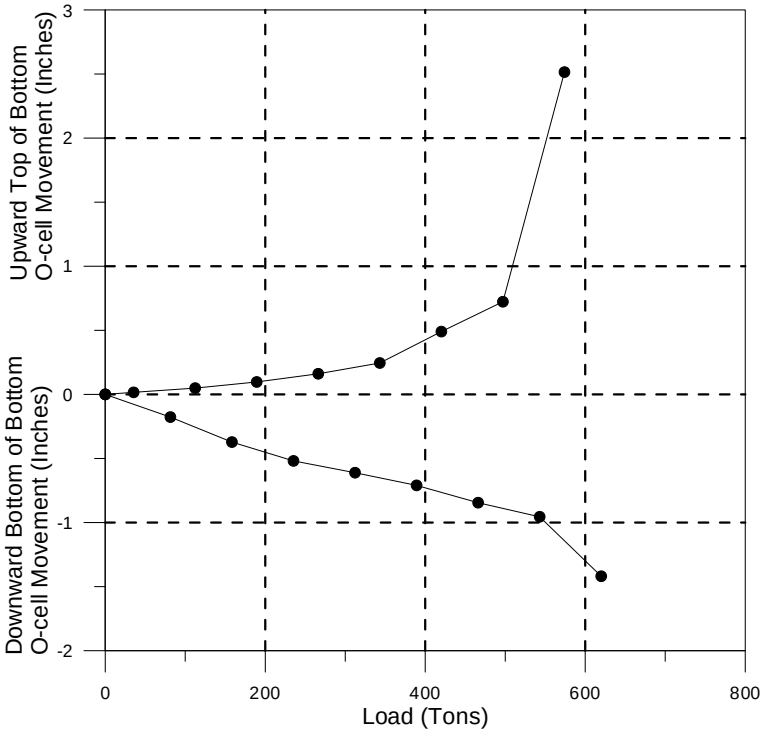

Figure 79
O-cell load settlement curve DS12

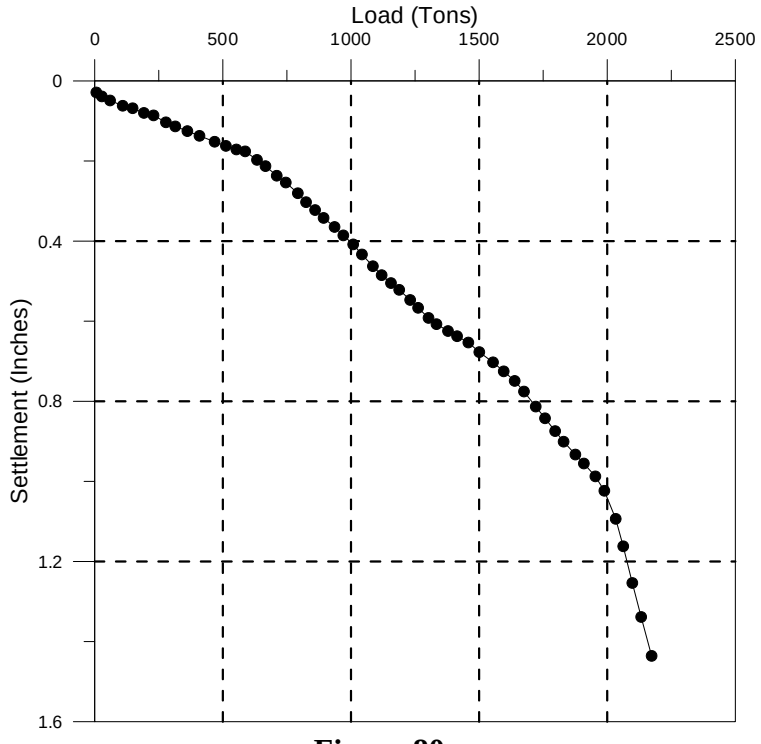

Figure 80
Equivalent top-down load settlement curve DS12

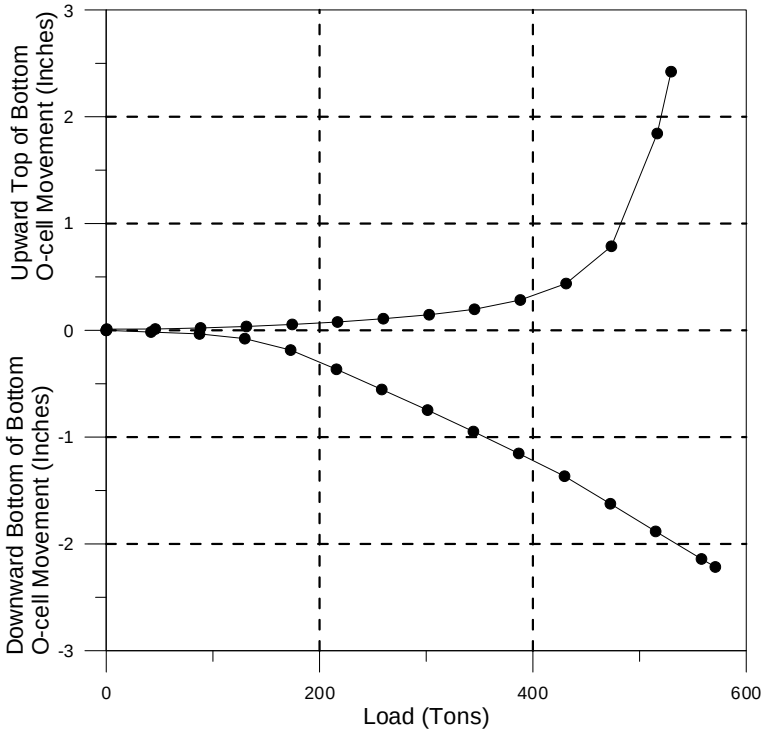

Figure 81
O-cell load settlement curve DS13

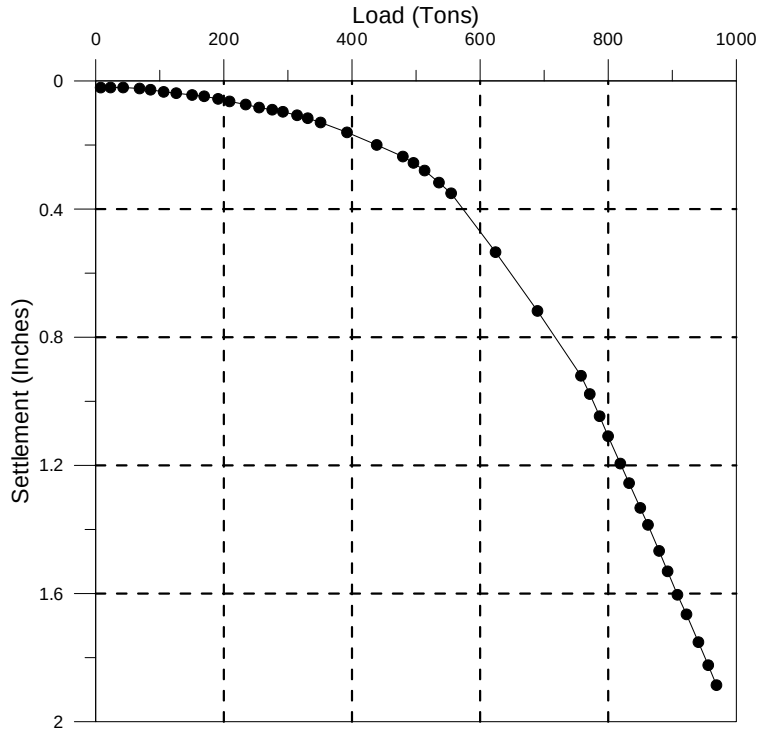

Figure 82
Equivalent top-down load settlement curve DS13

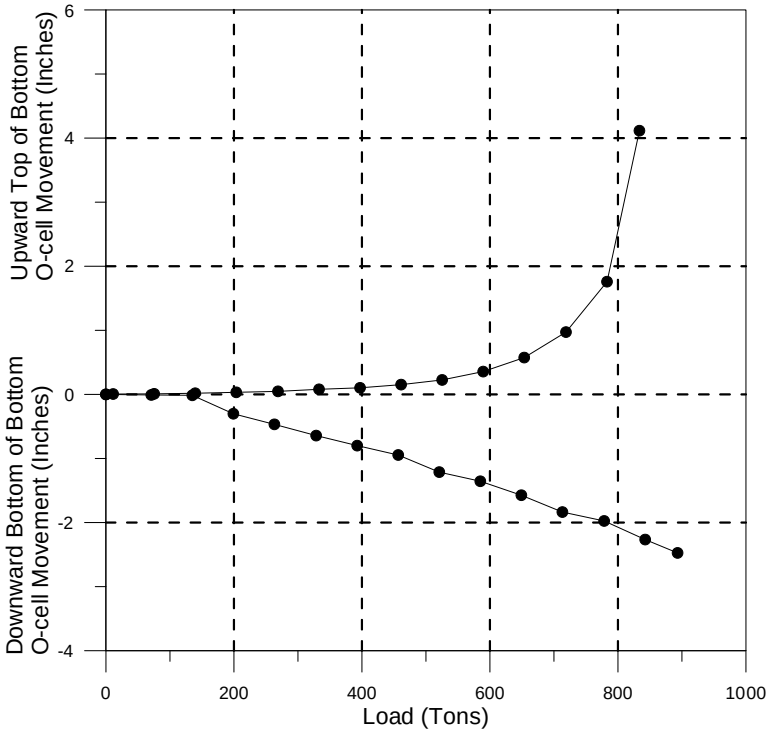

Figure 83
O-cell load settlement curve DS14

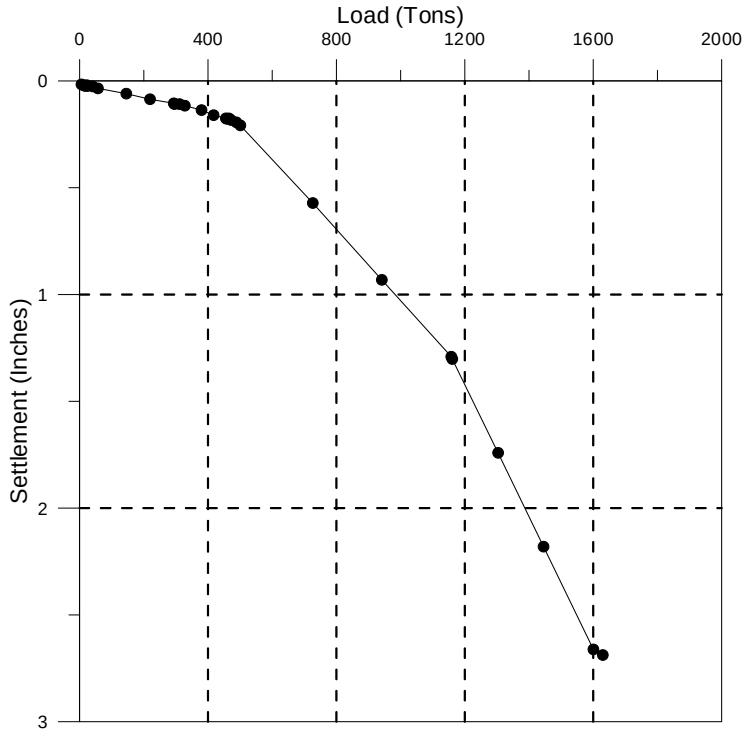

Figure 84
Equivalent top-down load settlement curve DS14

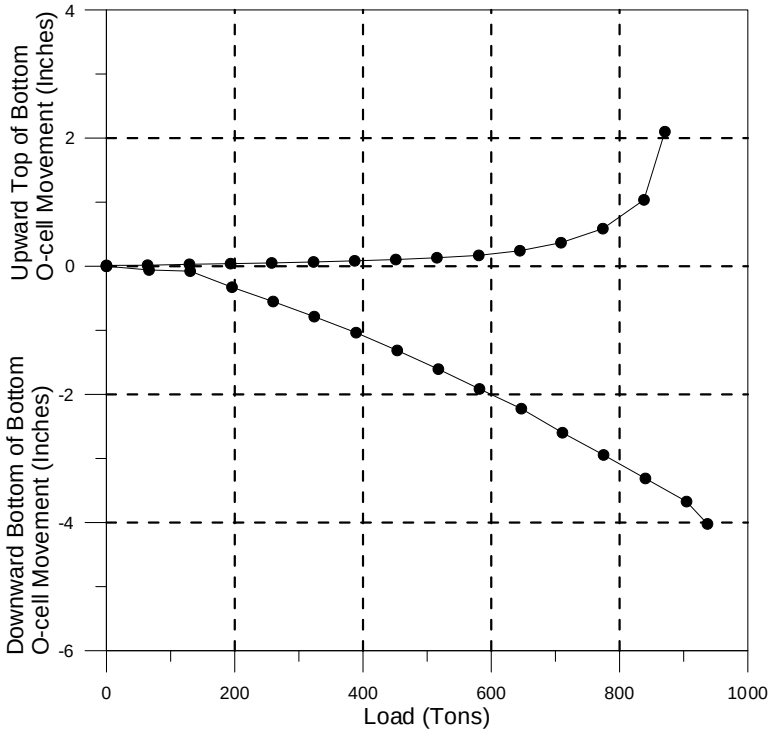

Figure 85
O-cell load settlement curve DS15

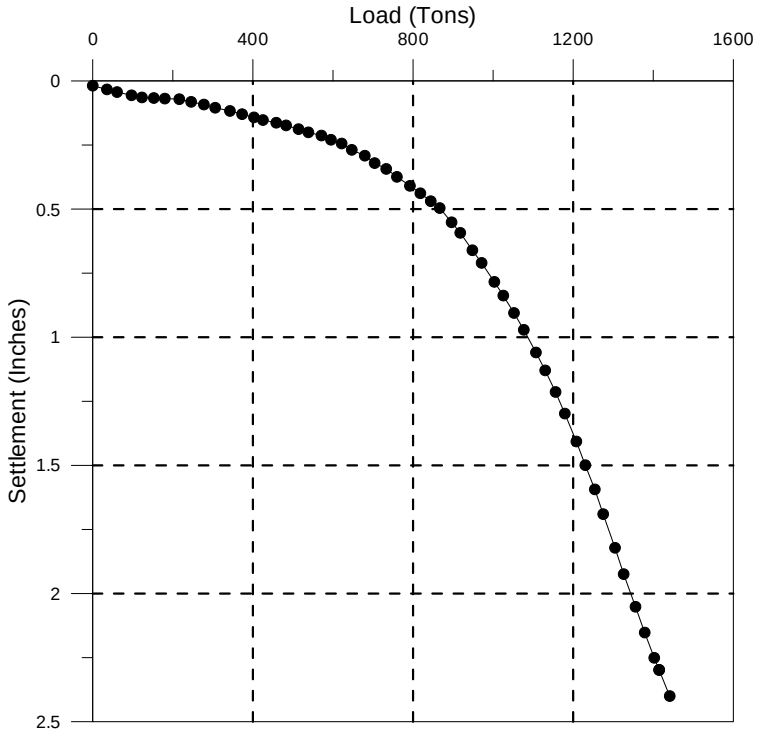

Figure 86
Equivalent top-down load settlement curve DS15

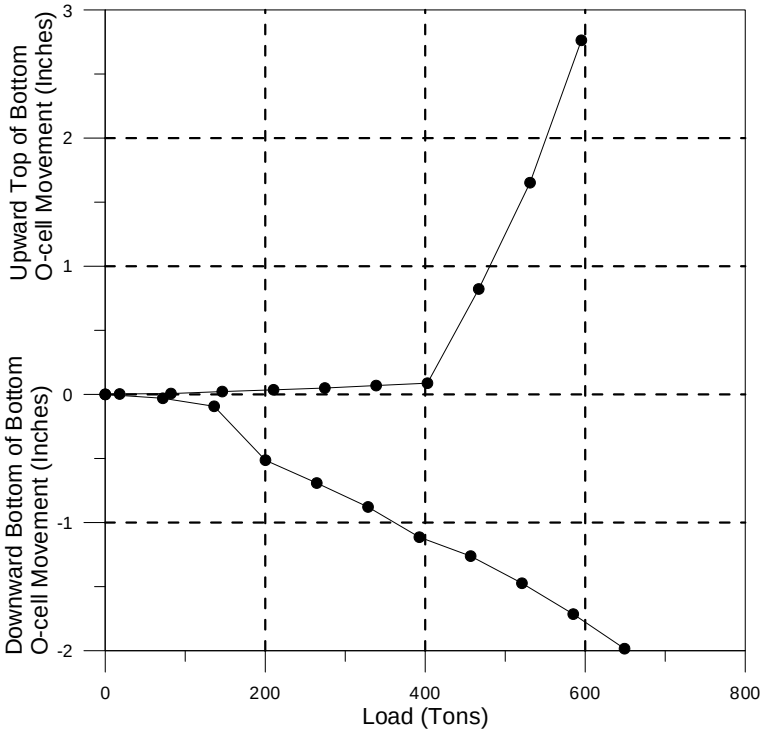

Figure 87
O-cell load settlement curve DS16

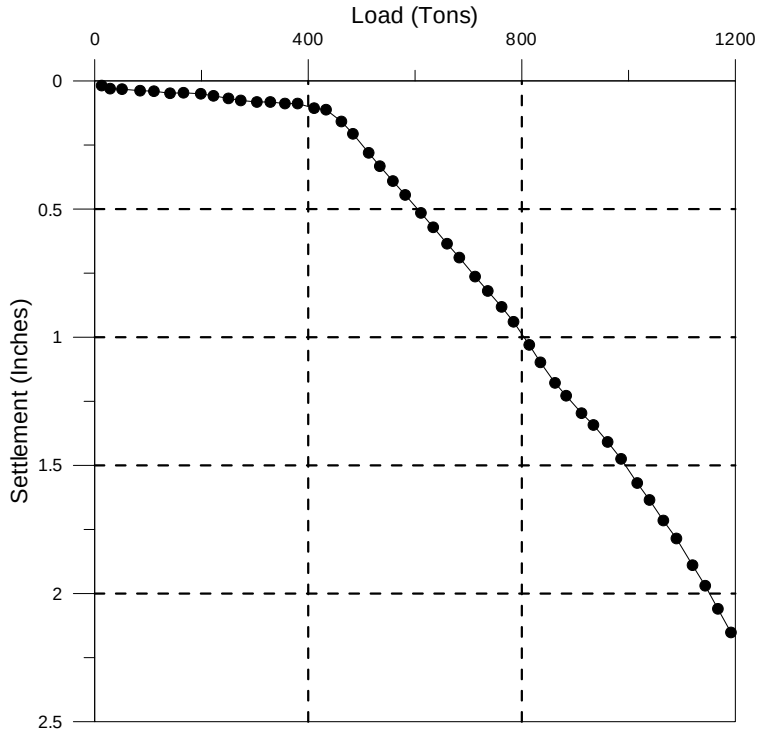

Figure 88
Equivalent top-down load settlement curve DS16

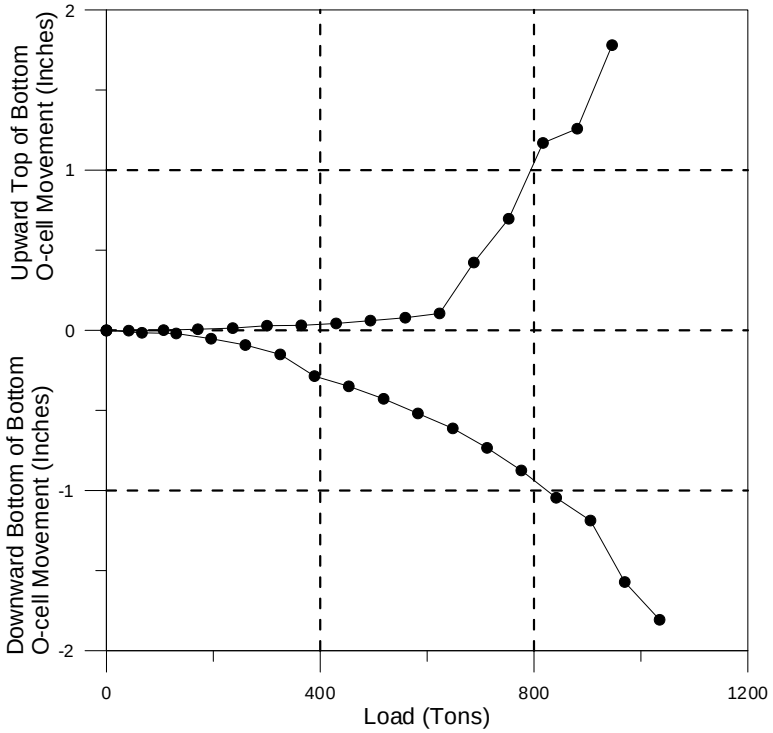

Figure 89
O-cell load settlement curve DS17

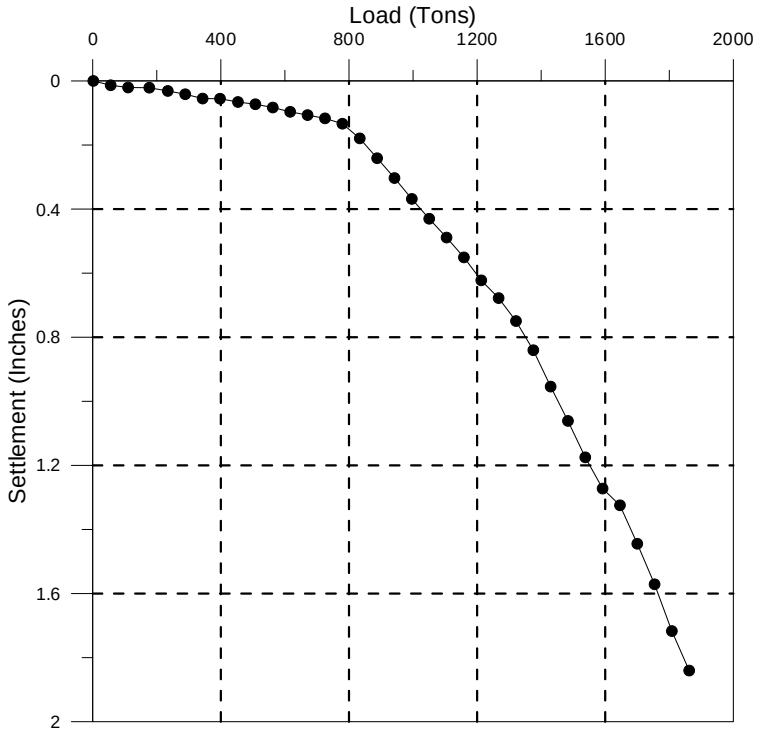

Figure 90
Equivalent top-down load settlement curve DS17

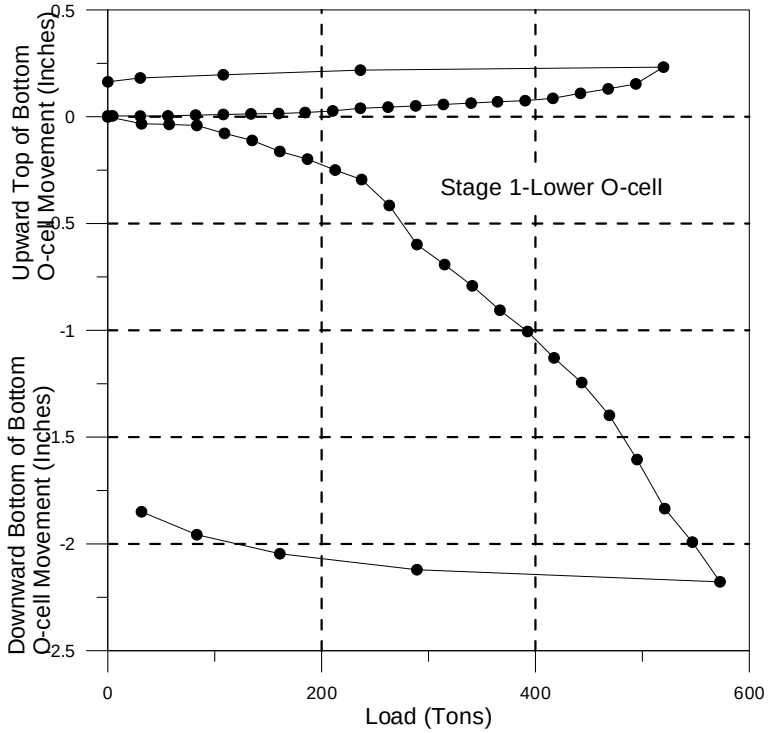

Figure 91

Lower O-cell load movement curves-stage 1 DS18

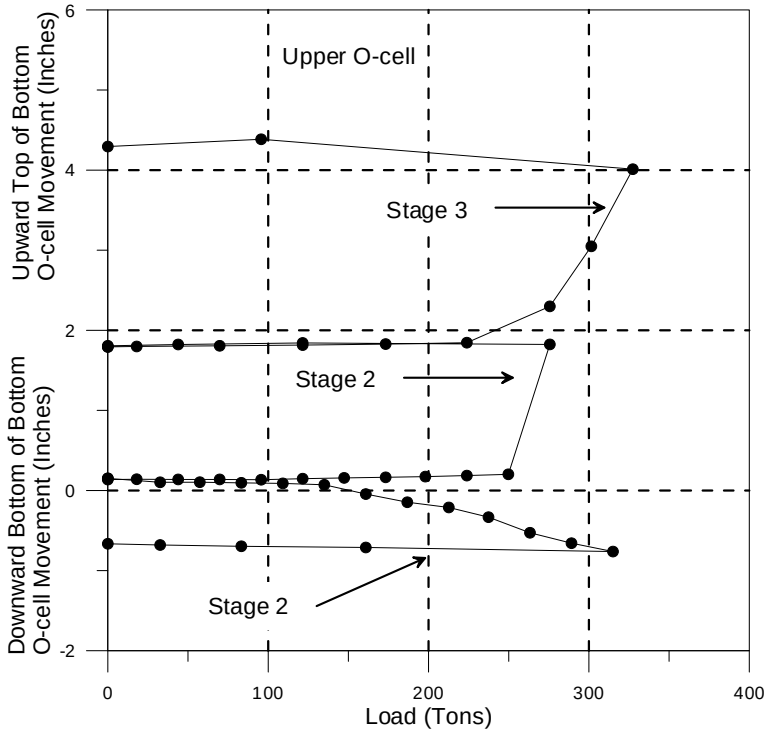

Figure 92

Upper O-cell load movement curves-stage 2 DS18

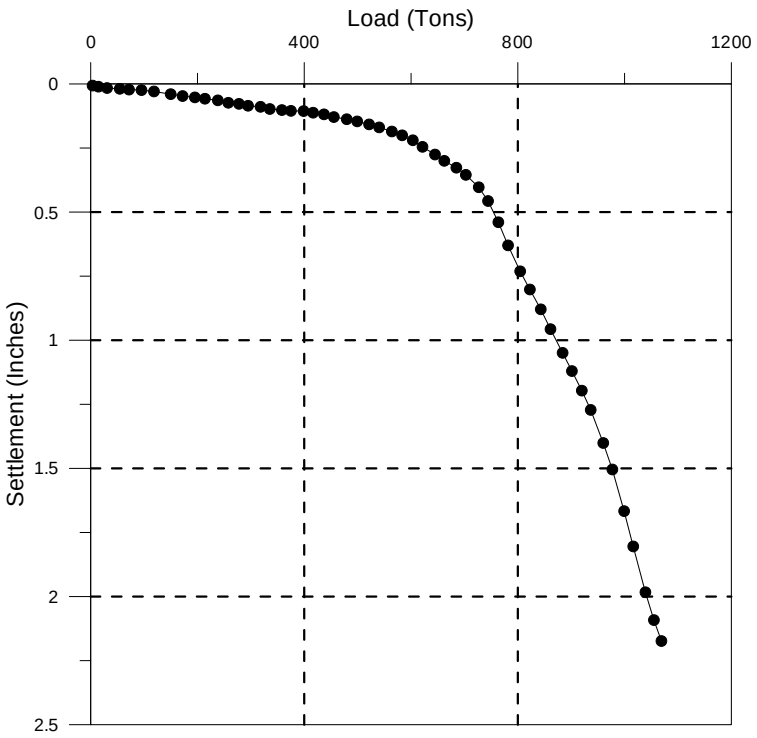

Figure 93
Equivalent top-down load settlement curve DS18

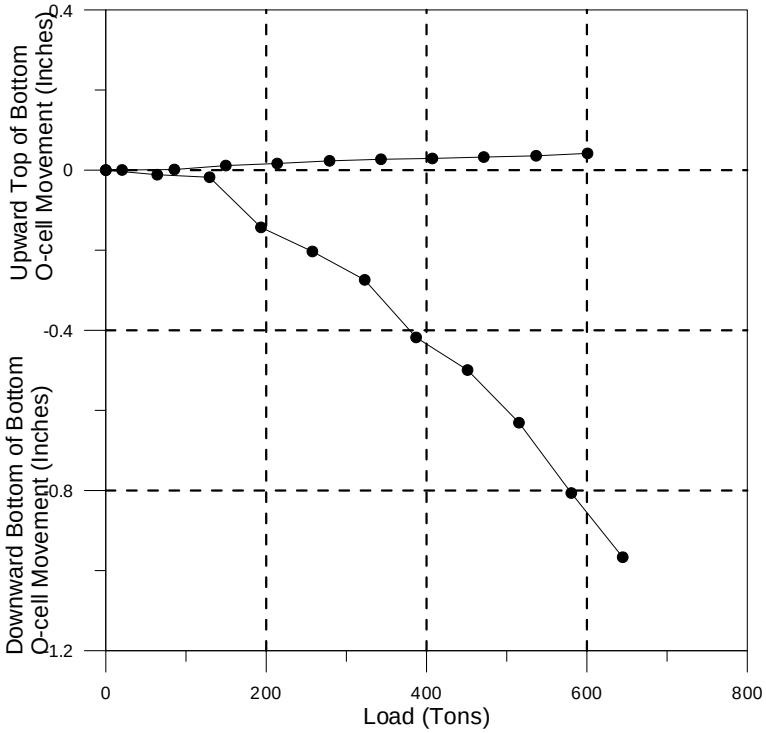

Figure 94
O-cell load settlement curve DS19

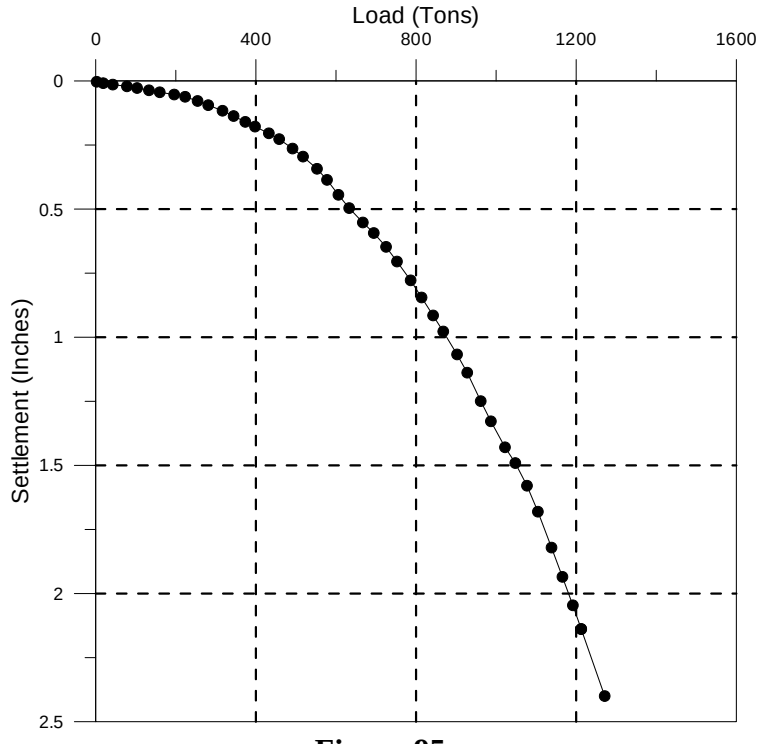

Figure 95
Equivalent top-down load settlement curve DS19

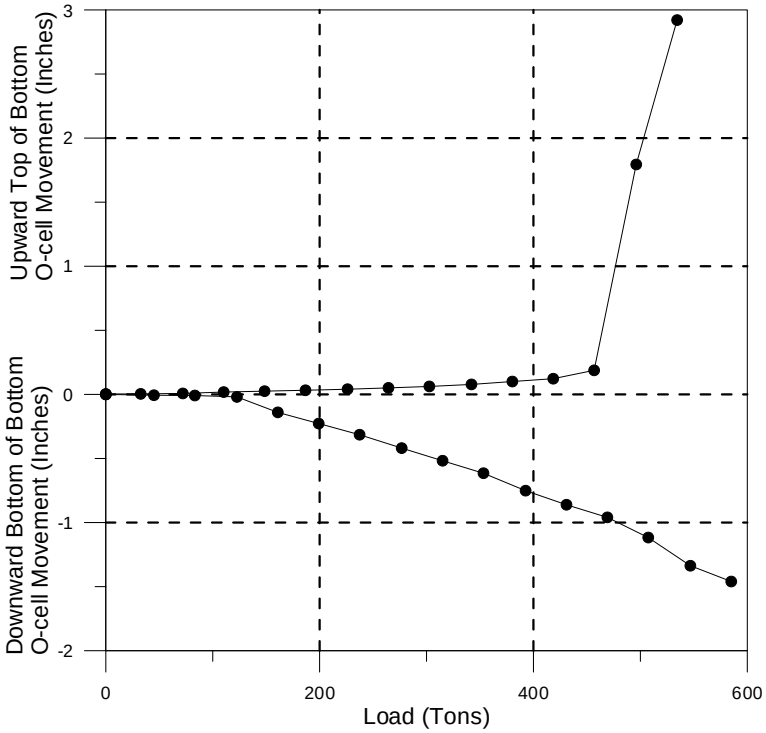

Figure 96
O-cell load settlement curve DS20

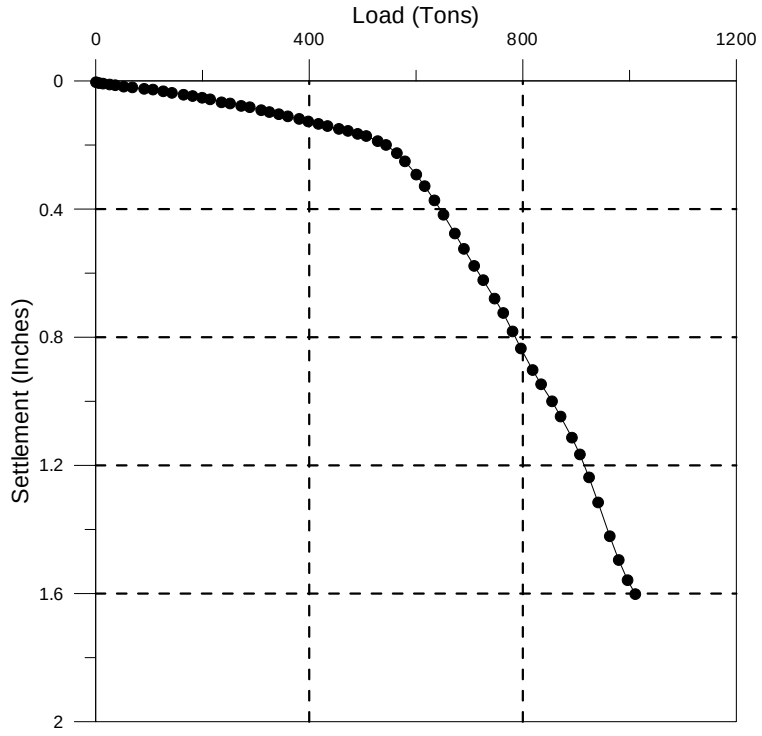

Figure 97
Equivalent top-down load settlement curve DS20

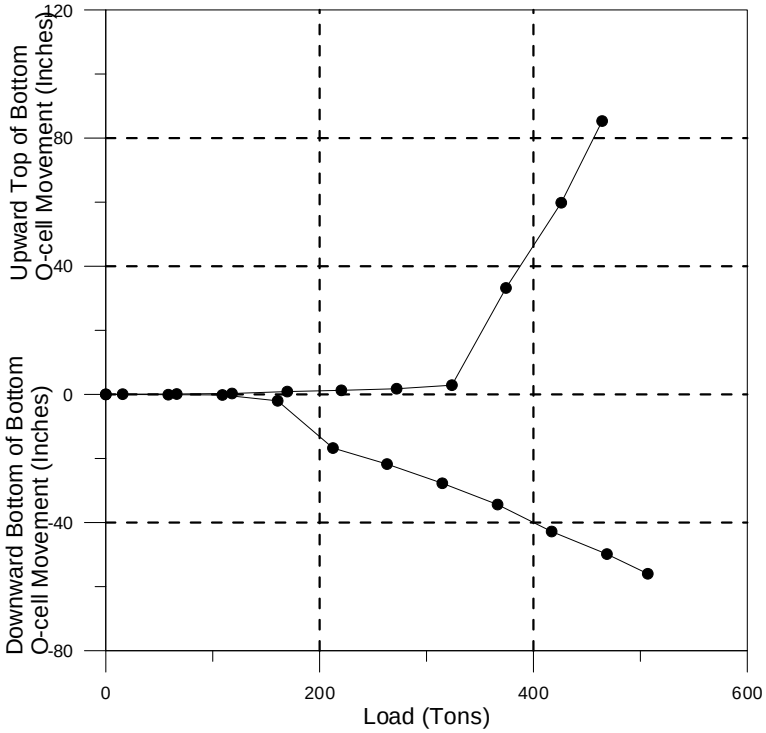

Figure 98
O-cell load settlement curve DS21

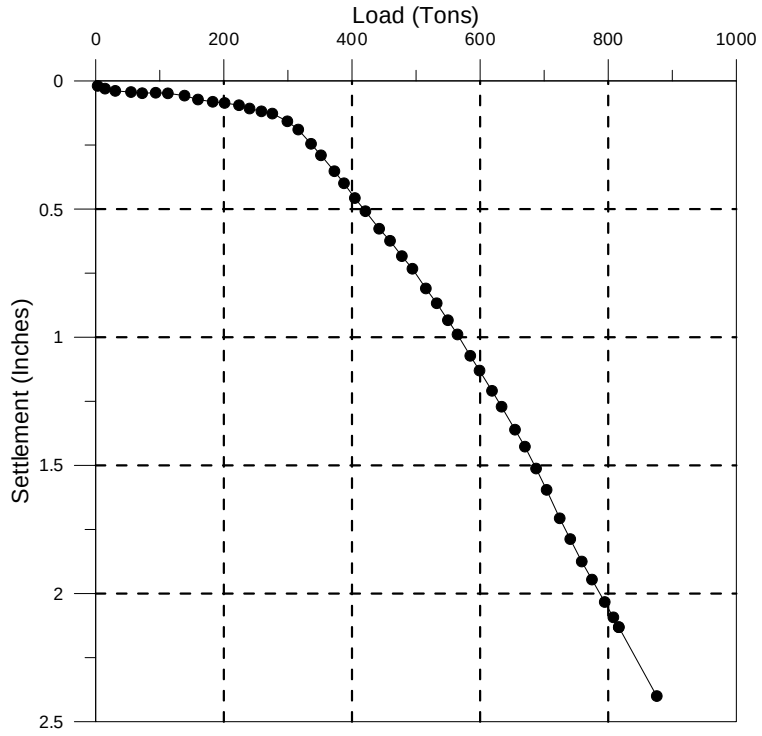

Figure 99
Equivalent top-down load settlement curve DS21

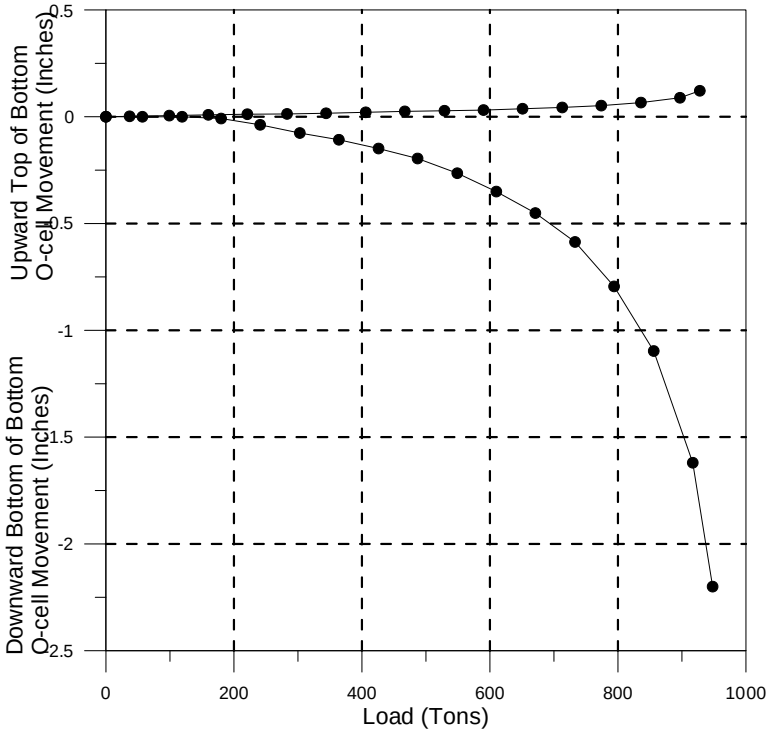

Figure 100
O-cell load settlement curve DS22

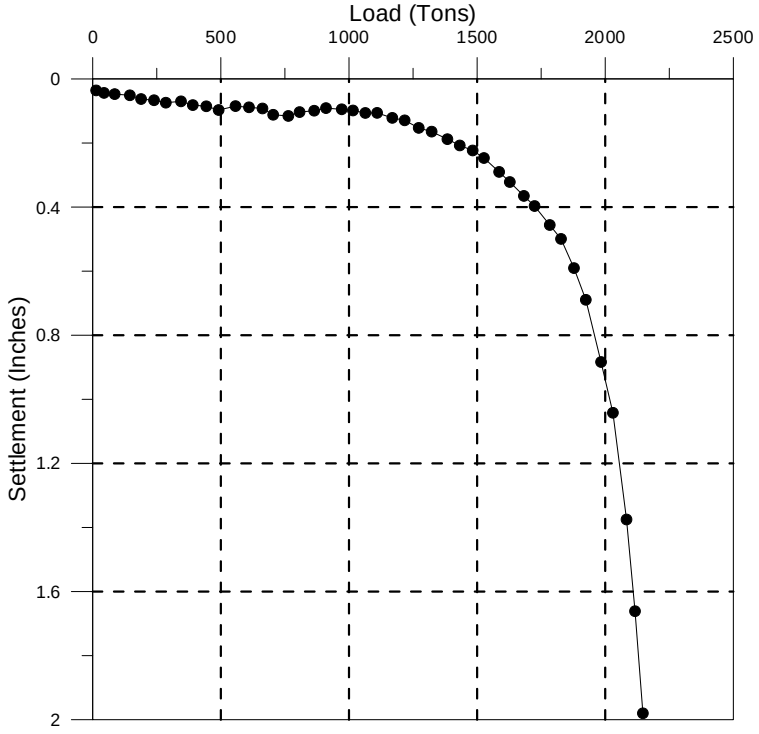

Figure 101
Equivalent top-down load settlement curve DS22

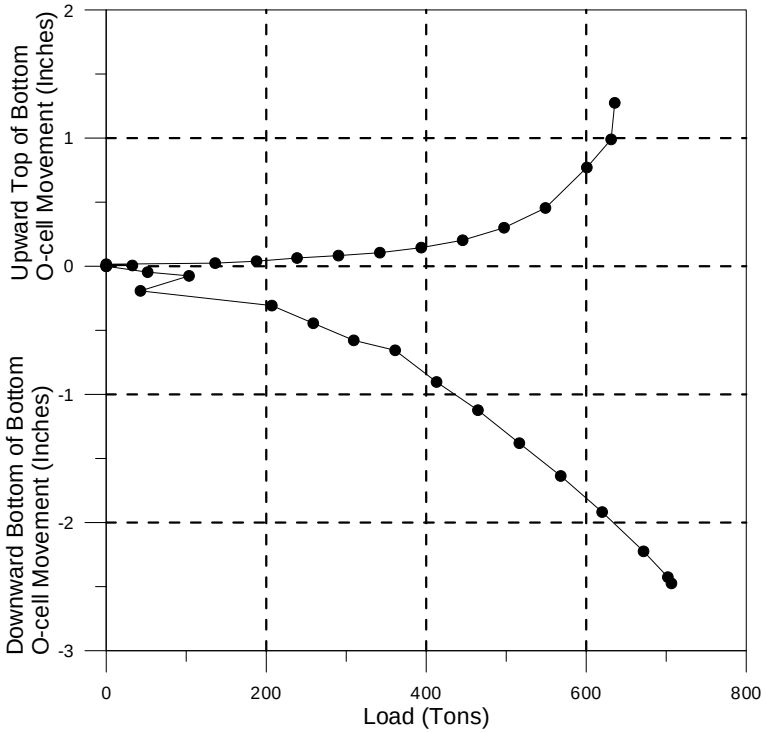

Figure 102
O-cell load settlement curve DS23

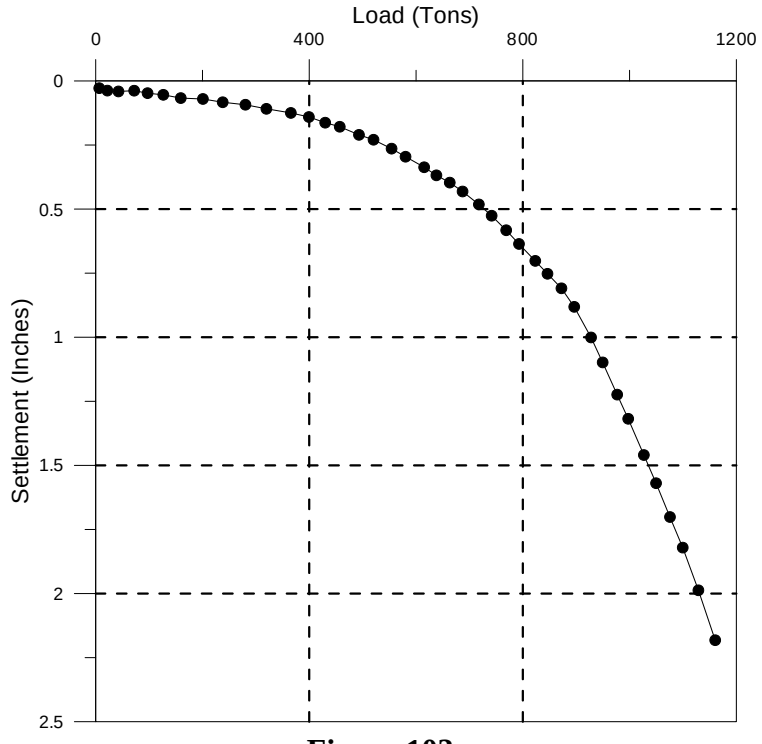

Figure 103
Equivalent top-down load settlement curve DS23

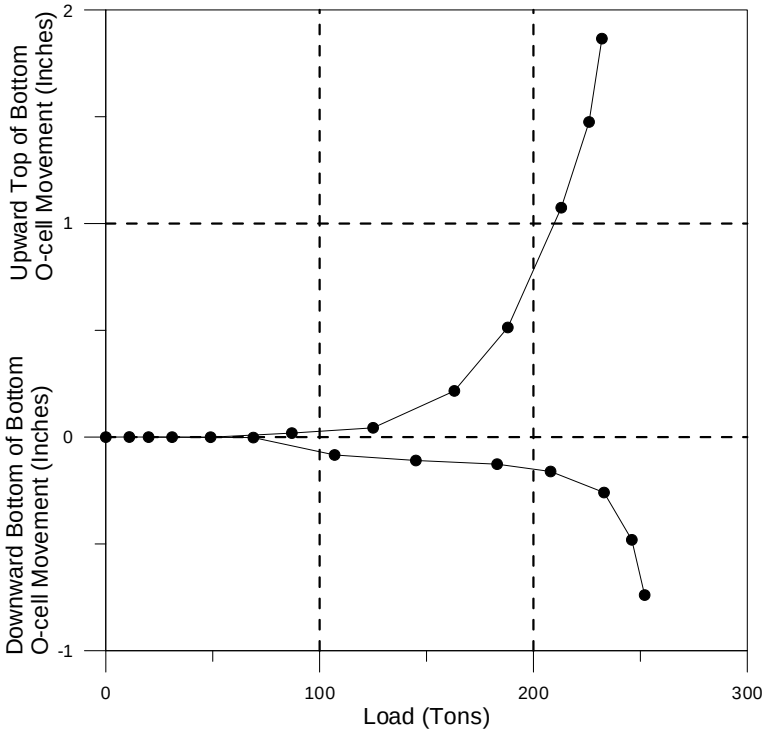

Figure 104
O-cell load settlement curve DS24

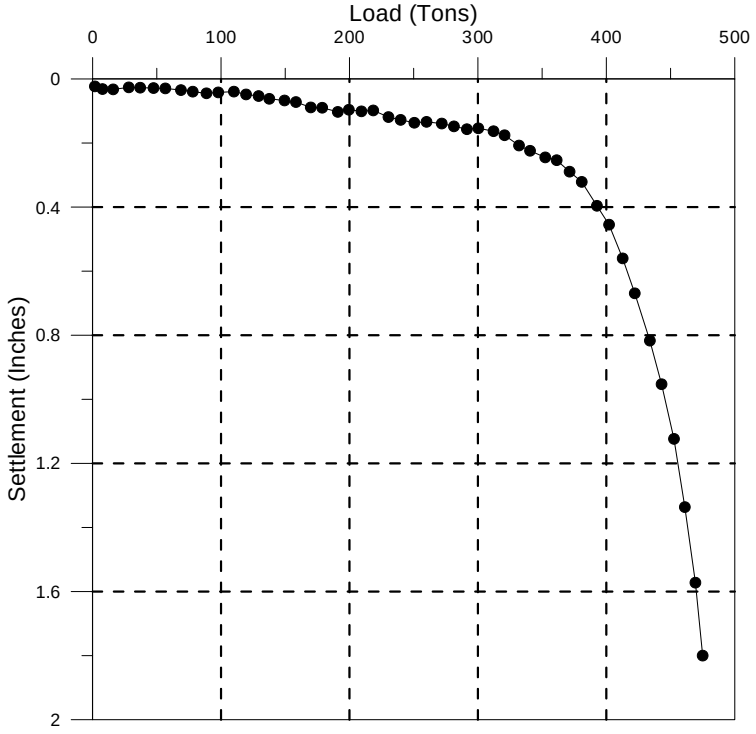

Figure 105
Equivalent top-down load settlement curve DS24

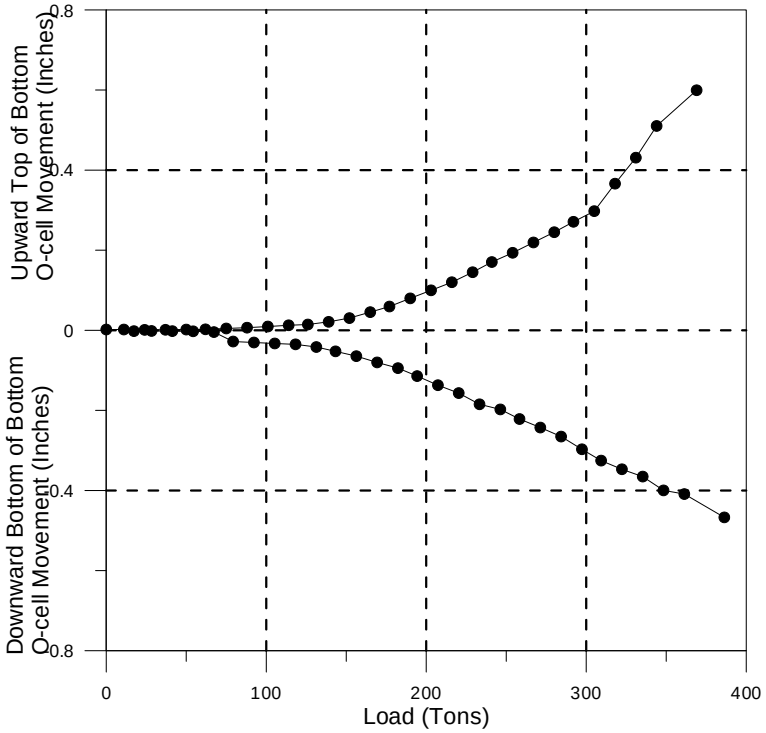

Figure 106
O-cell load settlement curve DS25

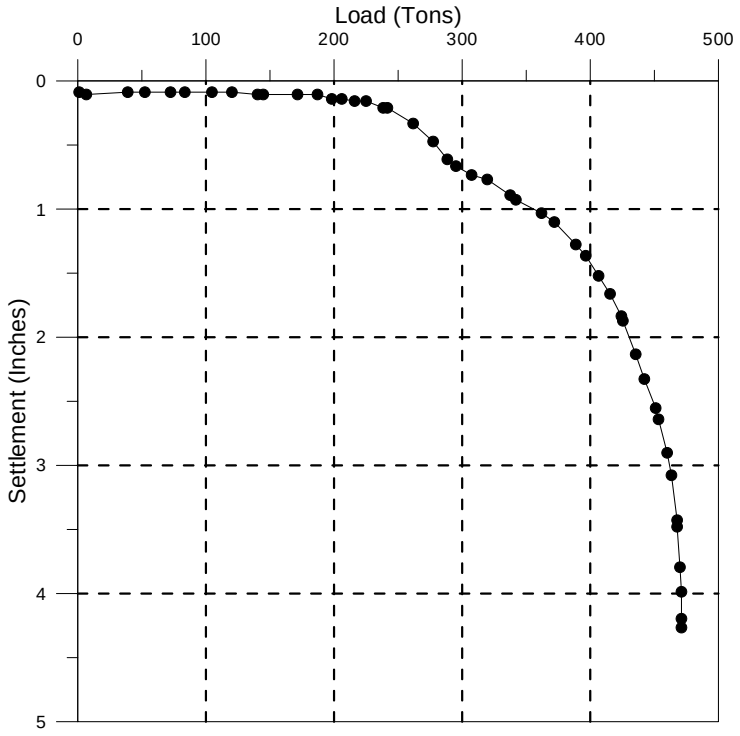

Figure 107
Equivalent top-down load settlement curve DS25

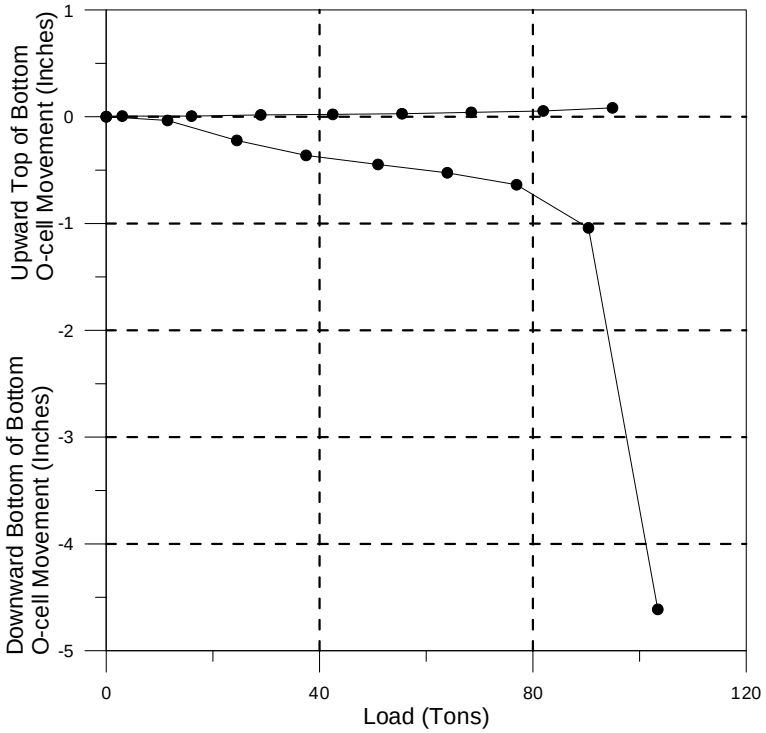

Figure 108
O-cell load settlement curve DS26

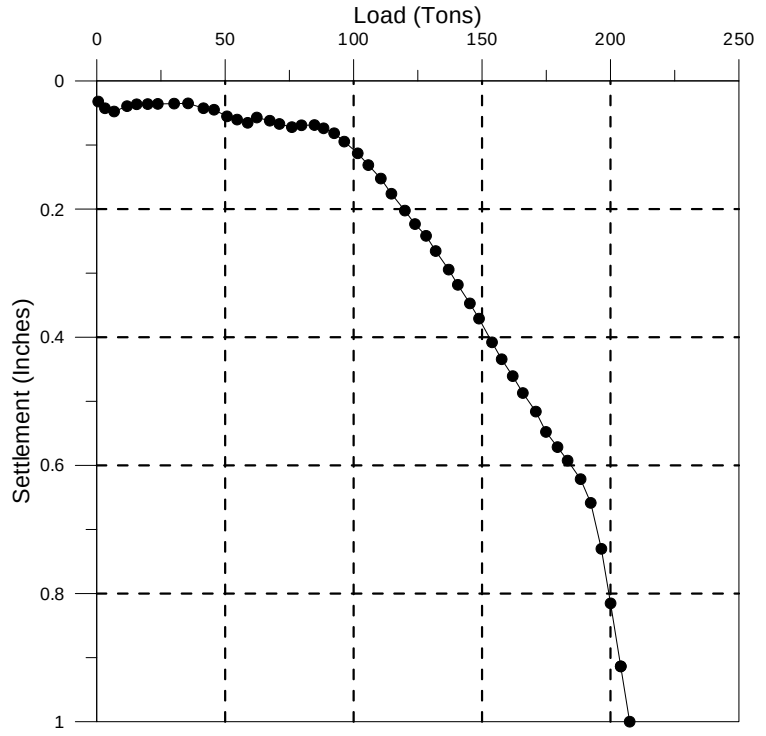

Figure 109
Equivalent top-down load settlement curve DS26

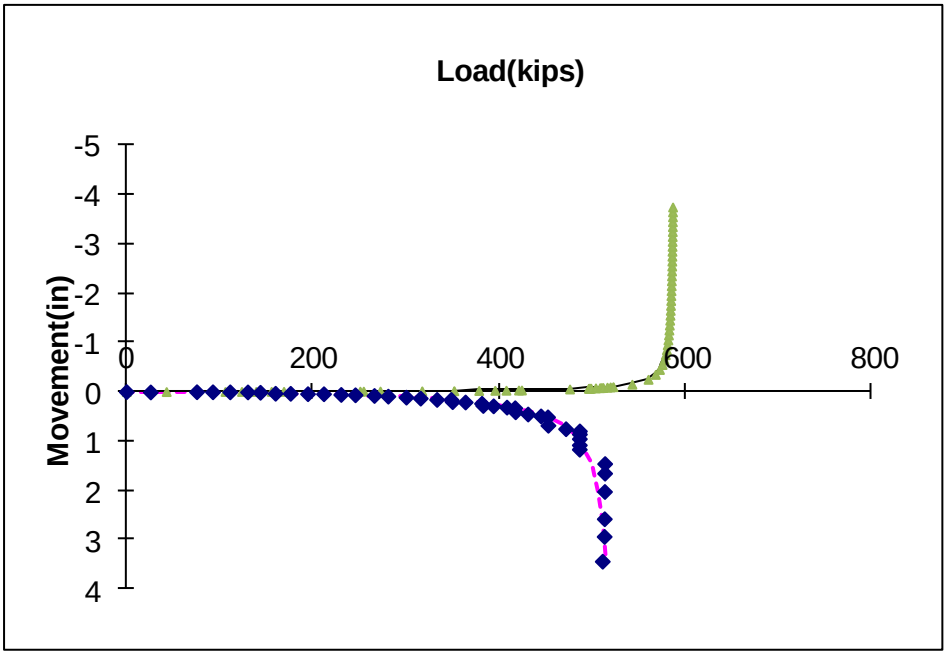

Figure 110
O-cell load settlement curve DS27

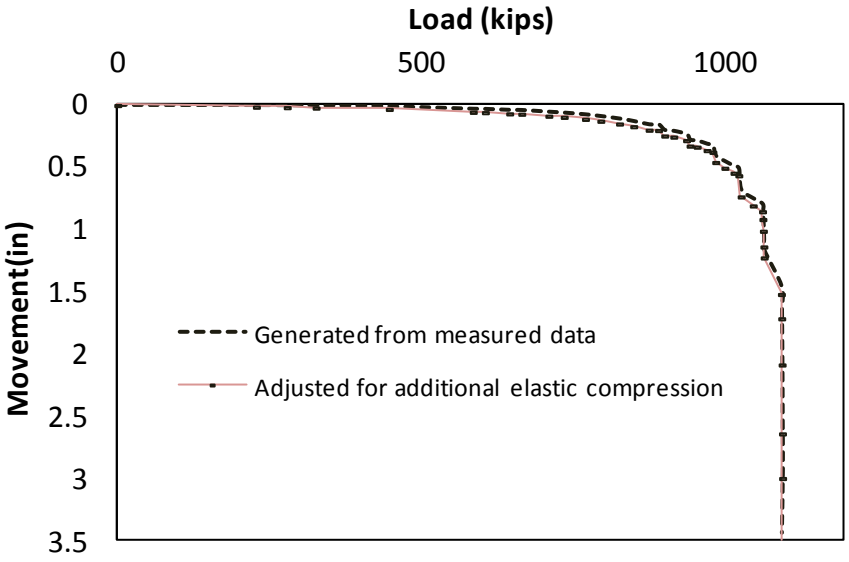

Figure 111
Equivalent top-down load settlement curve DS27

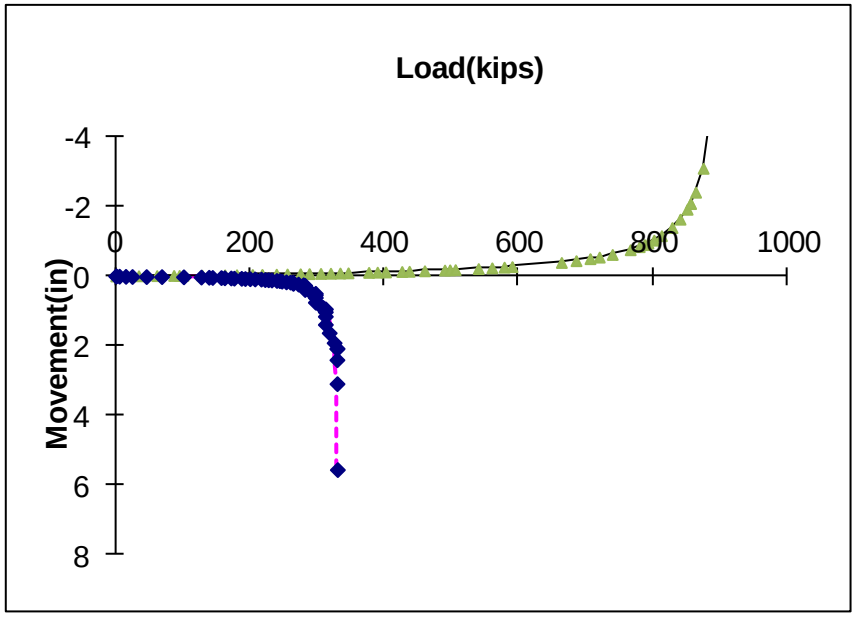

Figure 112
O-cell load settlement curve DS28

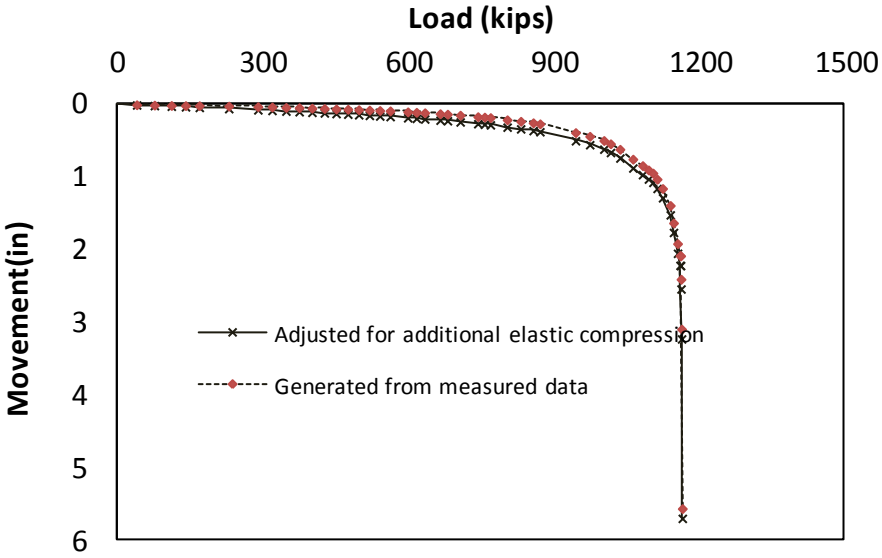

Figure 113
Equivalent top-down load settlement curve DS28

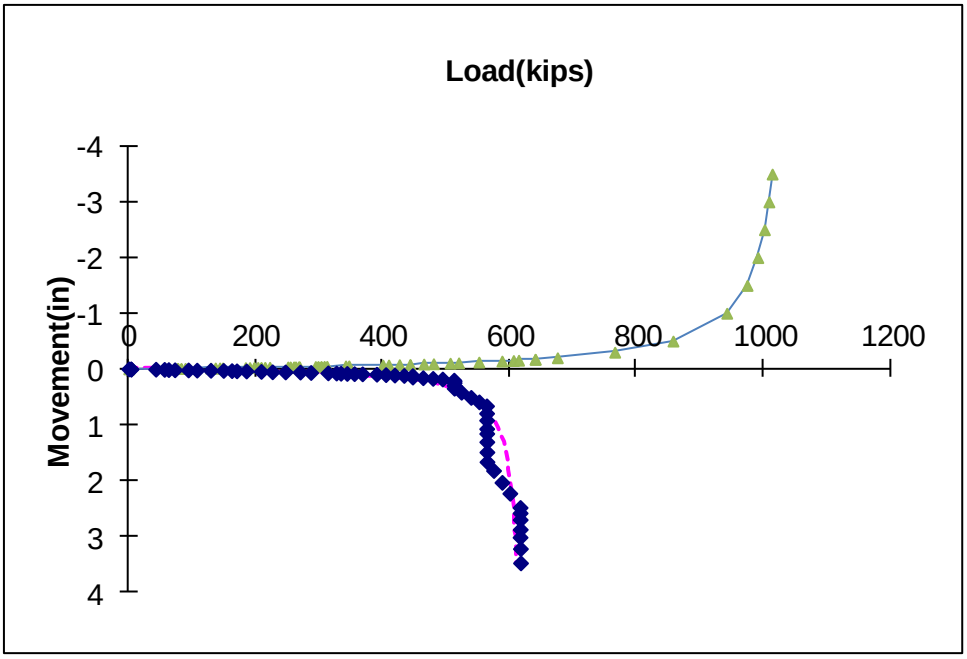

Figure 114
O-cell load settlement curve DS29

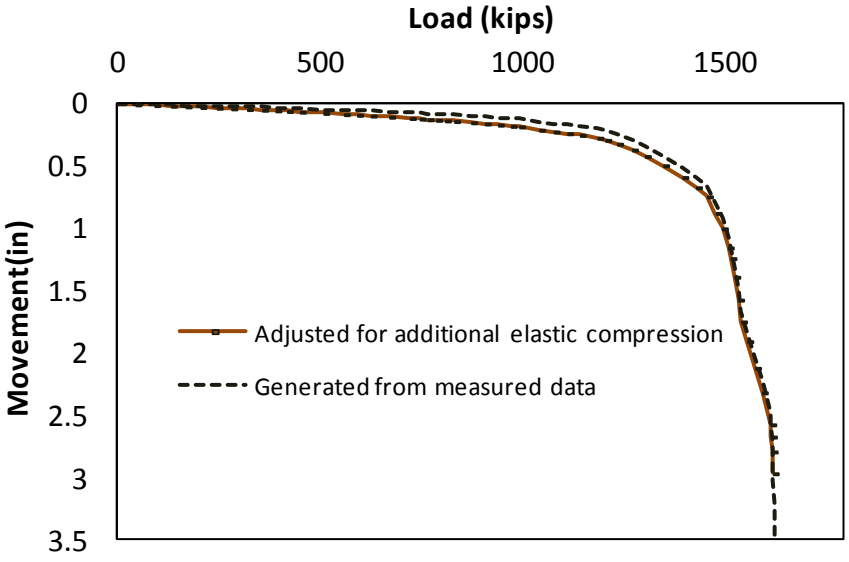

Figure 115
Equivalent top-down load settlement curve DS29

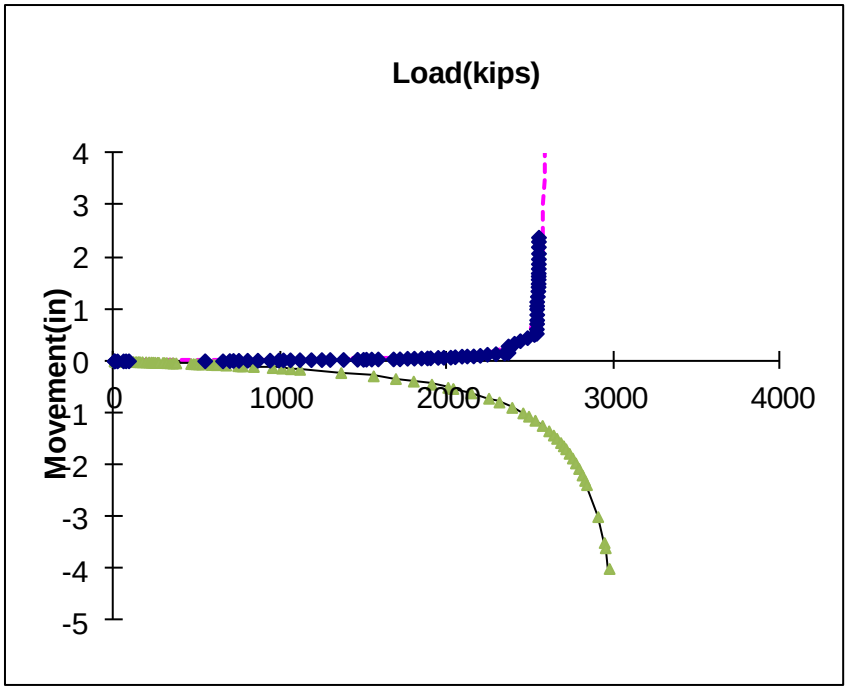

Figure 116
O-cell load settlement curve DS30

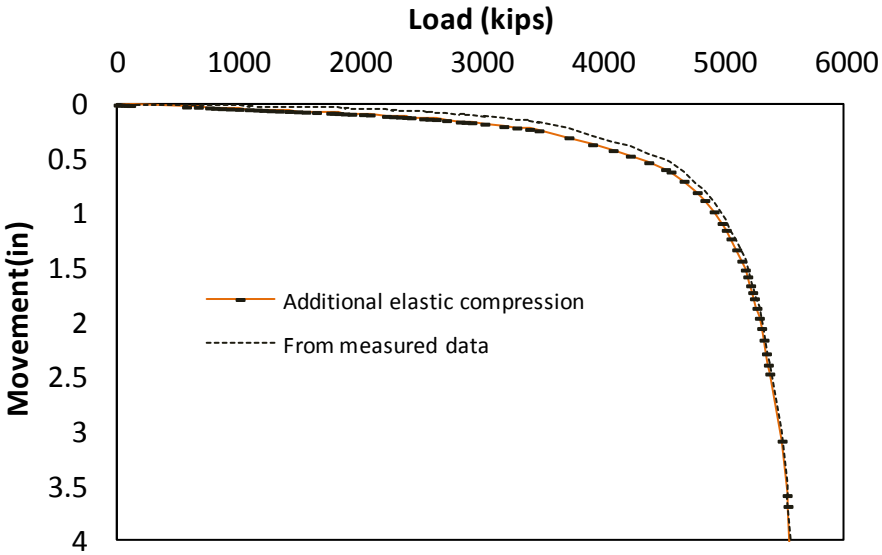

Figure 117
Equivalent top-down load settlement curve DS30

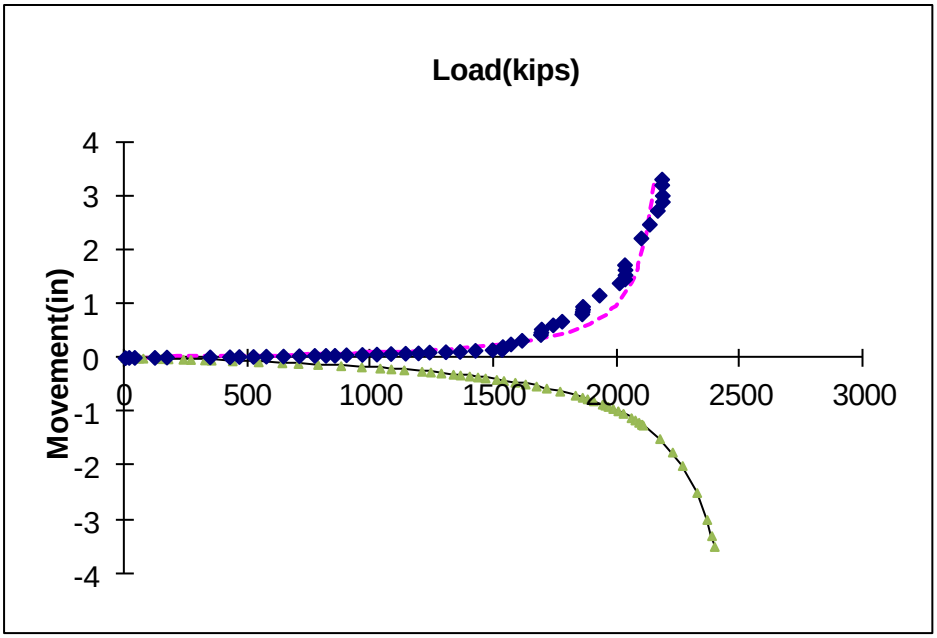

Figure 118
O-cell load settlement curve DS31

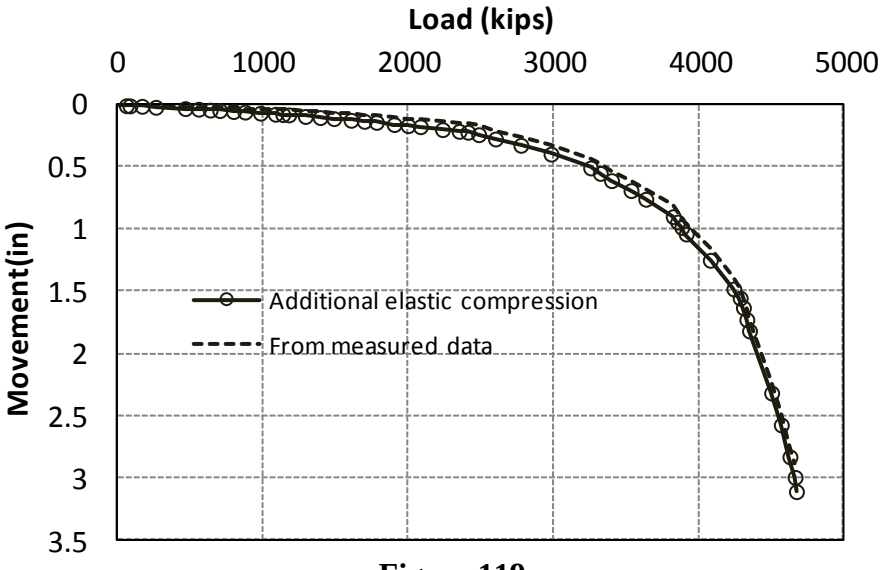

Figure 119
Equivalent top-down load settlement curve DS31

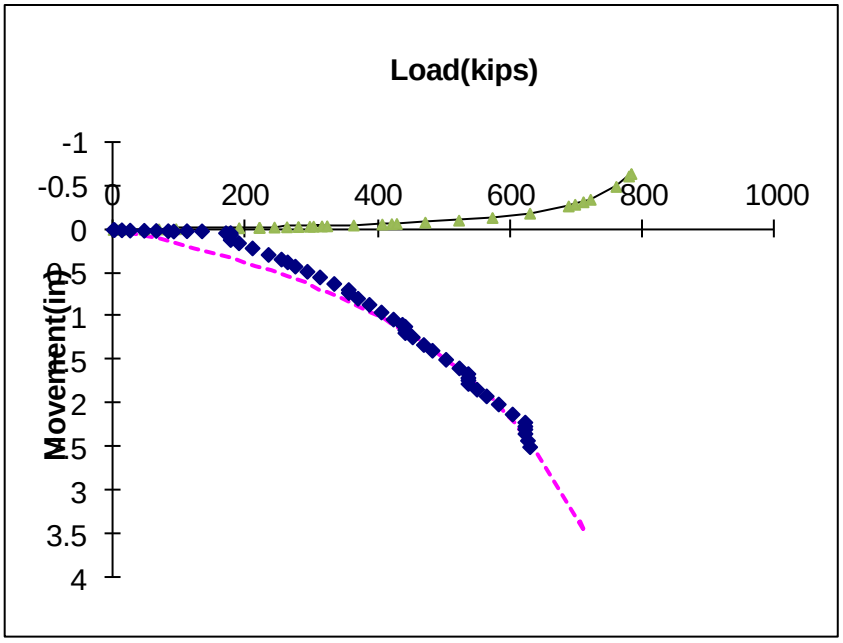

Figure 120
O-cell load settlement curve DS32

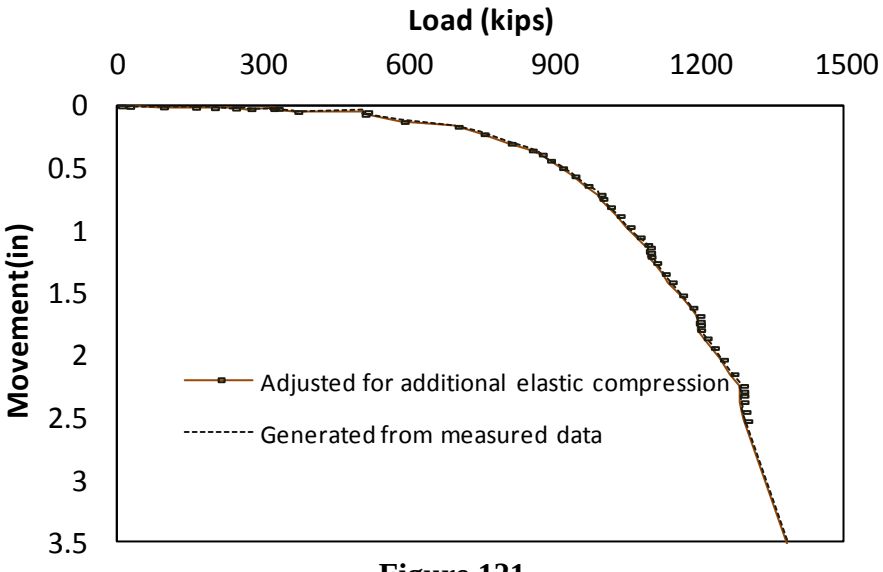

Figure 121
Equivalent top-down load settlement curve DS32

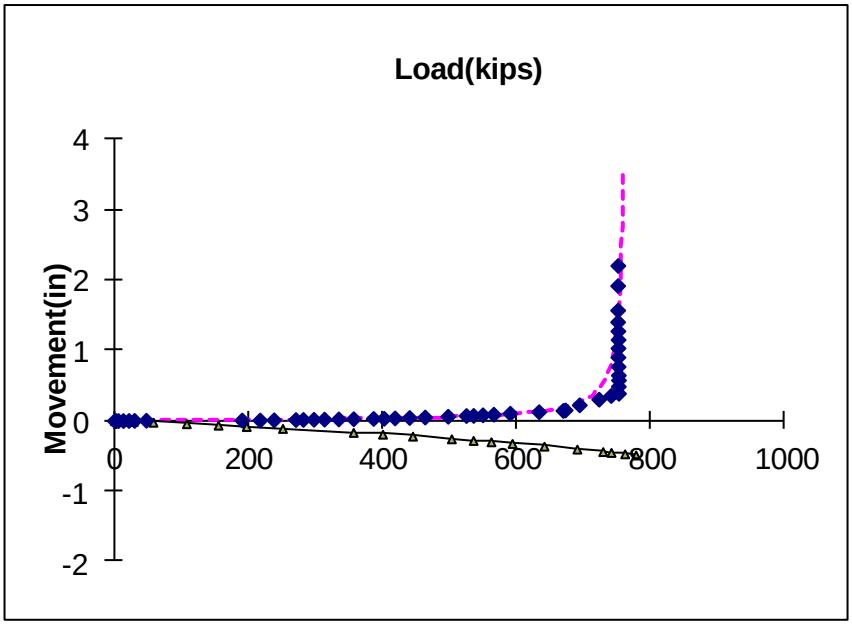

Figure 122
O-cell load settlement curve DS33

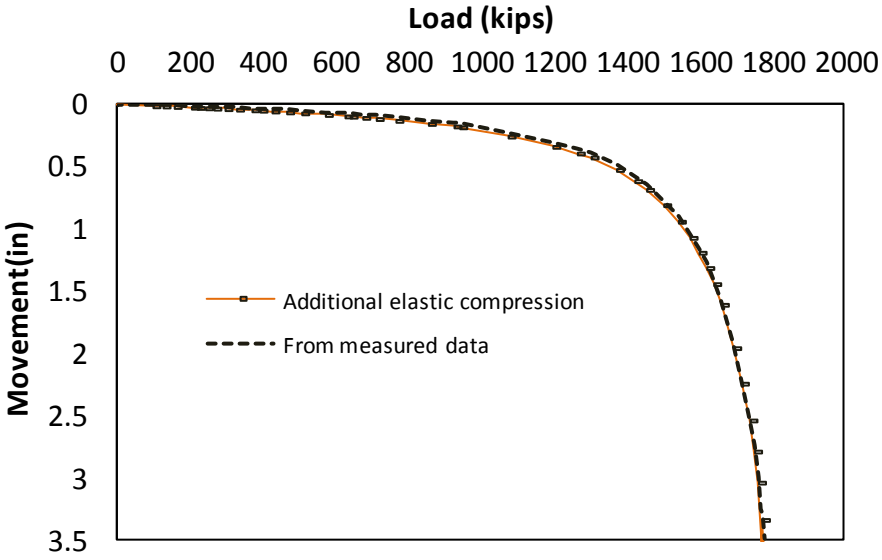

Figure 123
Equivalent top-down load settlement curve DS33

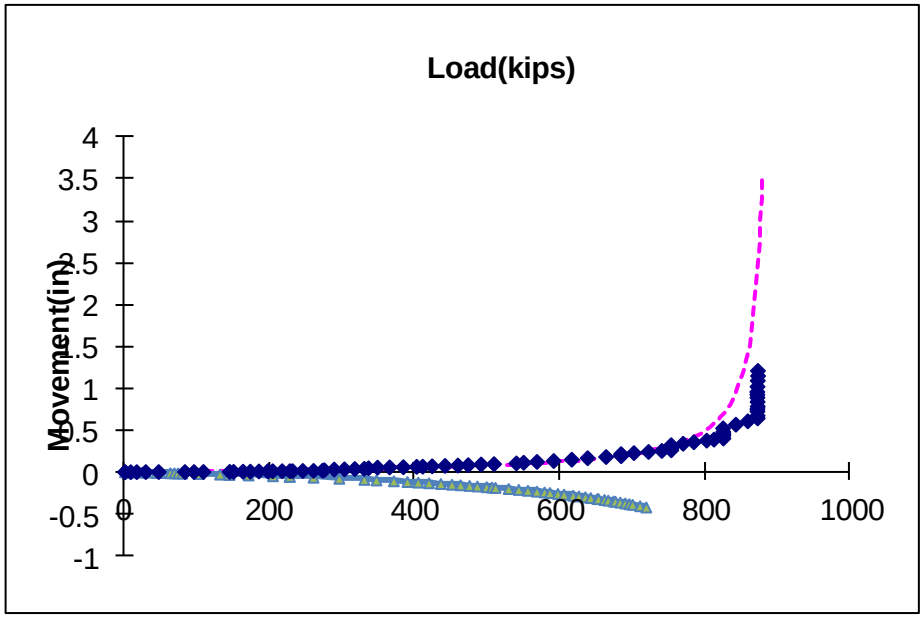

Figure 124
O-cell load settlement curve DS34

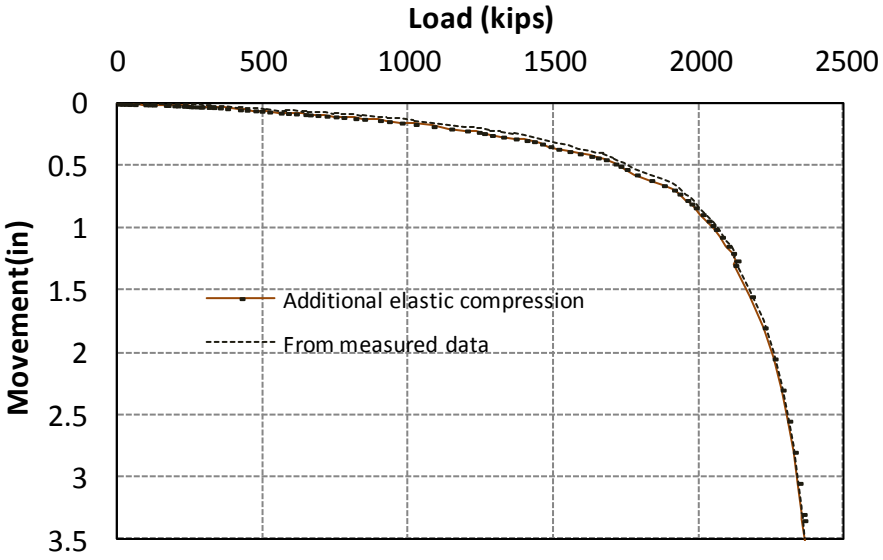

Figure 125
Equivalent top-down load settlement curve DS34